Tropical Clouds Life Cycles, Organization and Cloud Processes: Potential Impact of Aerosol
Part A

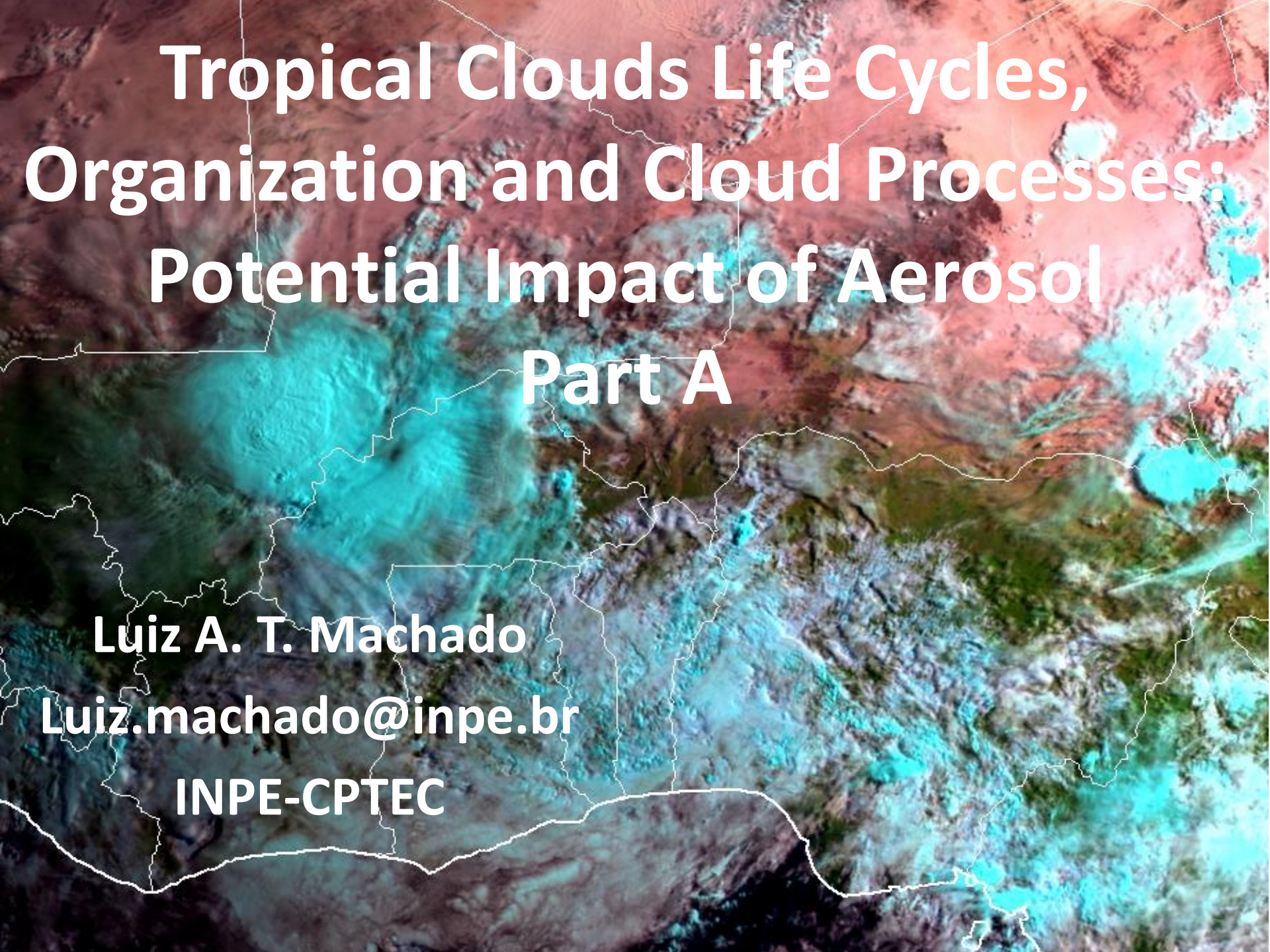

Luiz A. T. Machado
Luiz.machado@inpe.br
INPE-CPTEC

Two fundamentally different types of clouds exist, with different roles in the climate

- Convective clouds: Formed by rising due to buoyant instability of a column of air when air is humid and the lapse rate exceeds the moist adiabatic lapse rate

- Stratiform clouds: Formed by other sources of upward vertical motion such as lifting of warm air masses over cold air masses or boundary layer turbulence

Convective clouds

- Shallow (fair weather) cumulus
  - No or little precipitation
  - Moisten the lower troposphere by transporting water evaporated from the surface upward
  - Frequent enough to have a radiative impact

- Deep cumulonimbus
  - Responsible for the majority of Earth's precipitation
  - Warm and dry the atmosphere
  - Source of ~50% of cirrus clouds

(images courtesy NASA)

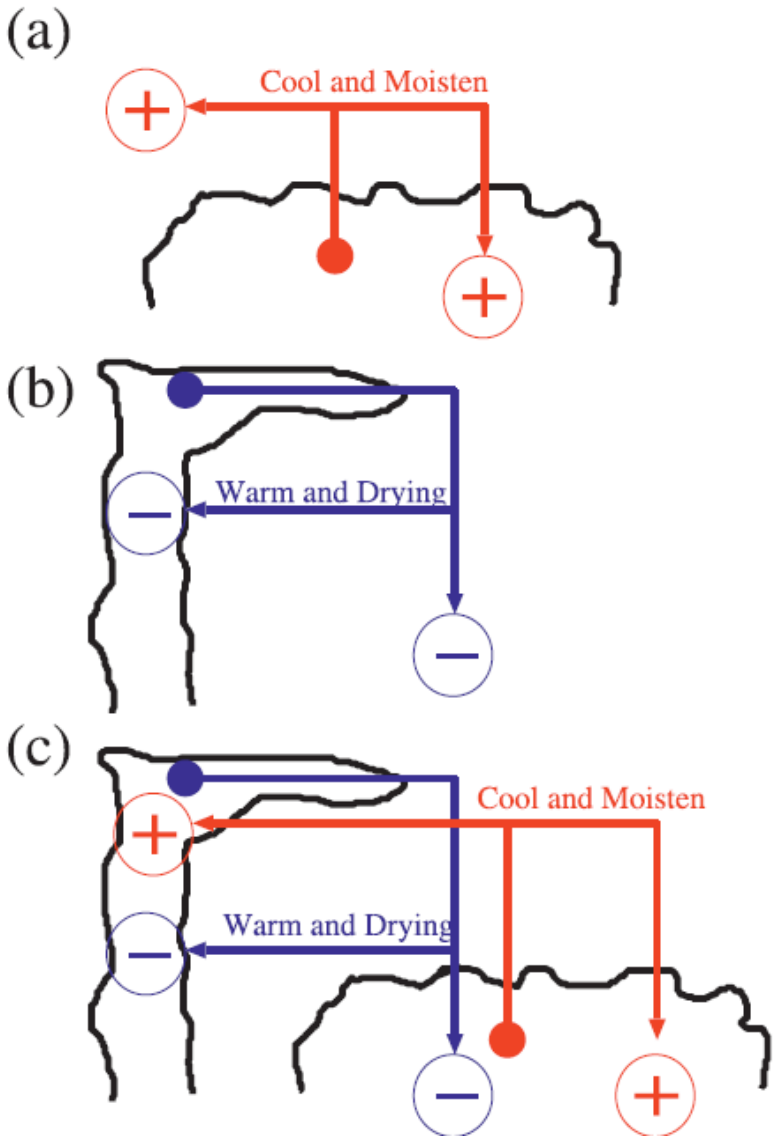

FIG. 1. Feedback loops for (a) shallow and (b) deep convection when they operate independently, and (c) when they are coupled. The arrows indicate the directions of feedbacks, and the plus and minus signs indicate positive and negative feedbacks, respectively. Here, feedbacks are defined in terms of the tendency for an increase of the cloud work function. Thus, positive and negative feedbacks lead to destabilization and stabilization of the system, respectively. In (a) shallow convection brings a positive feedback into the system, destabilizing itself, and also the conditions for deep convection by moistening and cooling the environment. In (b) deep convection brings a negative feedback into the system, stabilizing itself, and also the conditions for shallow convection by drying and warming the environment. In (c) the coupling of shallow and deep convection leads to a stable configuration by balancing the destabilization and stabilization tendencies (positive and negative feedbacks) of shallow and deep convection, respectively.

Yano, J. and R. Plant, 2012: Interactions between Shallow and Deep Convection under a Finite Departure from Convective Quasi Equilibrium. *J. Atmos. Sci.*, **69**, 3463–3470, https://doi.org/10.1175/JAS-D-12-0108.1

Stratiform clouds

- Low/middle clouds
  - Mostly liquid, but can be mixed-phase or ice at low temperatures
  - No or little precipitation (stratus, stratocumulus) or significant precipitation (nimbostratus)
  - Important for reflection of sunlight
  - Little greenhouse effect because they lie below the clear sky emission level
- High clouds
  - Almost exclusively ice
  - Optically thin with little reflection of sunlight (cirrus) or thick convective anvil clouds (cirrostratus) with significant reflection
  - Always produce snow which does not reach the ground; thick anvils produce rain at the ground
  - Strong greenhouse effect because they lie above the clear sky emission level

(images courtesy NASA)

Stratiform clouds are important primarily for their radiative effects. The global mean temperature is determined by the balance between absorbed sunlight and the Earth's emitted heat radiation.

Stratiform clouds, which cover a much larger area than convective clouds, are responsible for most of clouds' radiative effect on the climate.

Low-altitude stratiform clouds such as stratus and stratocumulus tend to be made of liquid and are optically thick and thus reflect significant sunlight. At the same time, they do not trap much more thermal radiation than the clear atmosphere does because they exist at altitudes where most of the atmosphere's water vapor (the most important greenhouse gas) resides. Thus these clouds have a net cooling effect on the current climate.

High stratiform clouds are almost always ice and can either be optically thin (cirrus) or optically thick (cirrostratus). Cirrus clouds reflect relatively little sunlight but strongly absorb thermal infrared radiation and re-emit it to space at the very low temperatures of the upper troposphere, and they thus have a net warming effect on the climate.

The Cloud Cluster Radiative Effect

Change in net radiative fluxes (W m^{-2})				
Region	Cloud type	Surface	Atmosphere	Top
Land	CS	−133	+98	−35
	Convective	−188	+71	−118
	Mesoscale anvil	−119	+104	−14
	Transition anvil	−164	+92	−71
	Cirrus anvil	−95	+111	+16
Ocean	CS	−160	+96	−64
	Convective	−218	+65	−153
	Mesoscale anvil	−146	+104	−41
	Transition anvil	−197	+92	+105
	Cirrus anvil	−118	+111	−7

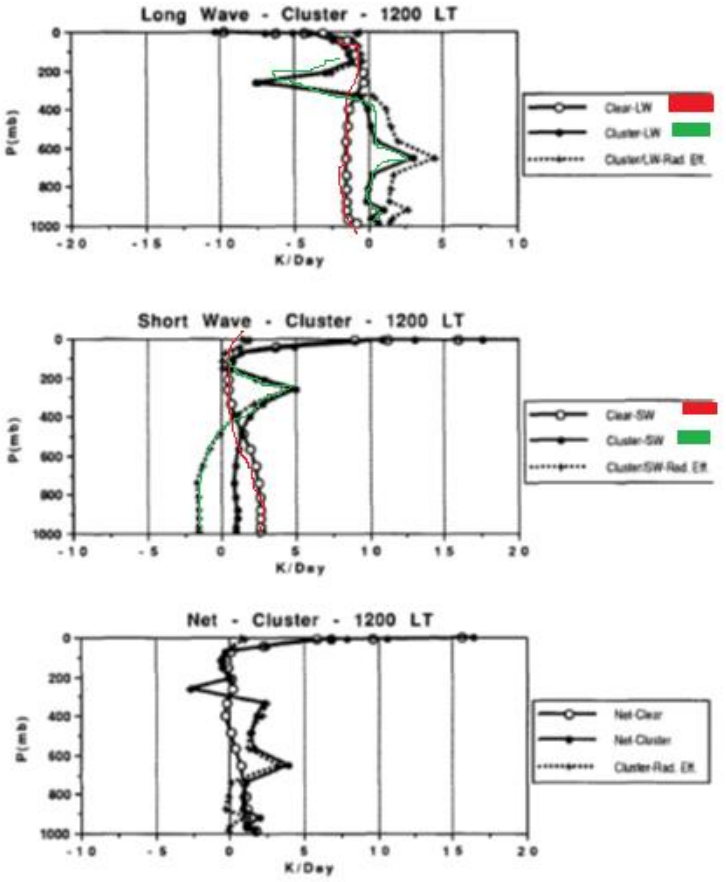

Based on the tropical cloud cluster mean properties it was computed, for 1200 LST, the heating-cooling rates of the longwave, short wave and the net effect. The change in net radiative flux, for land and ocean and for the different components of the cloud cluster is also presented in the Table above. Cloud cluster has a net cooling effect, mainly due to the convective parts of around 35 – 64 W m^{-2}.

Vertical profile heating-cooling rates for a typical cloud cluster of around 180-360 km radius, based on average cloud properties. The heating-cooling rates were computed for noontime over tropical region.

Machado, L. A. T., and W. B. Rossow, 1993: Structural characteristics and radiative properties of tropical cloud clusters. Mon. Wea. Rev., 121, 3234–3260.

$$\frac{\partial \rho E}{\partial t} + \nabla \cdot \mathbf{F}_{E'} = -\nabla \cdot \mathbf{F}_{\text{rad}} - \nabla \cdot \mathbf{F}_{\text{sfc}}$$

$$\mathbf{F}_{E'} = \rho(c_p T + gz + Lq)\mathbf{v}$$

$$E = (c_v T + gz + Lq), \qquad (1)$$

where ρ is the air density, $\mathbf{v}$ is the wind vector, and $\mathbf{F}_{\text{rad}}$ and $\mathbf{F}_{\text{sfc}}$ are the radiational heating/cooling in the surface/atmosphere and the nonradiational heating/cooling from the surface. These terms correspond to the main sources and sinks of energy in the atmosphere. This equation shows that local energy varies due to the divergence of energy flux and by radiative and surface divergence fluxes.

ABLE-2B				
Variables (W m^{-2})	Mean	Std dev	−95.0% conf.	+95.0% conf.
Net solar flux − TOA	272	23	263	280
OLR	217	24	208	226
Refl. solar rad. − TOA	131	24	122	140
Net radiation − TOA	55	15	48	59
Energy divergence flux	65	88	25	104
Energy storage	−10	87	−60	19
FluAmazon				
Variables (W m^{-2})	Mean	Std dev	−95.0% conf.	+95.0% conf.
Net solar flux − TOA	280	36	268	294
OLR	218	33	206	230
Refl. solar rad. − TOA	143	35	130	156
Net radiation − TOA	62	12	58	67
Energy divergence flux	50	71	21	78
Energy storage	12	72	−16	43

Machado, L. A. T. (2000). The Amazon Energy Budget Using the ABLE-2B and FluAmazon Data, J. Atmos. Sci., 57(18), 3131–3144

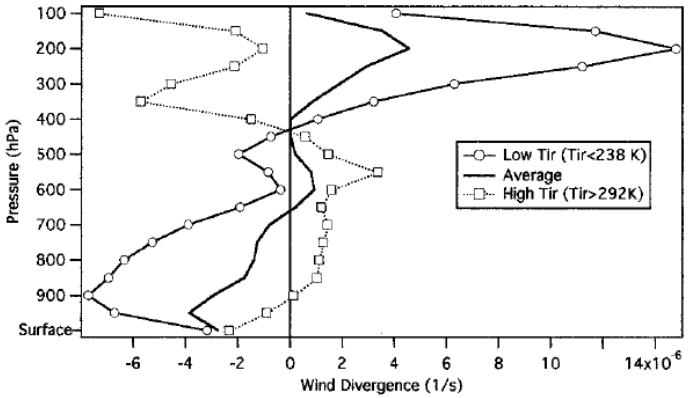

FIG. 5. Average wind divergence profile for the condition of low Tir (Tir $<$ 238 K), mean Tir, and high Tir (Tir $>$ 292 K), for ABLE-2B and FluAmazon.

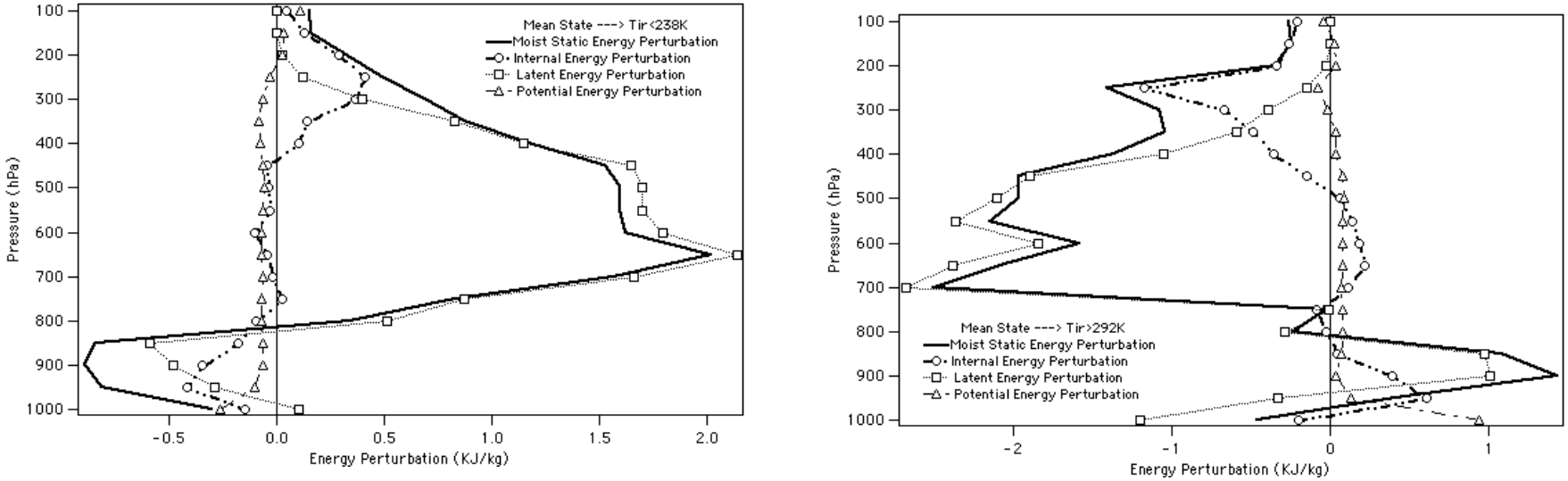

FIG. 3. Profiles of the energy perturbation (moist static energy, internal energy, latent, and potential) from the average state to the condition defined by (a) Tir $<$ av_Tir $- 1.5\sigma$ (typical of high clouds situation Tir $<$ 238 K) and (b) Tir $>$ av_Tir $+ 1.5\sigma$ (typical of low clouds situation Tir $>$ 292 K).

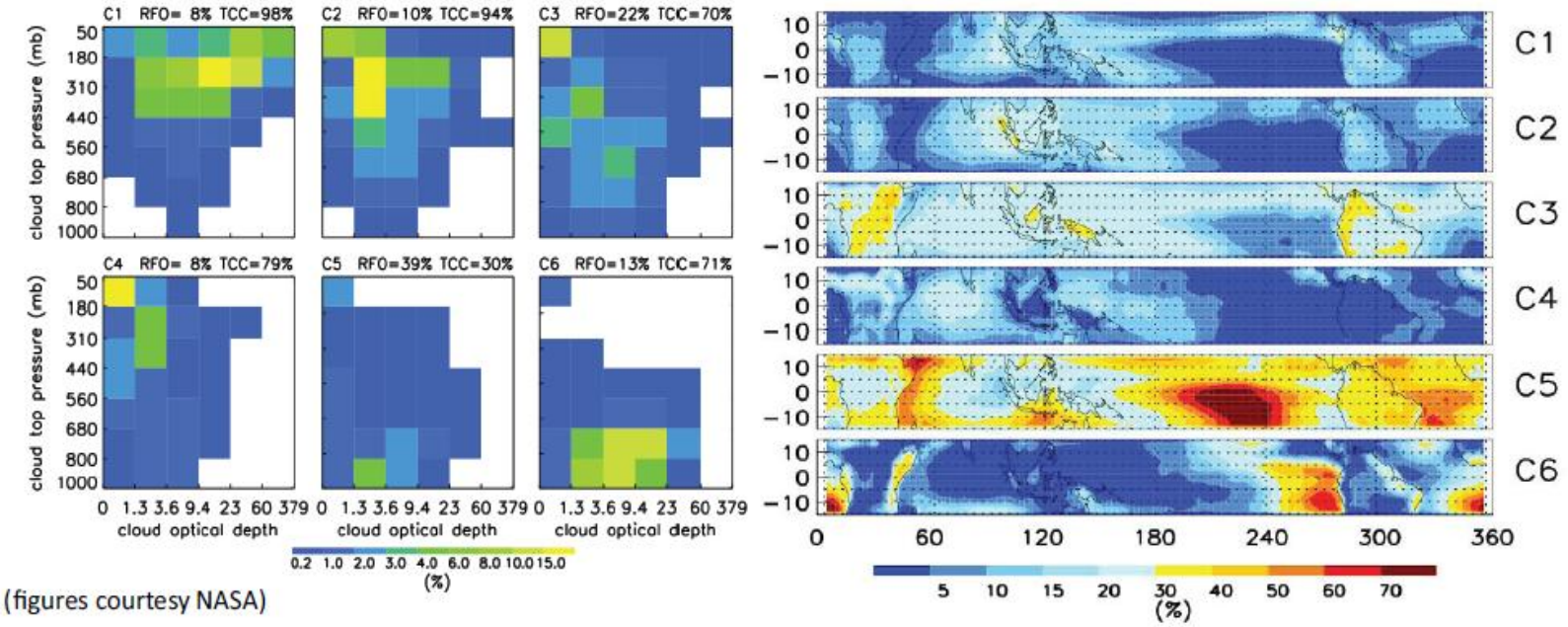

(figures courtesy NASA)

Tropical clouds can be organized into 6 categories in weather satellite images by their optical thickness (which determines how much visible sunlight they reflect) and their emission of thermal infrared radiation to space (which depends on how high their tops are):

- *Disturbed (precipitating) conditions*: Organized deep convection (WS1), cirrostratus and anvil clouds (WS2), and isolated deep, midlevel and shallow convection (WS3)
- *Suppressed (fair weather, drizzle) conditions*: Cirrus (WS4), shallow cumulus (WS5), and stratocumulus (WS6)

Cloud Cluster and Lifetime Observed by Satellite

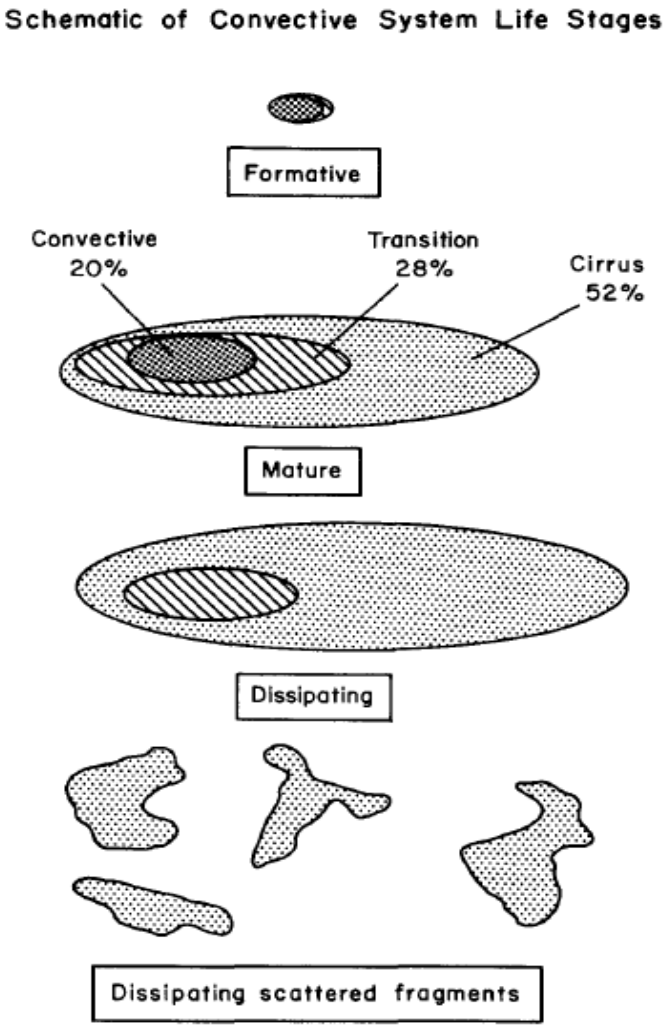

Cloud Clusters can be defined in the range of Brightness Temperature smaller of around 255K, mostly of the studies employ 235K.

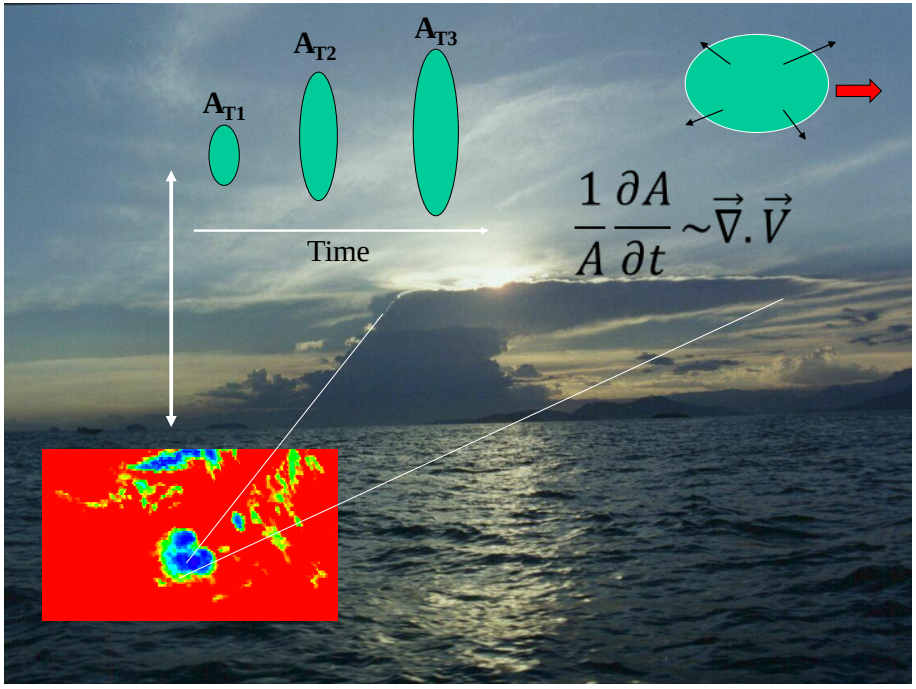

Machado, L. A. T., and W. B. Rossow, 1993: Structural characteristics and radiative properties of tropical cloud clusters. Mon. Wea. Rev., 121, 3234–3260.

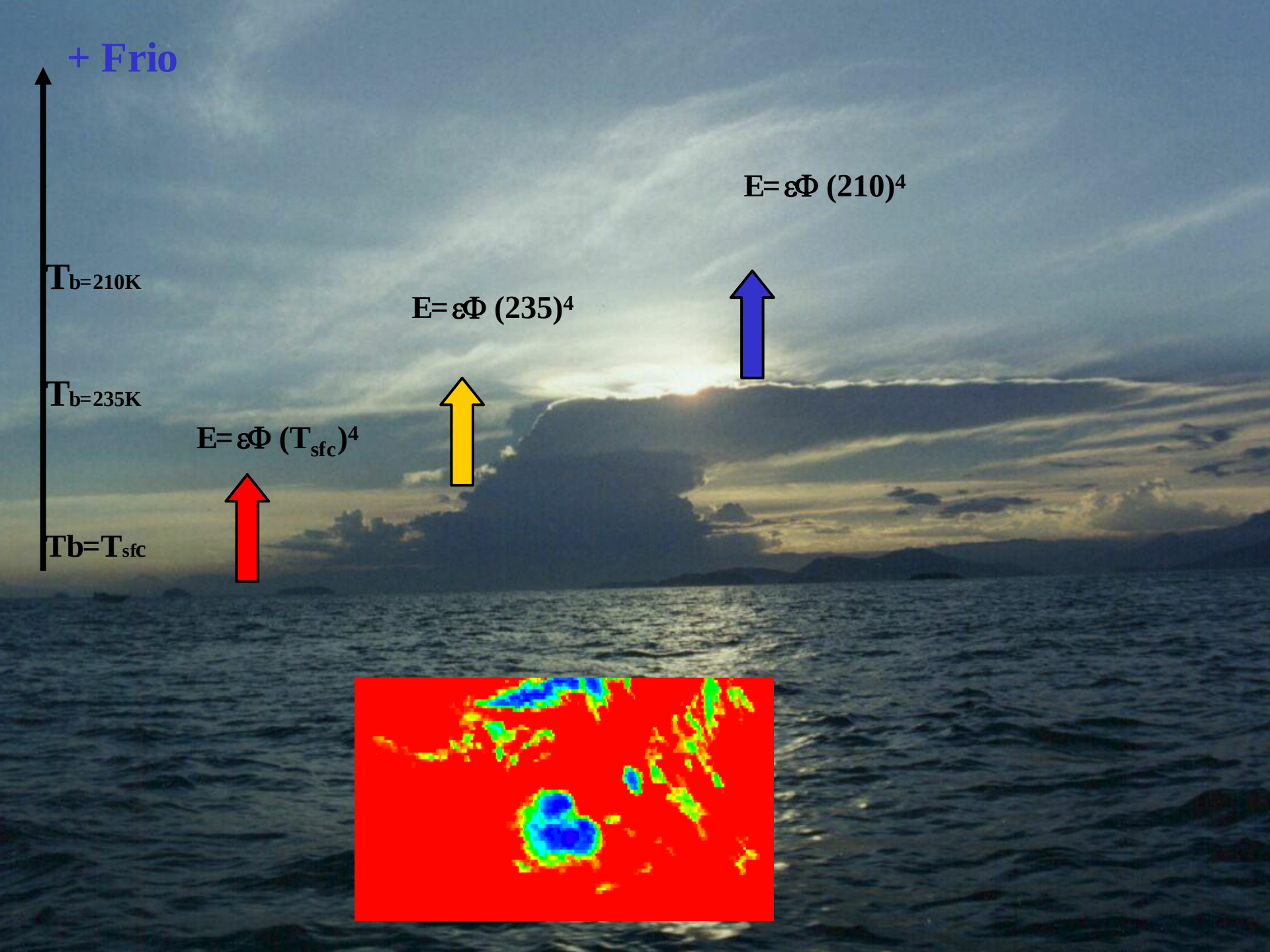
+ Frio
$T_{b=210K}$
$T_{b=235K}$
$Tb=T_{sfc}$
$E=\varepsilon\Phi\ (T_{sfc})^4$
$E=\varepsilon\Phi\ (235)^4$
$E=\varepsilon\Phi\ (210)^4$

The Cloud Size Distribution

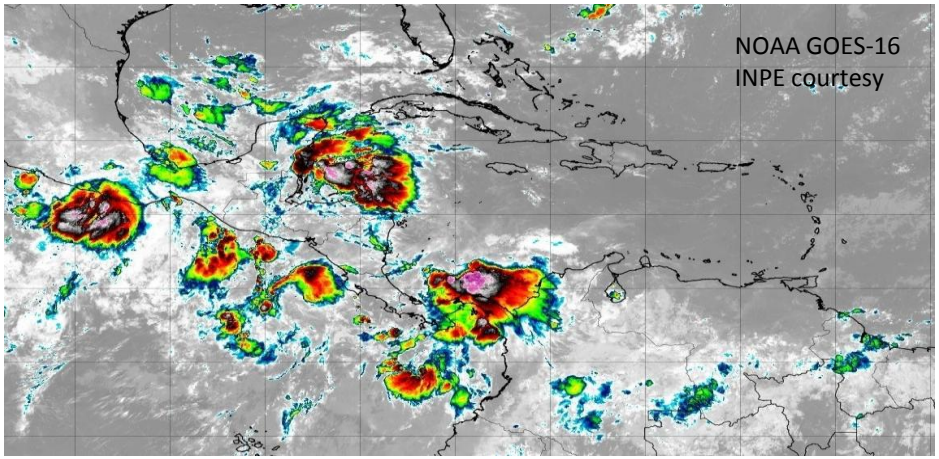

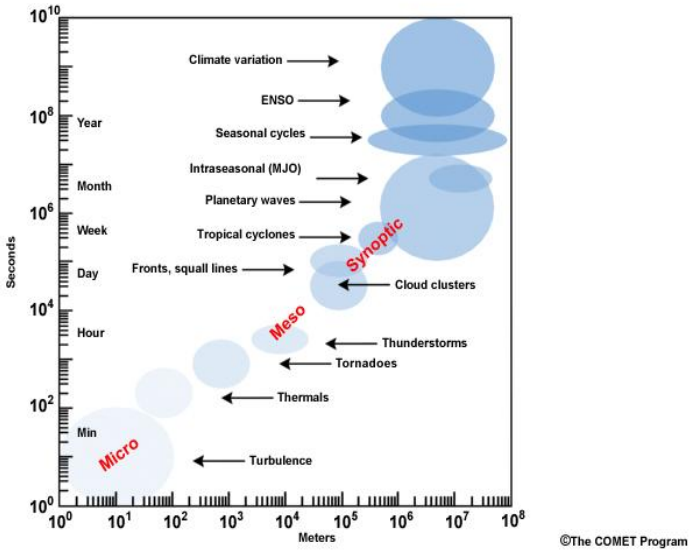

radii and N(r) is the number of cloud cluster with size r and A is a constant. This size parameterization implies in the nearly same contribution to the cloud cover by all cloud cluster

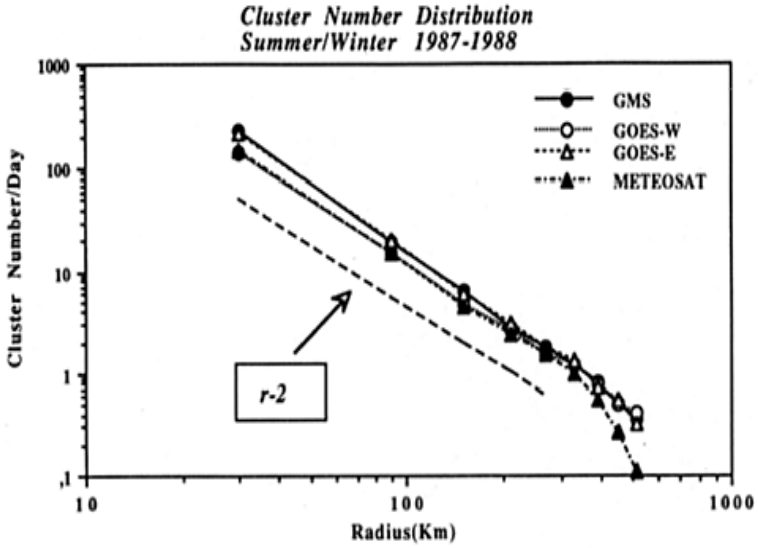

Machado, L. A. T., and W. B. Rossow, 1993: Structural characteristics and radiative properties of tropical cloud clusters. Mon. Wea. Rev., 121, 3234–3260.

Thresholds and the Cloud Cluster Size Distribution

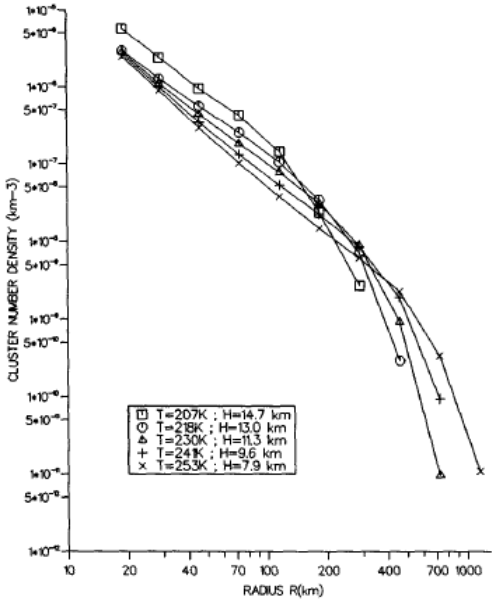

FIG. 2. Normalized cluster number density $N(\Delta R)$ versus cluster equivalent radius for the five thresholds studied and on the average over the whole region, and summers 1983–88.

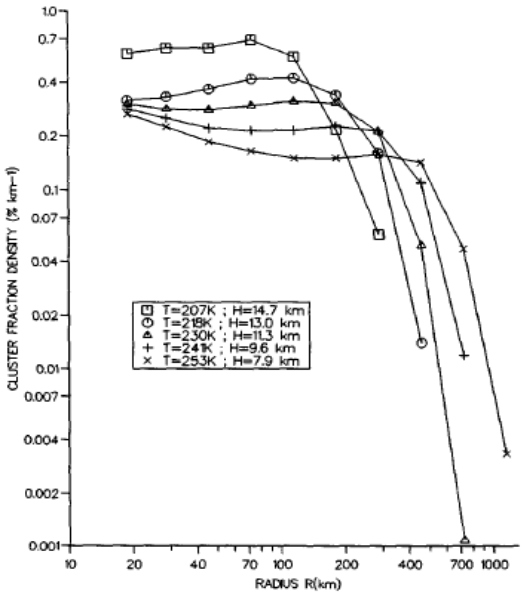

FIG. 3. Same as Fig. 2 but for cluster fraction density $S(\Delta R)$.

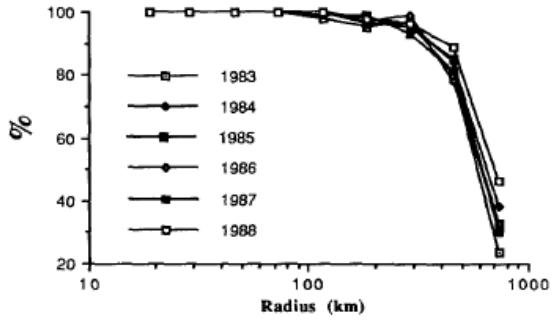

FIG. 4. Average probability of finding at least one cloud in each radius class for threshold 253 K, summers 1983–88, and the whole region.

Machado LAT, Desbois M, Duvel JP. 1992. Structural characteristics of deep convective systems over tropical Africa and the Atlantic Ocean. Mon. Weather Rev. ***120****: 392–406.*

Cloud Cluster Number Density and fraction density, number density describes the number of cloud cluster in a given area for each size range and fraction density describes the area fraction covered by each size range. The thresholds change the absolute value however its do not change the shape of the distribution. It is clear that size distribution follow a specific distribution up to a breaking radius. This breaking radius defines the typical sizes of cloud clusters for a specific threshold. Colder thresholds are associated to smaller cloud organization. The breaking radius is related to the temporal probability of observing cloud clusters with larger radius in a specific area and threshold. This breaking radius is very stable from year to year in despite of large total cloud cover variability and set up the scale of the cloud clusters for a specific threshold, region and season.

The Modulation of the Cloud Size Distribution by Diurnal Cycle

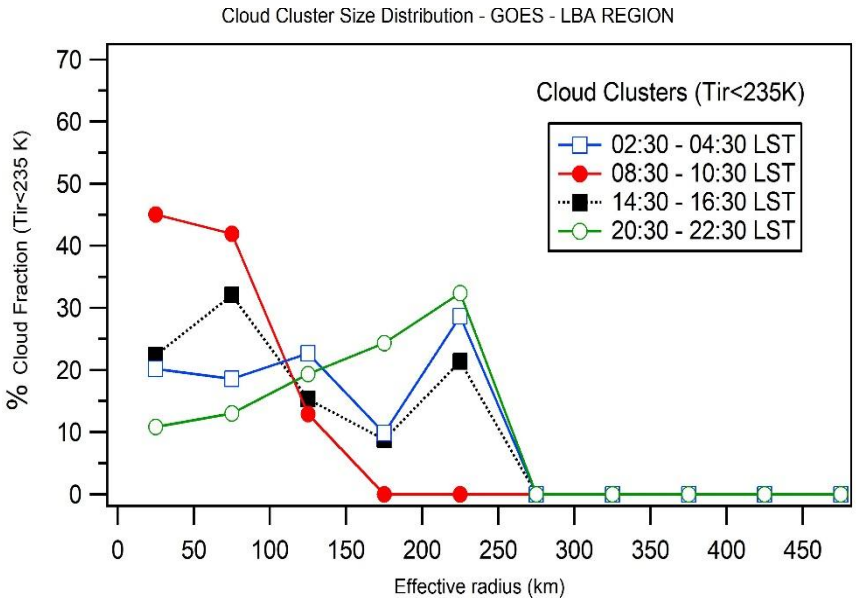

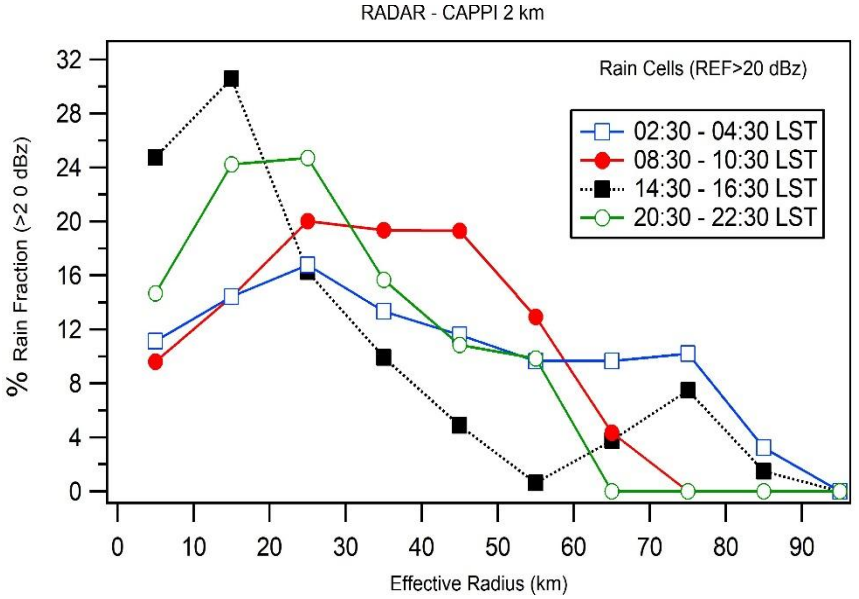

Diurnal cycle change the size distribution from the climatology distribution from the standard N(r)= $A.r^{-2}$. Figures above are for Amazonas collected during TRMM-LBA field campaign. On the left side are the rain cell size distribution, the rainfall at 2 km height and on the right side are the cloud cluster size distribution for a 235K threshold. It is clear the increase in size from early morning to the night. Also one can note the differences between cloud and rain. The rainfall in the early morning are a result of clouds of reduced size. From the other side at 2030–2230 LST almost the entire high cloud cover is organized into large convective systems, but the rain cells are smaller. There is a preferential size organization for cloud and rainfall.

The Modulation of the Cloud Size Distribution by Synoptic Systems

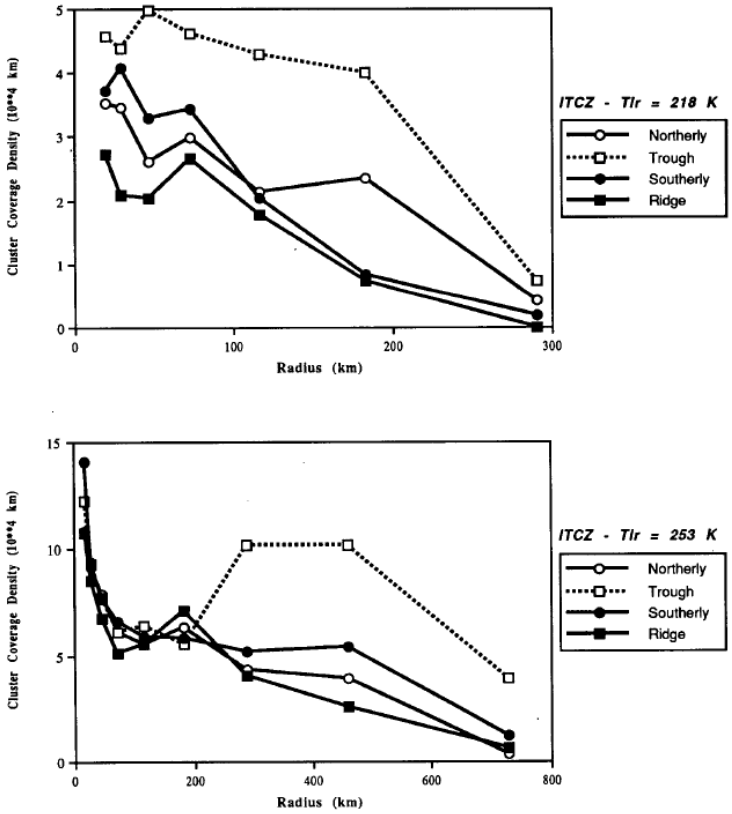

FIG. 10. Easterly wave modulation of the cluster coverage density $S(\Delta R)$ versus cluster radius over the ITCZ region (a) for threshold T_{IR} = 218 K, and (b) for threshold T_{IR} = 253 K.

Easterly waves, in Africa, modulates de cloud cluster number distribution, the system with effective radius around 200-400 km are typical in the trough (system is defined by 253 K – cloud organization in middle to high levels clouds). At colder thresholds (218K), associated to the more intense parts of the cloud cluster easterly waves modulated the number of cluster at all sizes, in the trough there is a larger number of these more convective cells.

The same is observed by looking cold fronts penetration and others synoptic systems.

Machado, L. A. T., J. P. Duvel, and M. Desbois, 1993: Diurnal variations and modulation by easterly waves of the size distribution of convective cloud clusters over West Africa and the Atlantic Ocean.Mon. Wea. Rev, ***121,*** *37–49*

The Cloud Lifetime and Size Relationship

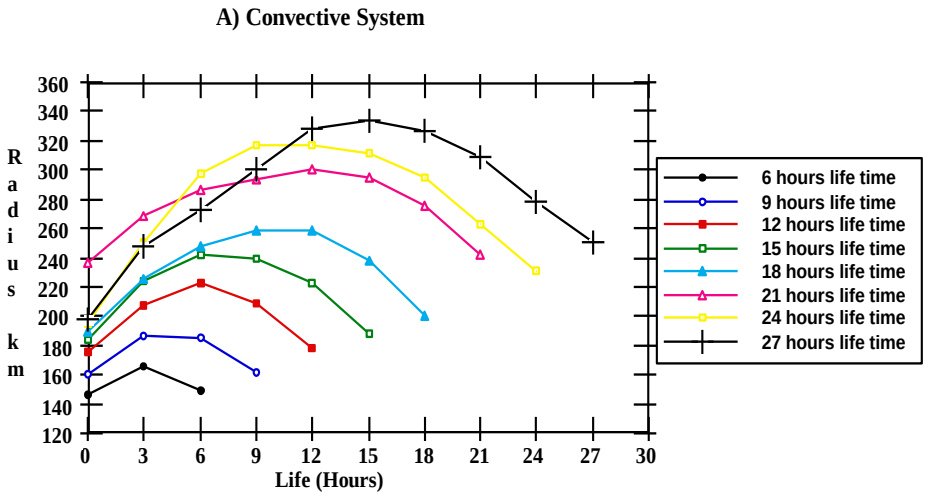

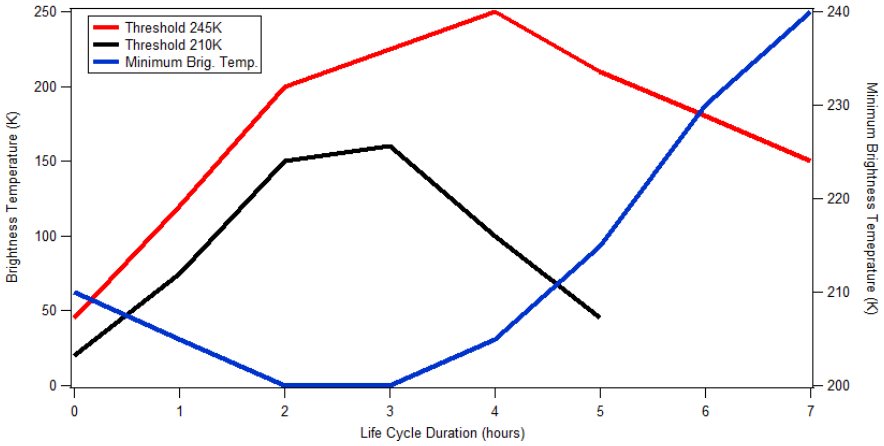

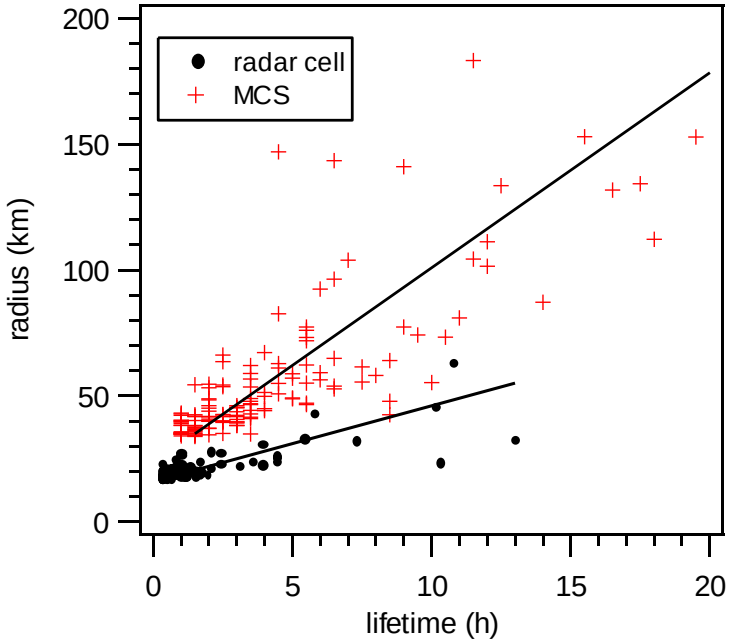

There is a linear relationship between lifetime and radius. This relationship is observed for cloud clusters as well as rain clouds (using weather radar). The threshold employed set up the specific space-time scale of the cloud organization. Cloud Clusters evolve from the initiation to the mature stage (stage when the area expansion is close to zero) and to the dissipation stage when cloud clusters reduce in size up to the fragmentation. The warmer threshols continue to increase in size when the average cloud cluster minimal brightness temperature is already increasing and the convective cells merged inside the cloud cluster is decreasing in size.

The Cloud Area Expansion

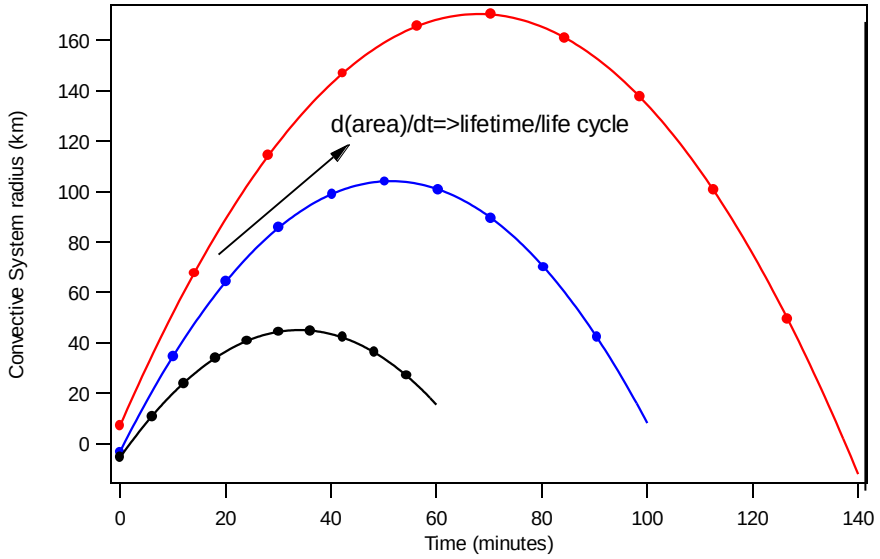

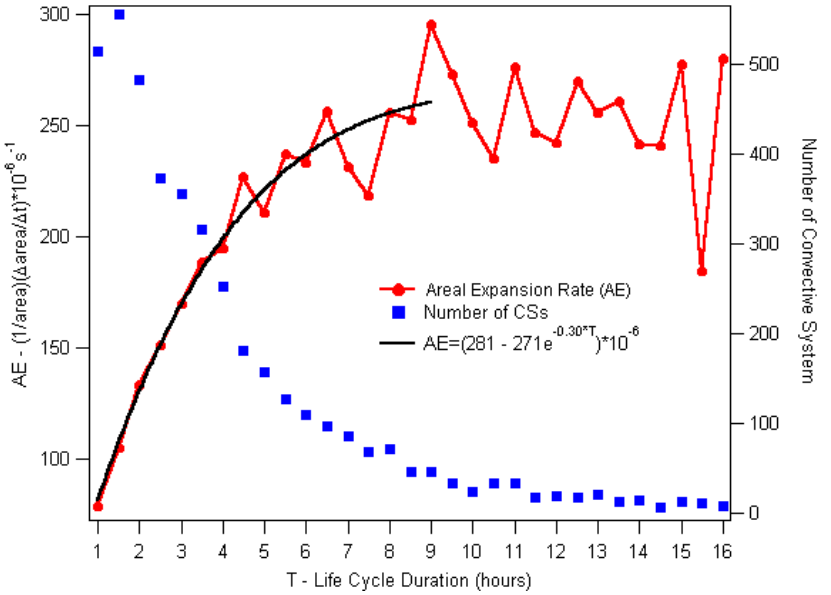

Cloud clusters with larger size stay for longer than smaller one as showed before. Larger cloud clusters show in the initiation phase a larger Normalized Area Expansion (NAE) than system with shorter duration. The NAE in the initiation is related to the cloud cluster lifetime. The NAE is related to the mass flux of the convective process, larger mass flux longer and larger the system will be.

The Cloud Area Expansion

$$\frac{1}{A}\frac{\partial A(div,cond)}{\partial t} = \frac{1}{A}\frac{\partial A(div)}{\partial t}\Big|_{cond=cte} + \frac{1}{A}\frac{\partial A(cond)}{\partial t}\Big|_{div=cte}$$

$$\frac{1}{A}\frac{\partial A(div)}{\partial t}\Big|_{cond=cte} = \nabla.V$$

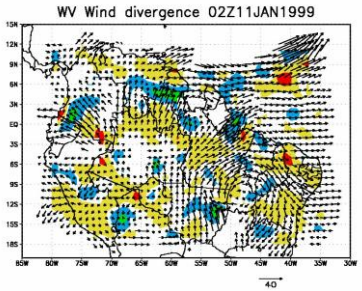

$$\frac{1}{A}\frac{\partial A(div,cond)}{\partial t} = \nabla.V + \frac{1}{A}\frac{\partial A(cond)}{\partial t}\Big|_{div=cte}$$

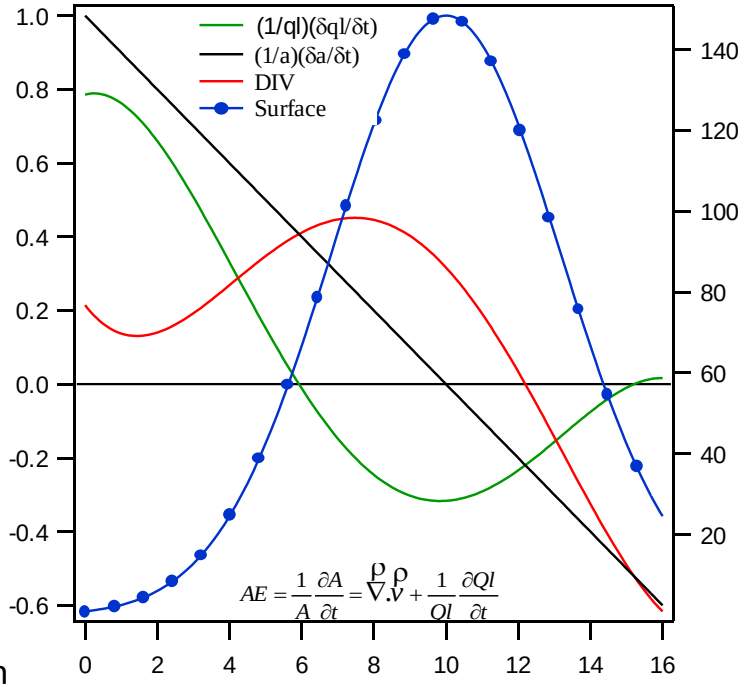

$Ql = \rho_l.A.H$ The liquid water content of the convective system

and

$$\frac{\partial Ql}{\partial t} = \rho_l.A\frac{\partial H}{\partial t} + \rho_l.H\frac{\partial A(cond)}{\partial t}$$

$$\frac{\partial H}{\partial t} \cong 0 - Cloud\ top\ close\ to\ tropause$$

ρl is the liquid water density
H is the convective system height

$$\frac{1}{A}\frac{\partial A}{\partial t} = \nabla.V + \frac{1}{Ql}\frac{\partial Ql}{\partial t}$$

The area time rate depends from the expansion from the wind advection and also by the condensation/evaporation process.

The Cloud Area Expansion

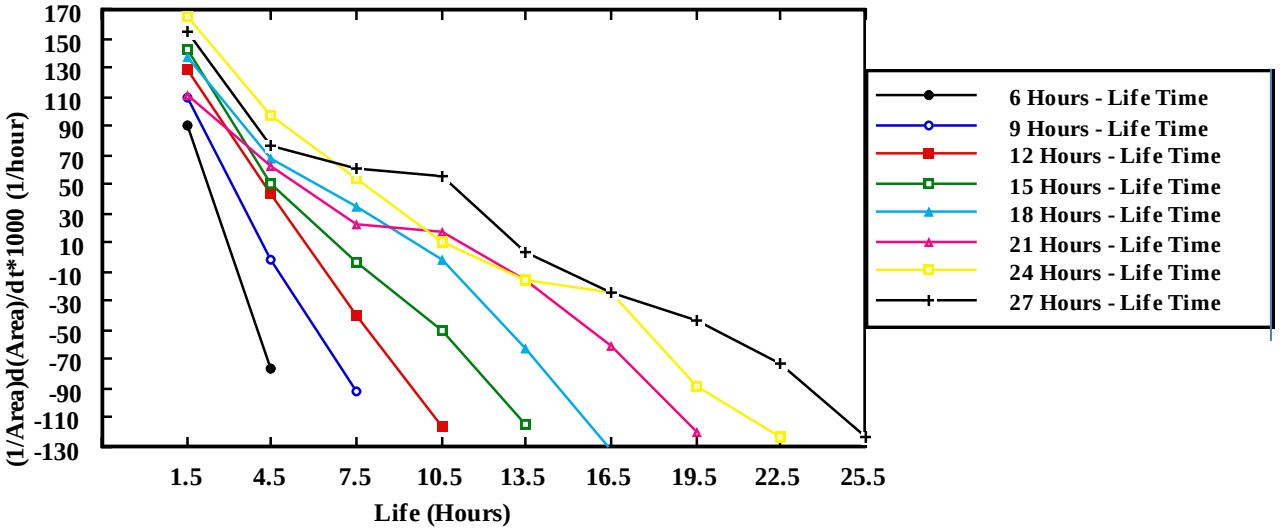

The Normalized Area Expansion change nearly linearly during the Cloud cluster lifecycle. Stronger the NAE in the initiation, longer the system lifetime. The system, in the beginning. expand mainly by the condensation process, the upper level wind divergence become more and more important as the system evolve to the Maturation. In the dissipation the system reduce area mainly by upper level wind convergence, evaporation(sublimation) and fragmentation. If the NAE is followed one can roughly forecast the change in size of the cloud cluster.

The Cloud Cluster and Rain Cell Lifetime

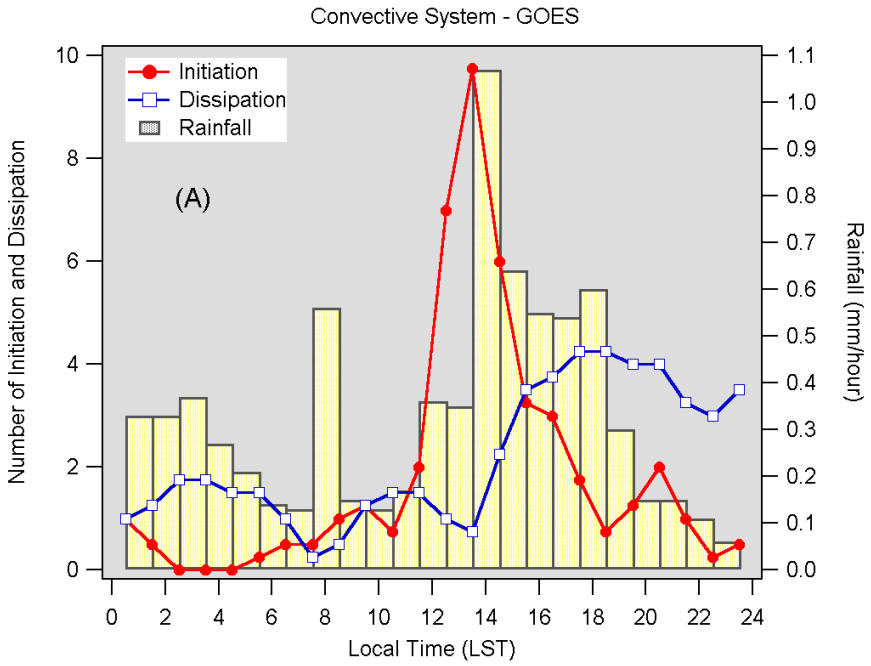

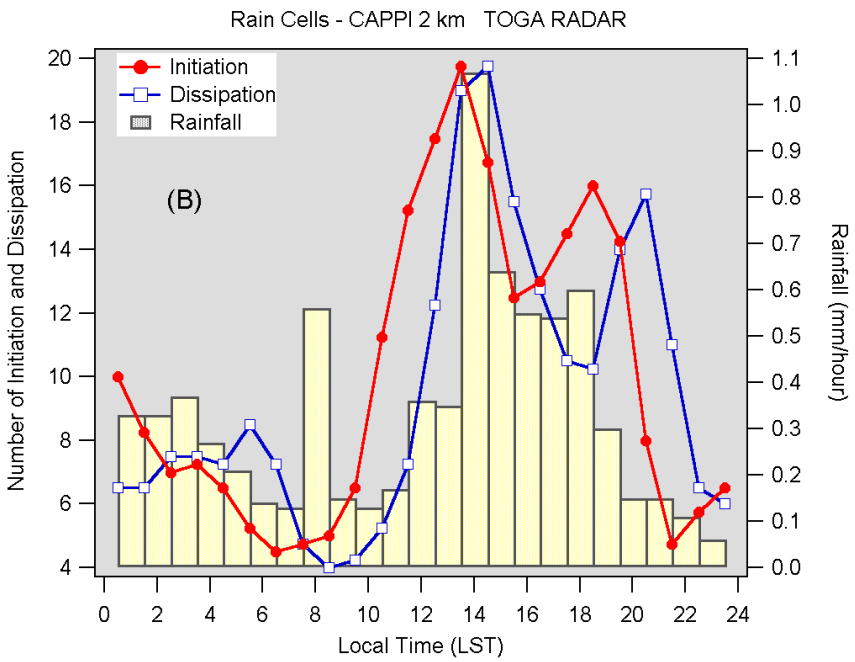

The examples above are for Amazonas convection. Cloud clusters is mainly initiated at 1400 LST but dissipation varies, the majority of the lifetime duration are around 4-6 hours. The maximum rain rate is close to the initiation when system is growing. Rain cells, from another side, is also initiated at the same time, but the lifetime is much smaller around one hour. The maximum convective activity occurs in the phase between initiation and mature time step.

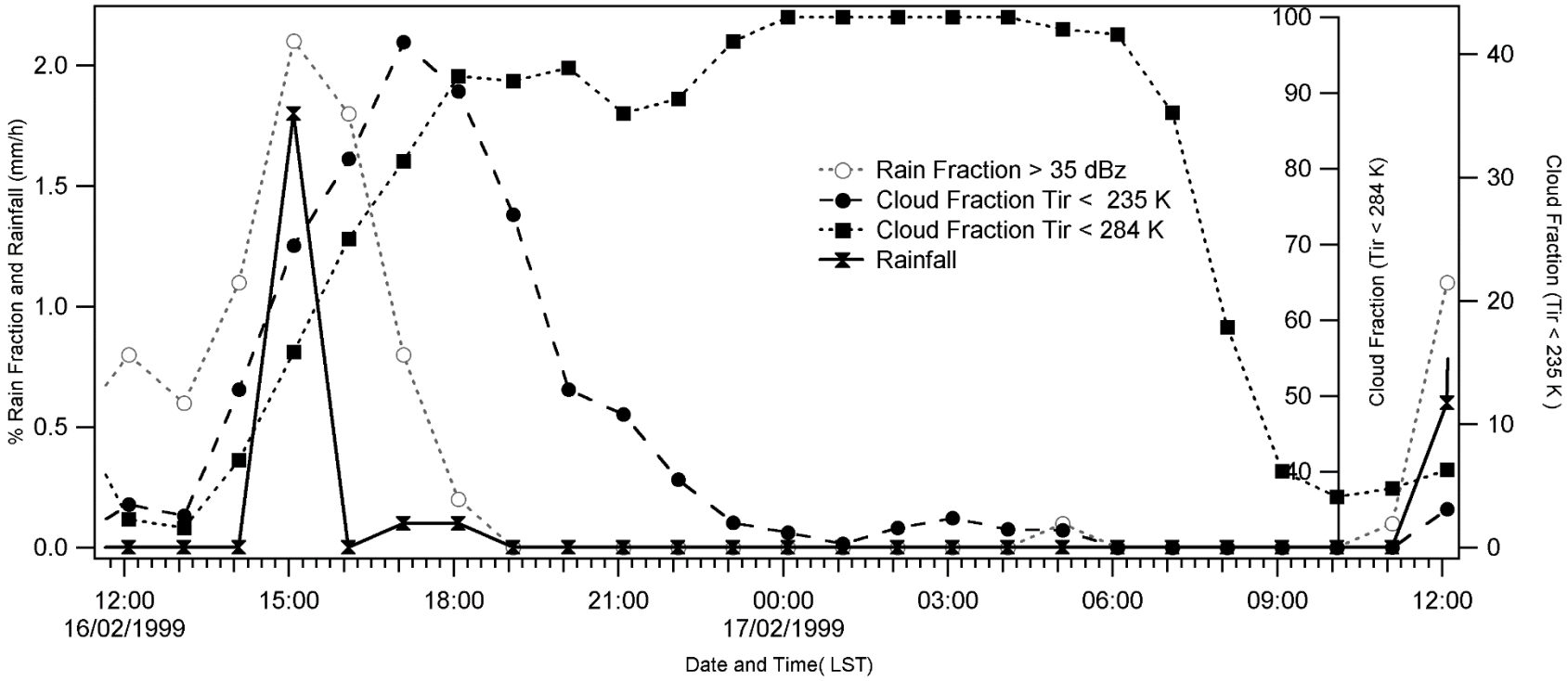
% Rain Fraction and Rainfall (mm/h)
2.0
1.5
1.0
0.5
0.0
100
90
80
70
60
50
40
Cloud Fraction (Tir < 284 K)
40
30
20
10
0
Cloud Fraction (Tir < 235 K)
Rain Fraction > 35 dBz
Cloud Fraction Tir < 235 K
Cloud Fraction Tir < 284 K
Rainfall
12:00
16/02/1999
15:00
18:00
21:00
00:00
17/02/1999
03:00
06:00
09:00
12:00
Date and Time(LST)

Composite of the reflectivity vertical profile at different lifetime RACCI/LBA

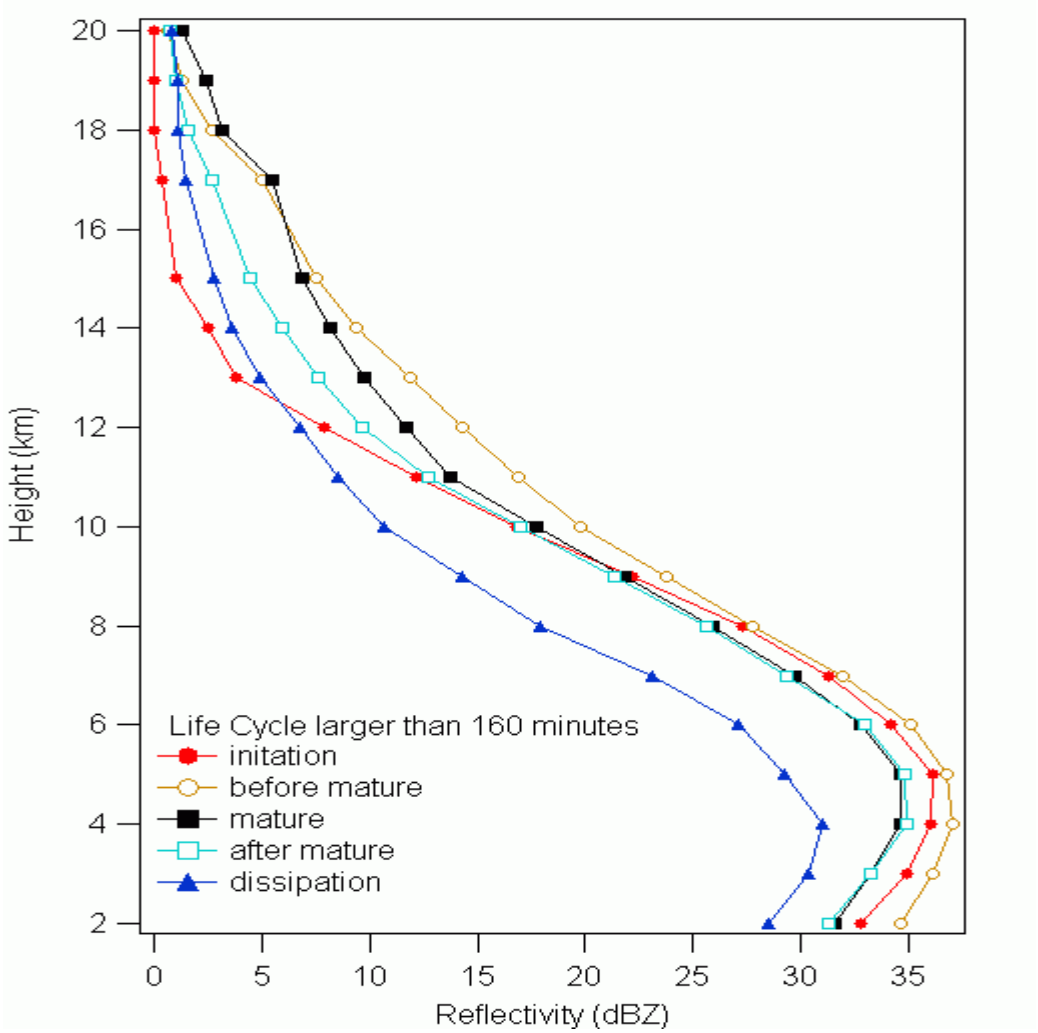

These figures show the increase of the ice phase as the cloud evolves to the mature stage.

Cloud with longer lifetime show intense liquid water phase at the initiation stage.

Cloud Cluster and Lifetime Observed by Radar

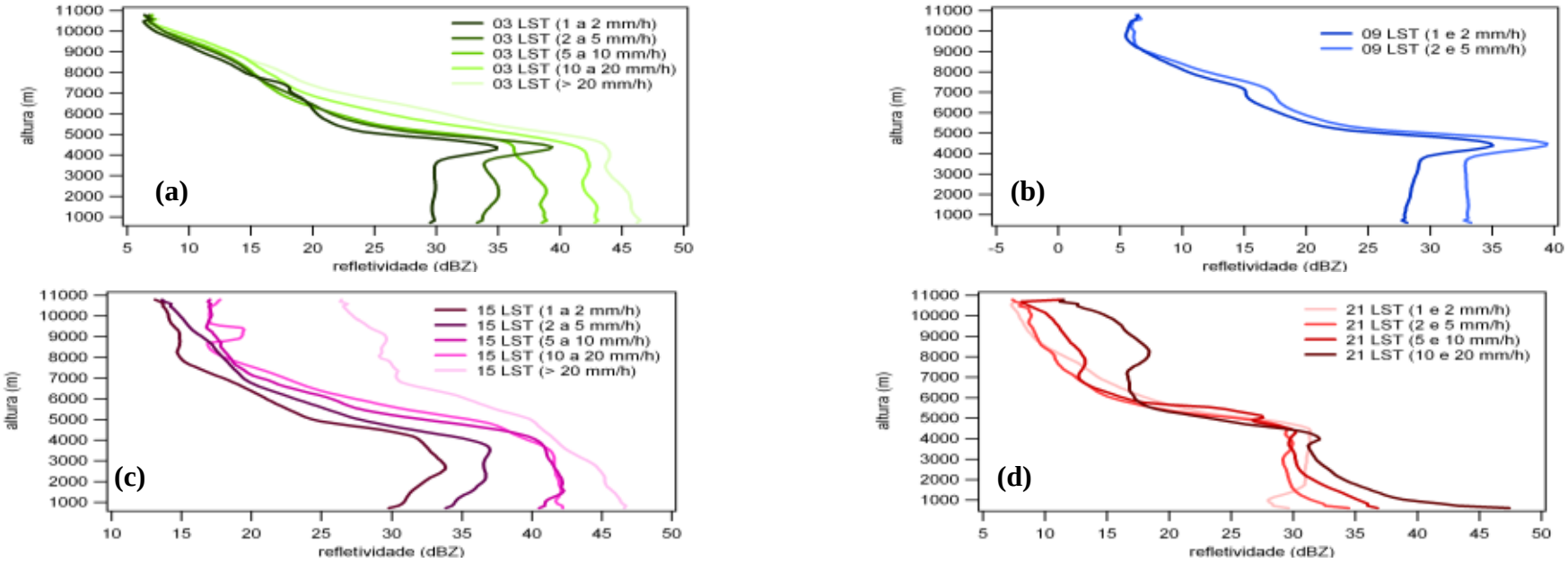

Amazonas Vertical Pointing Radar profiles corresponding to different rainfall intensities and time intervals: (a) 03:00 LST, (b) 09:00 LST, (c) 15:00 LST and (d) 21:00 LST

These reflectivity vertical profiles of Amazonas convective clouds separated by rain rate and local time describe the cloud life cycle. At 15:00 LST convective cloud starts do develop and these are the typical profile of convective cloud initiation (except for the rain rate above 20.0 mm/h). Very few ice formation and maximum liquid water at around the melting layer. The profile with rainfall above 20.0 mm/h or the one later at 21:00 LST (rain rate above 5 mm/h) the ice layer is well developed, this is the mature stage. It is interesting to see the increase of ice content and rainfall, this is the base of passive microwave rainfall estimation over land. At night or early morning the profiles are typical of the stratiform cloud deck in the dissipation phase. The maximum reflectivity pic around the melting layer is a result of the melting ice and is called bright band.

Martins, R.C.G., Machado, L.A.T., Costa, A.A. Characterization of the microphysics of precipitation over Amazon region using radar and disdrometer data. (2010) Atmospheric Research, 96 (2-3), pp. 388-394.

Squal LineBelém - RHI

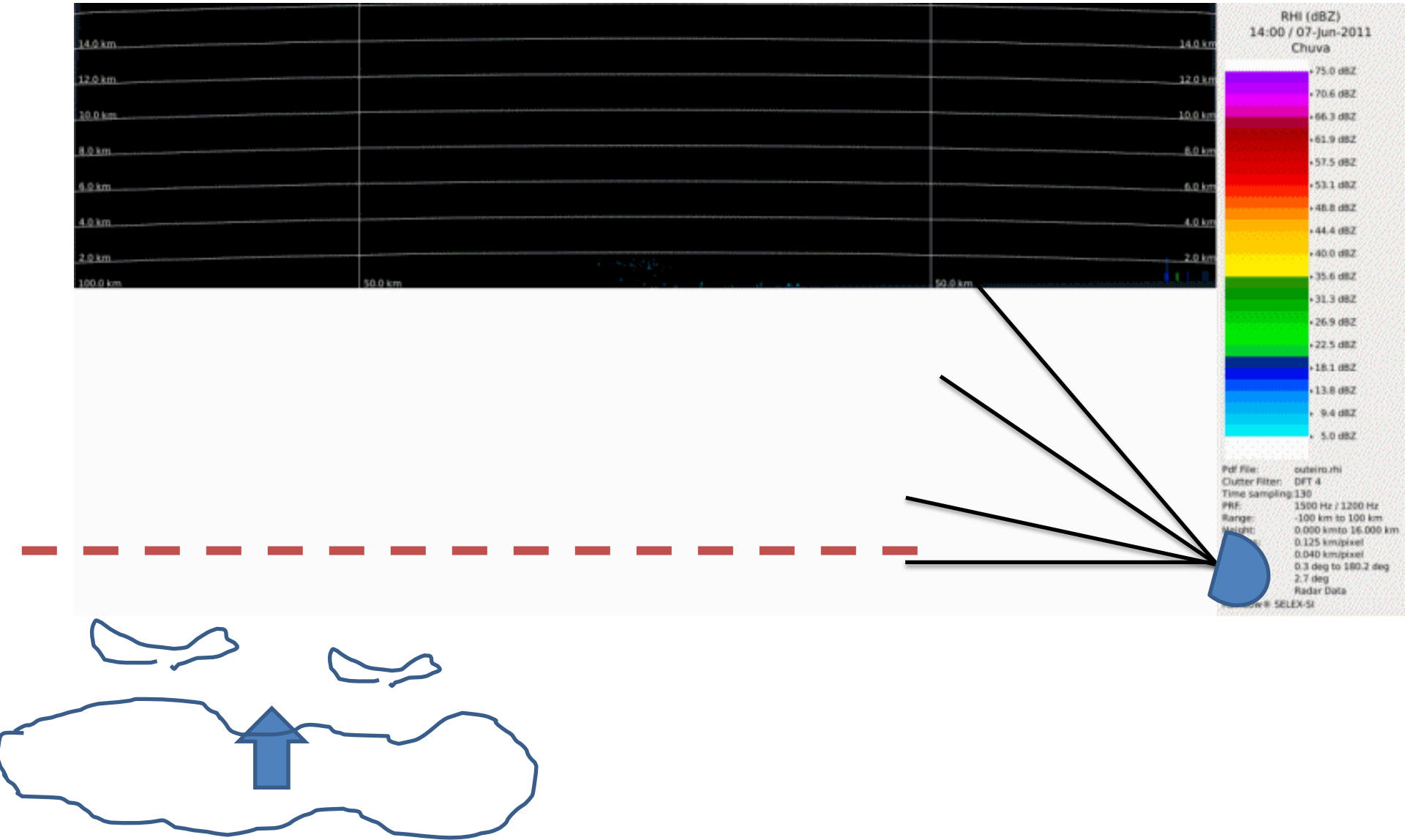

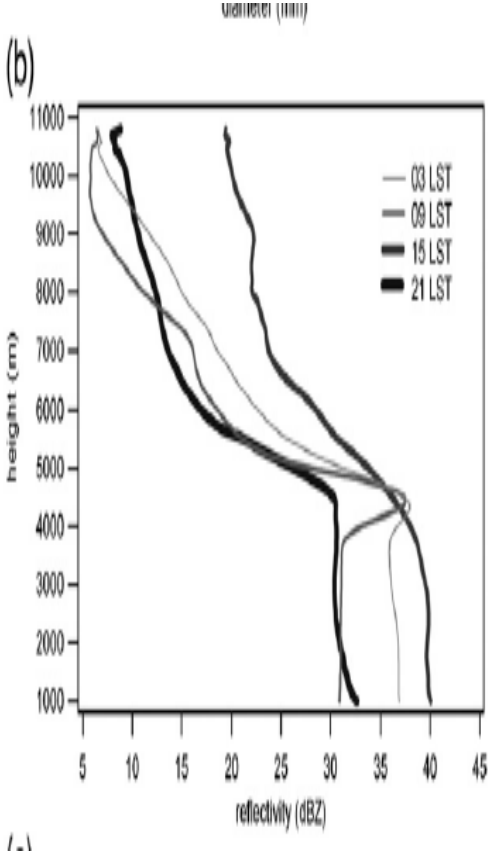

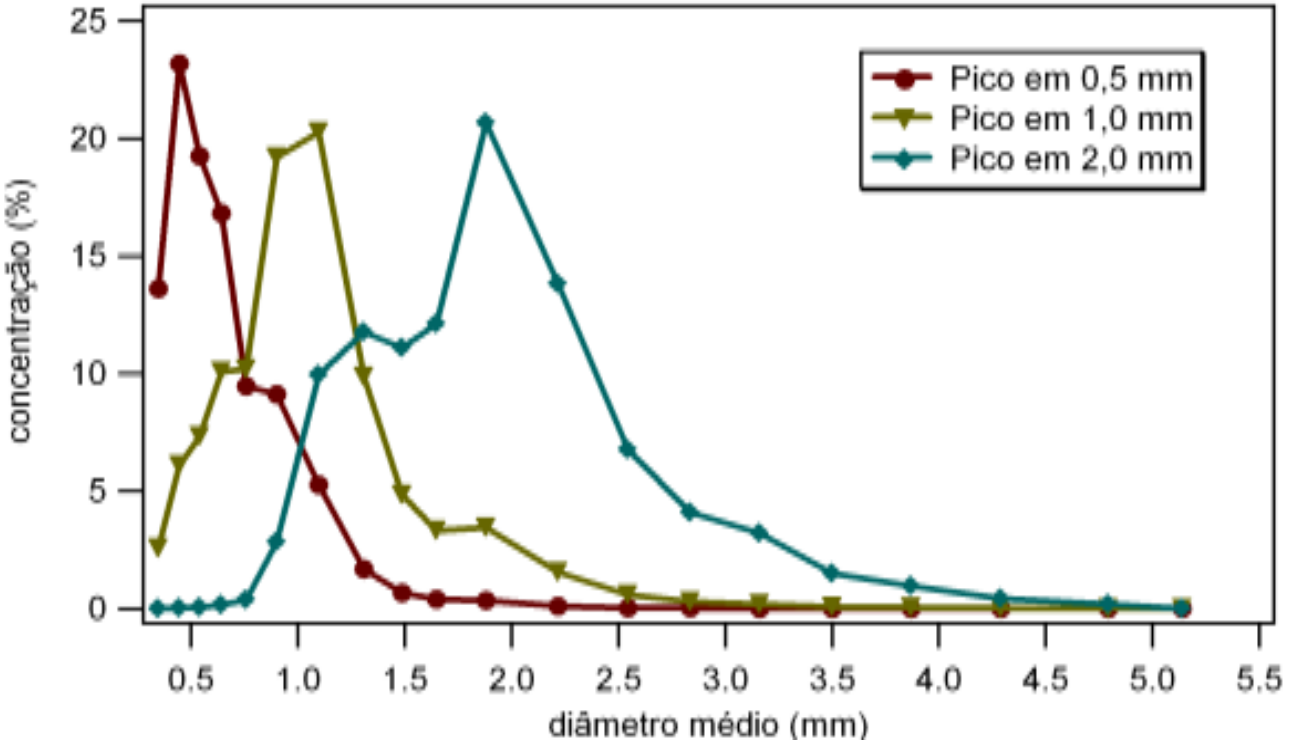

82% of the Amazon (LBA region – wet season) DSD can be explained by these 3 distributions

A physically-based identification of Vertical Profile of Reflectivity

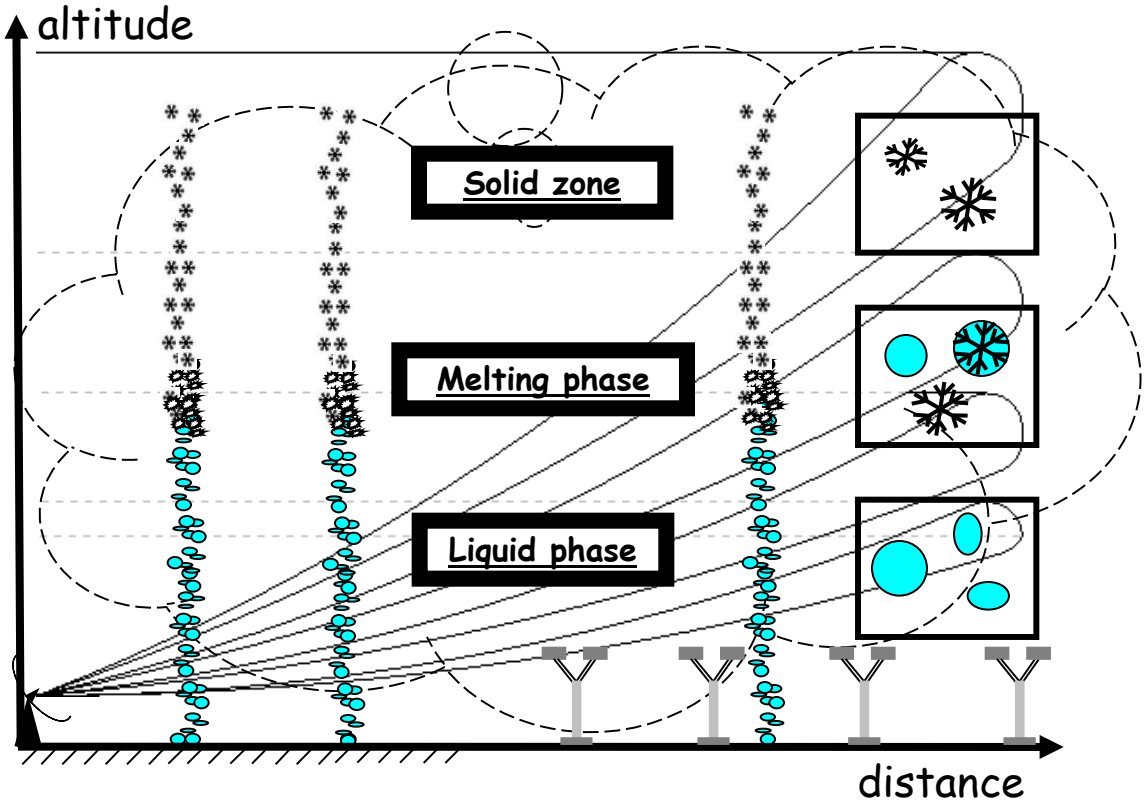

Goal: use radar measurements to retrieve a physically-based representation of the Vertical Profile of Reflectivity and characterize links between physical processes of rainfall at ground and aloft.

Comprehensive ‘Phase Diagram’ for Ice Crystal Habit

(from: Bailey and Hallett (2009)

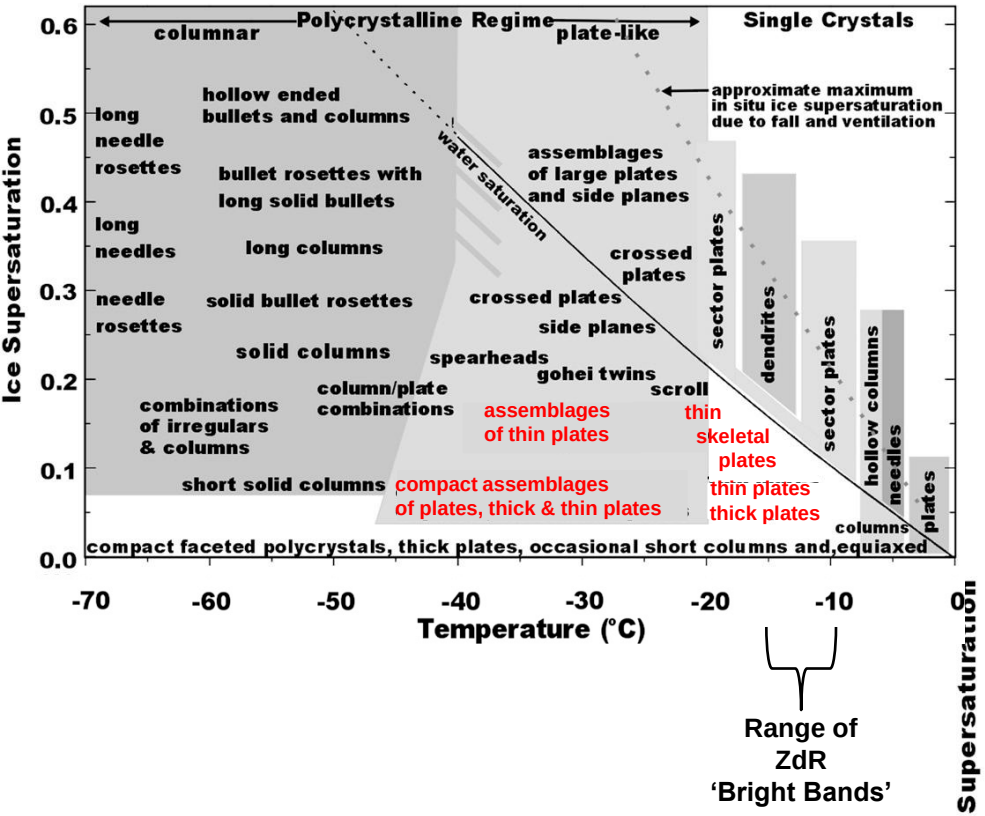

Range of ZdR ‘Bright Bands’

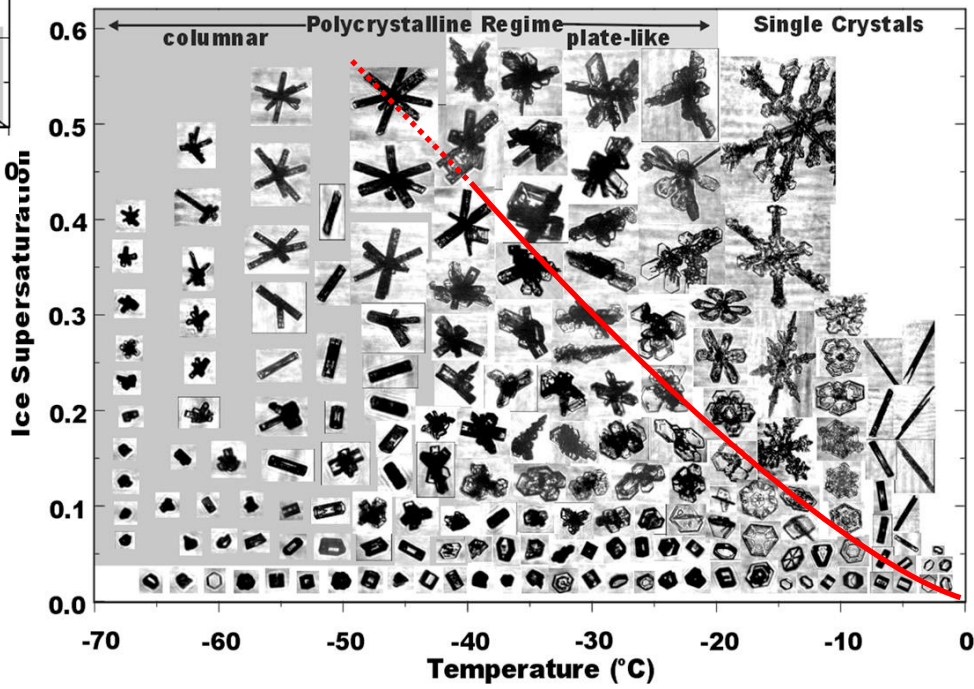

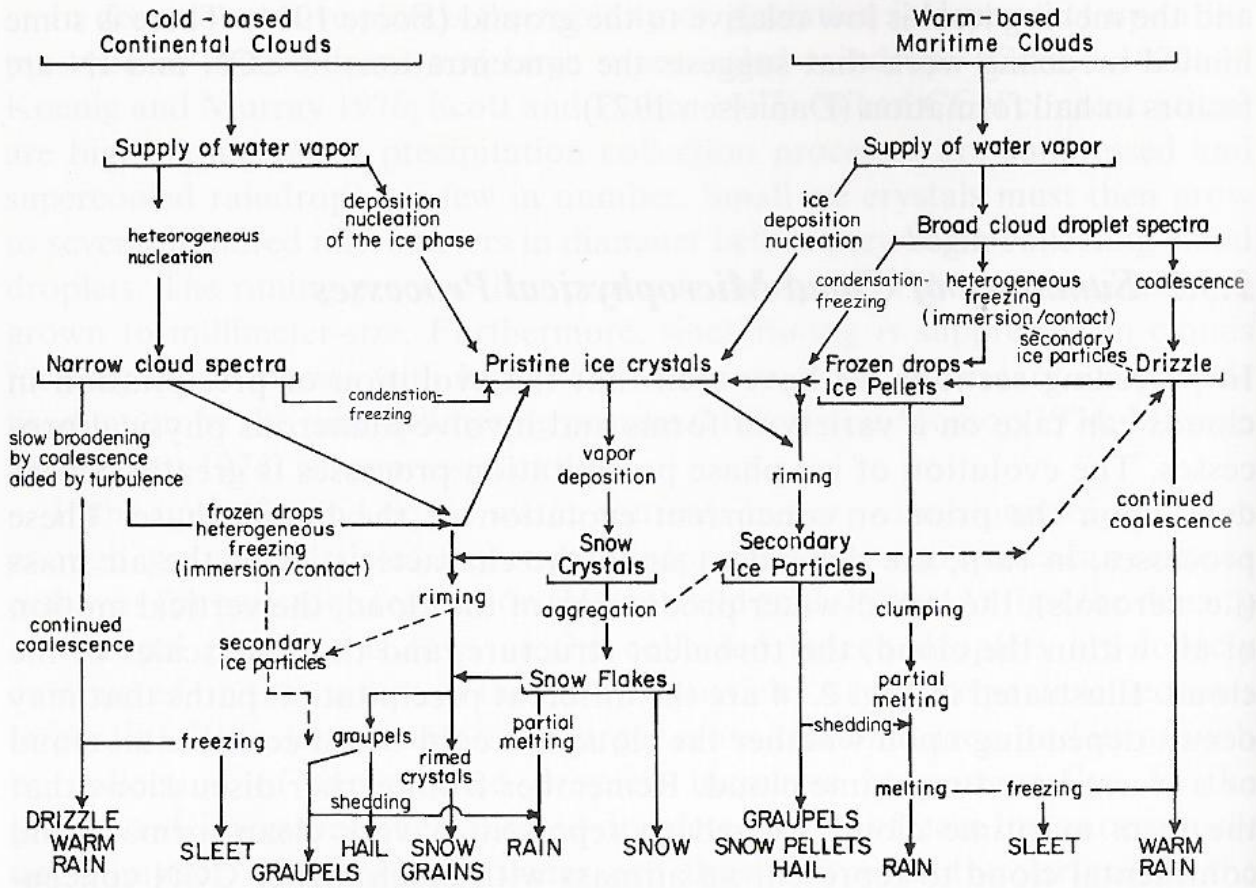

Fig. 2.14 Flow diagram describing microphysical processes, including different paths for precipitation formation. From Cotton and Anthes (1989) with permission of W.R. Cotton

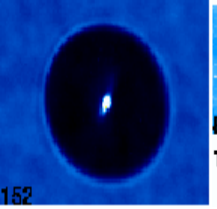

Sphere

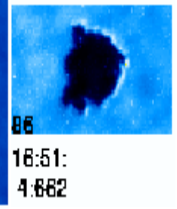

Small Irregular

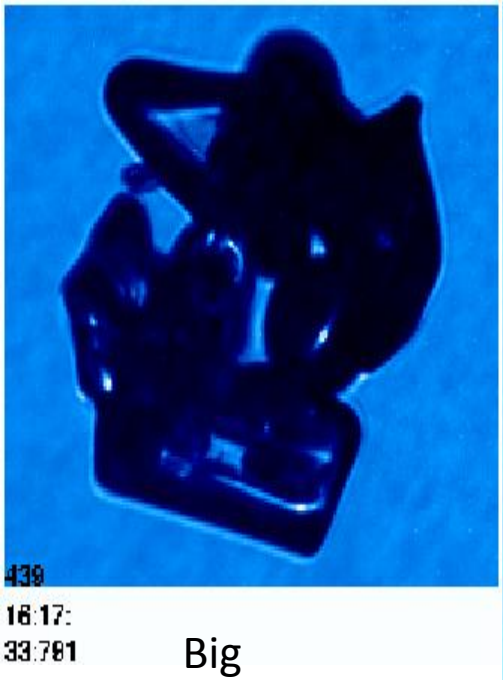

Big Irregular

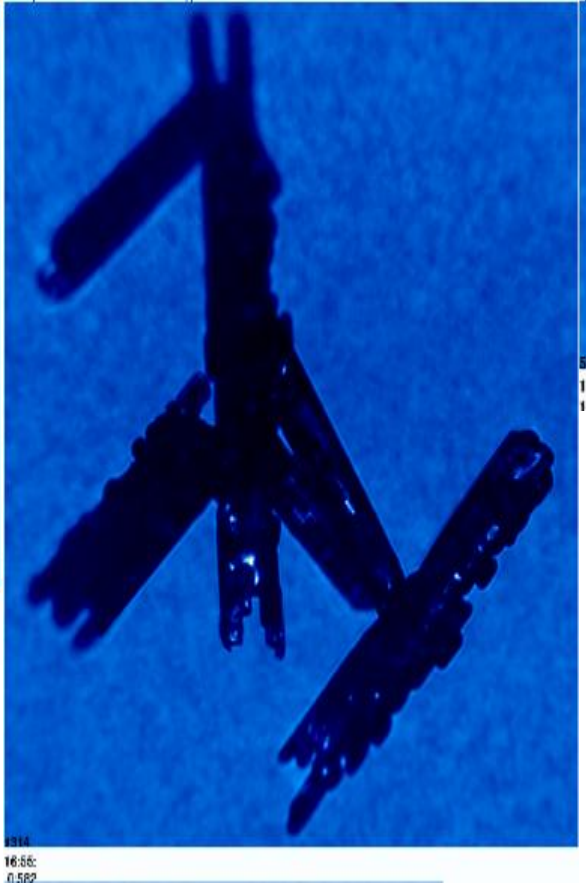

Roset te

Budding Rosette

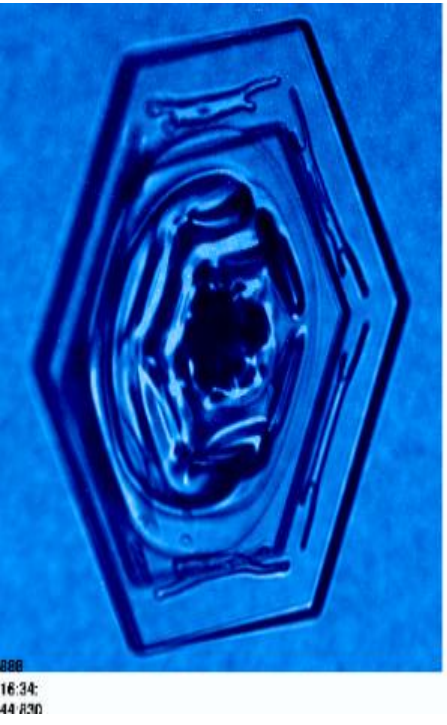

Plate

Column

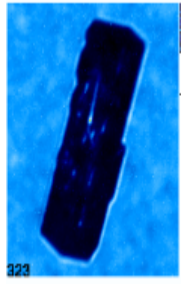

Cristais observados no dia 22/Fev/2014 – nuvens Cu isoladas

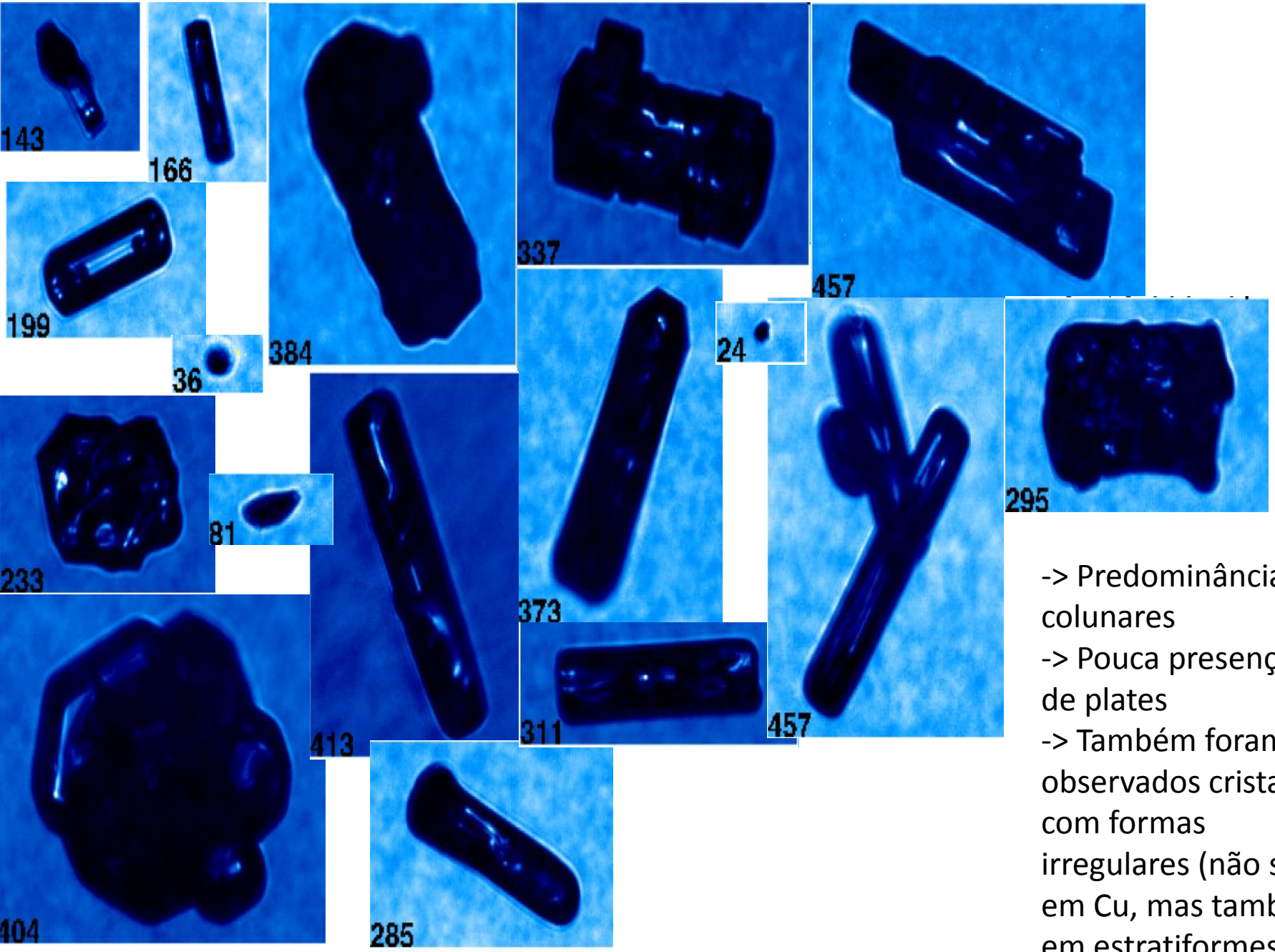

-> Predominância de colunares
-> Pouca presença de plates
-> Também foram observados cristais com formas irregulares (não só em Cu, mas também em estratiformes)

Cristais observados no dia 19/Mar/2014 – Nuvens estratiformes, com chuva desde

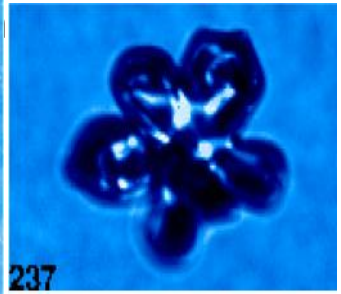

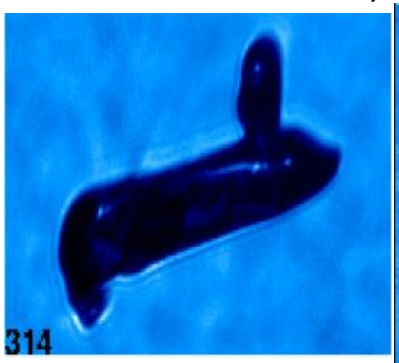

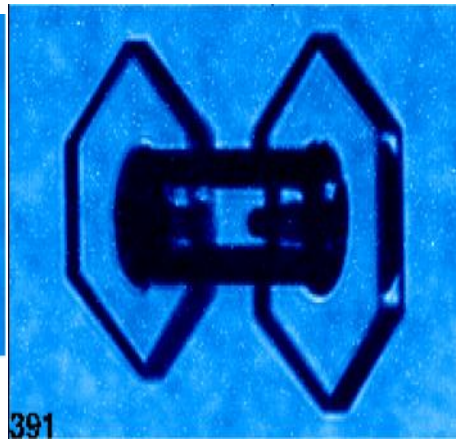

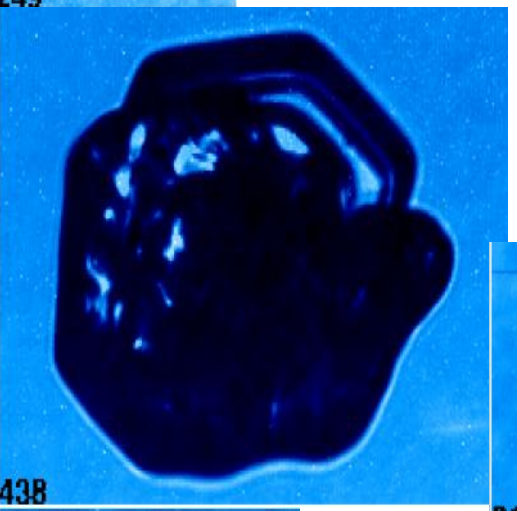

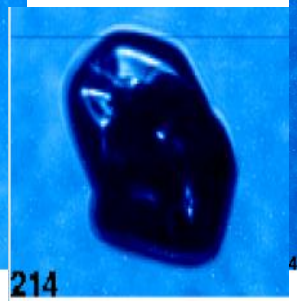

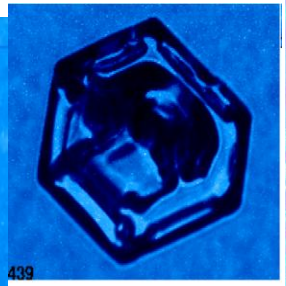

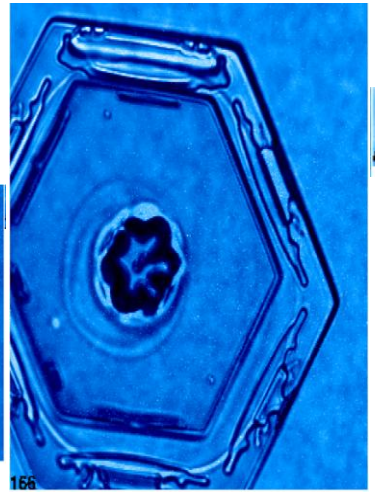

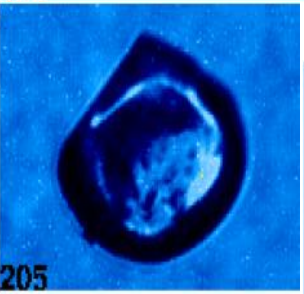

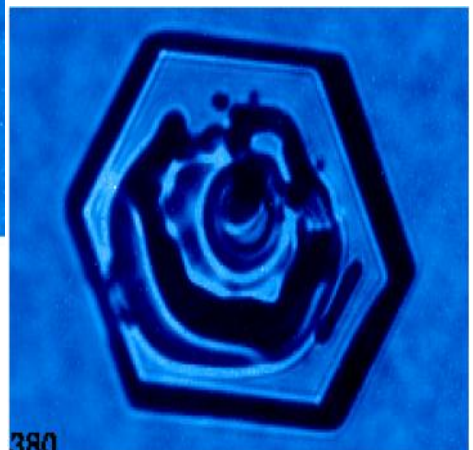

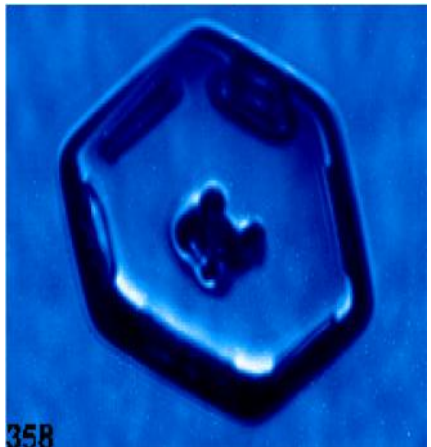

-> Há presença de colunares, mas o regime de crescimento de plates é mais eficiente

-> Casos com crescimento de plates nas extremidades de

2009 08 24, 10:31 UT, 4700 m, 3.2ºC. Max HWLWC=2.45 gm-3. N of Bareilly.
No rain.

Daniel Rosenfeld

2009 08 24, 10:29 UT, 5530 m, -1.6ºC. Max HWLWC=2.91 gm-3. N of Bareilly.
The cloud had isolated small rain drops.

Daniel Rosenfeld

2009 08 24, 10:24 UT, 6270 m, -4.8ºC. Max HWLWC=1.05 gm-3. N of Bareilly. Some small rain drops were at the edge of the cloud.

Daniel Rosenfeld

2009 08 24, 10:14 UT, 6720 m, -8.1ºC. Max HWLWC=1.66 gm-3. N of Bareilly.
The cloud has supercooled rain drops.

Daniel Rosenfeld

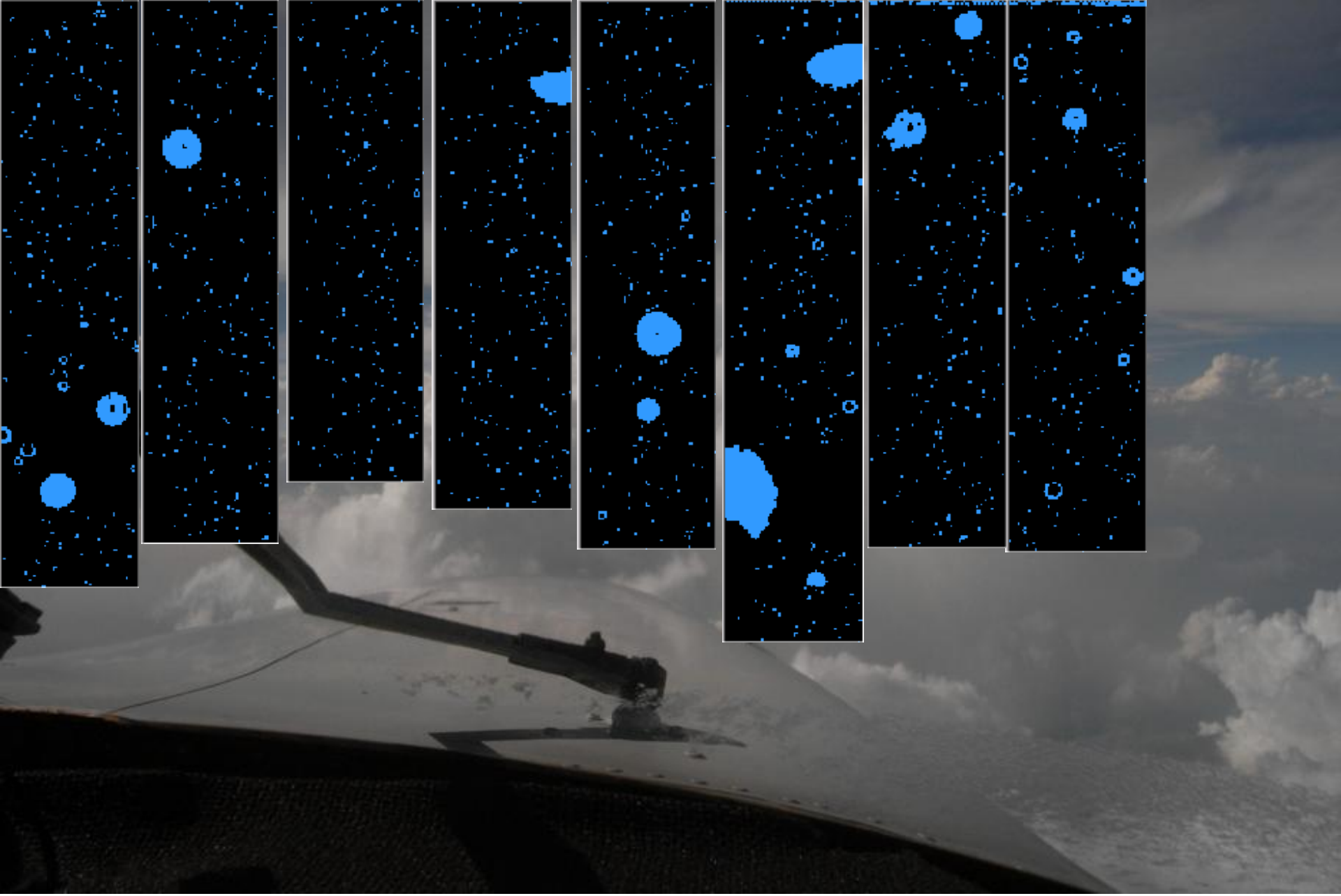

2009 08 24, 10:03 UT, 7350 m, -11.8ºC. Max HWLWC=0.87 gm-3. N of Bareilly.
The cloud has small raindrops and larger freezing rain drops.

Daniel Rosenfeld

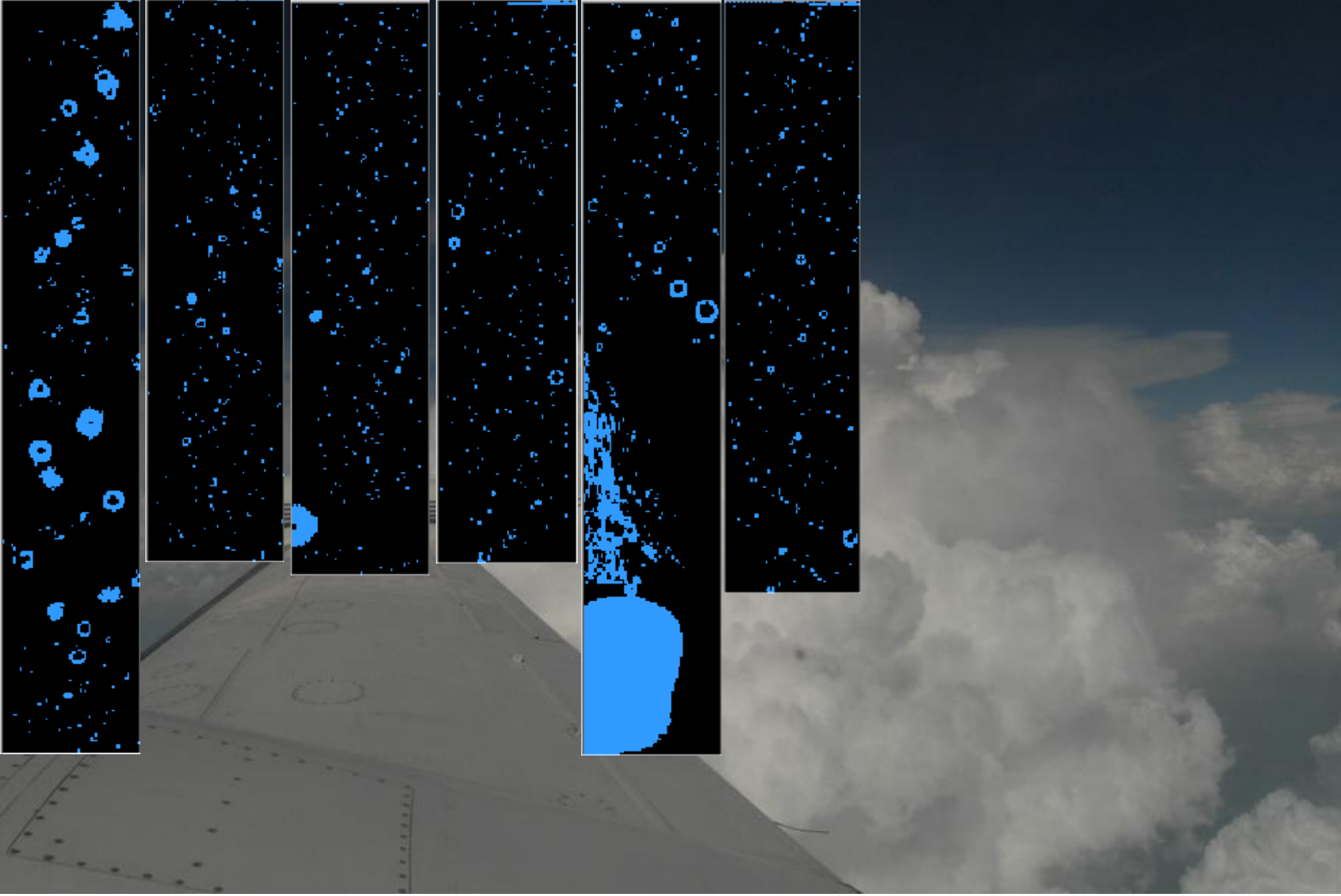

2009 08 24, 10:00 UT, 7700 m, -14.7ºC. Max HWLWC=1.45 gm-3. N of Bareilly.
The cloud has small rain drops, large freezing rain drops and small graupel.

2009 08 24, 9:57 UT, 8130 m, -17.1ºC. Max HWLWC=0.49 gm-3. N of Bareilly.
The cloud is glaciating, with frozen rain drops, small graupel and ice crystals.

Daniel Rosenfeld

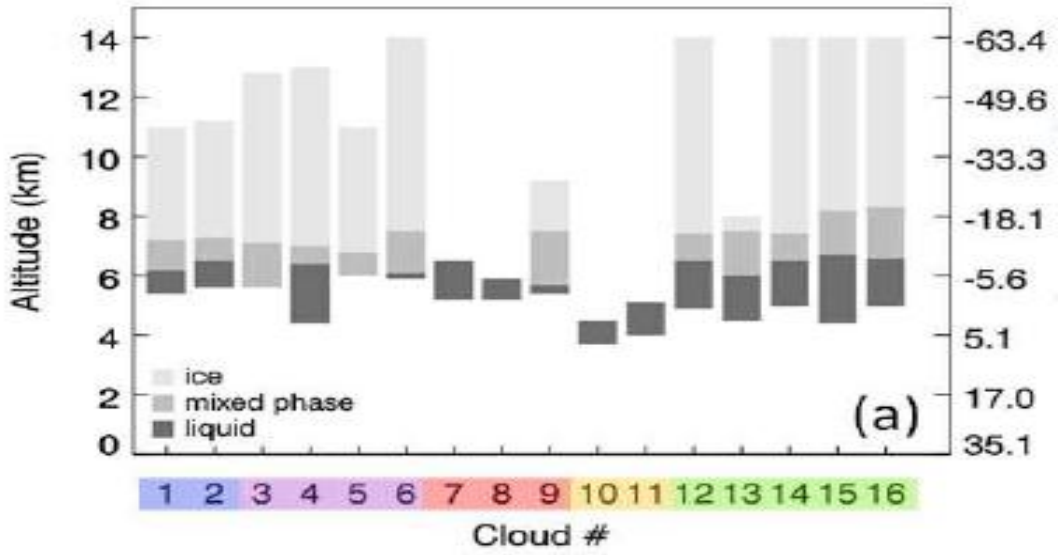

Vertical distribution of the phase state of particles in tropical deep-convective clouds as derived from cloud-side reflected solar radiation measurements. Evelyn Jäkel1, Manfred Wendisch1, Trismono C. Krisna1, Florian Ewald2,3, Tobias Kölling2, Tina Jurkat3, Christiane Voigt3, Micael A. Cecchini4, Luiz A. T. Machado, Armin Afchine5, Anja Costa5, Martina Krämer5, Meinrat O. Andreae6,7, Ulrich Pöschl6, Daniel Rosenfeld8, and Tianle Yuan. ACPD 2017

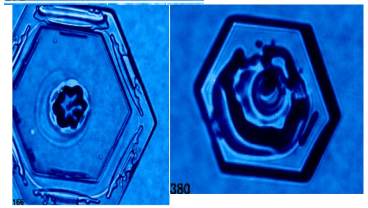

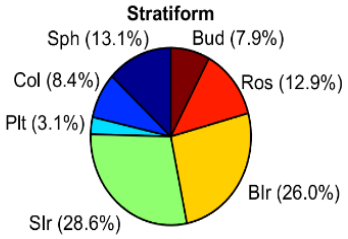

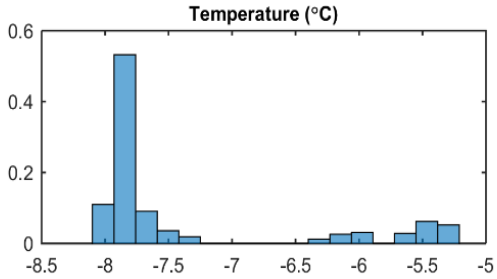

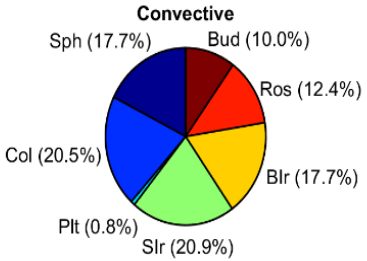

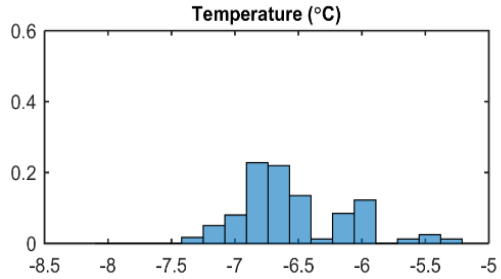

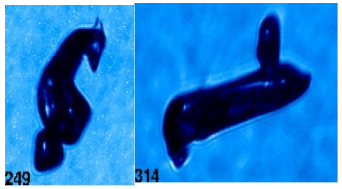

Frequency of occurrence of different ice crystals types for stratiform and convective clouds near Manaus. Histograms show the respective dispersion of the temperature of the measurements. Crystal types considered are: 1) Sph: spheroids, 2) Col: columns, 3) Plt: plates, 4) Sir: small irregular (<200µm), 5) Blr: big irregular (>200µm), 6) Ros: rosette and 7) Bud: budding rosette. You may also want to include some of the actual images of the crystals that were observed under diferente conditions.

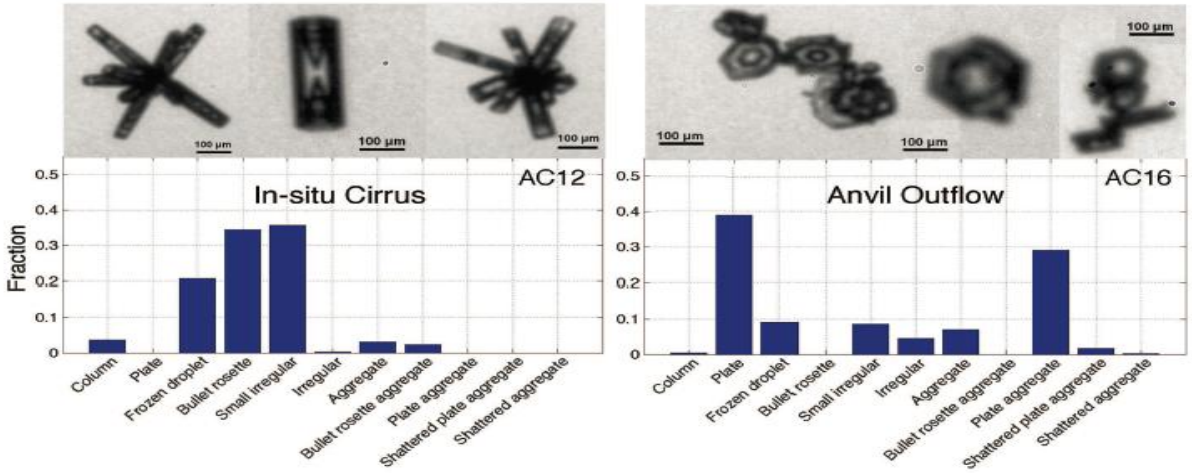

932 FIG. 14. Statistical analysis of the ice microphysical properties of ambient in–situ cirrus sampled during flight
933 AC12 and of an anvil outflow of a tropical convective system sampled during flight AC16. The analysis is based
934 on stereoscopic images taken by the PHIPS–HALO probe, which was newly developed for HALO.

The ACRIDICON–CHUVA campaign to study tropical deep convective clouds and precipitation using the new German research aircraft HALO by Manfred Wendisch, Ulrich P¨oschl, Meinrat O. Andreae , Luiz A. T. Machado , Rachel Albrecht, Hans Schlager k, Daniel Rosenfeld et al. - Bulletin of American Met. Soc. 2016

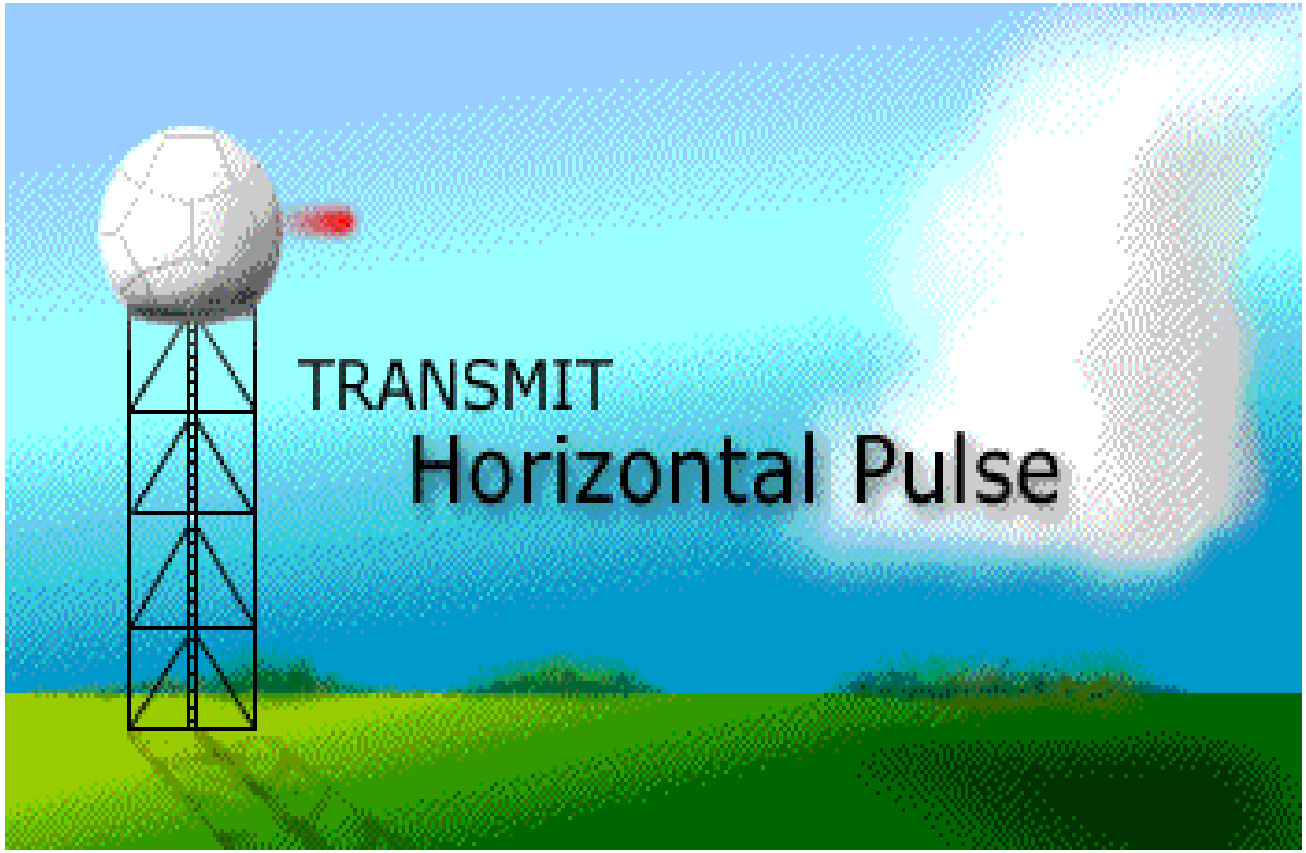
TRANSMIT
Horizontal Pulse

graupel

granizo

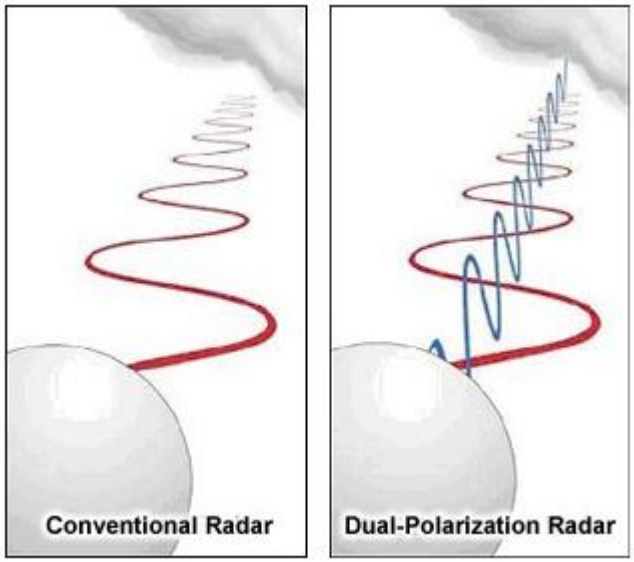

NOAA

Neve

$$Z = \sum_{i=1}^{n} D_i^6$$

Zdr= ZH/Zv

Chuva – contribuição a Modelagem

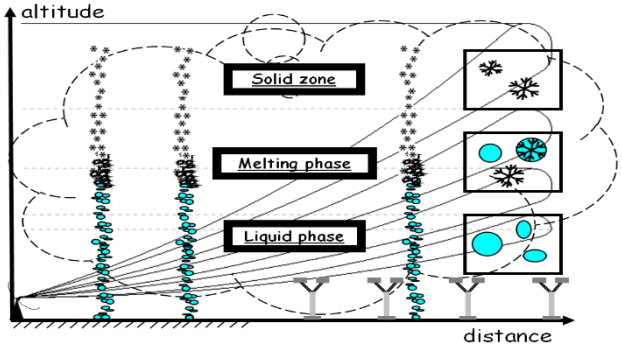

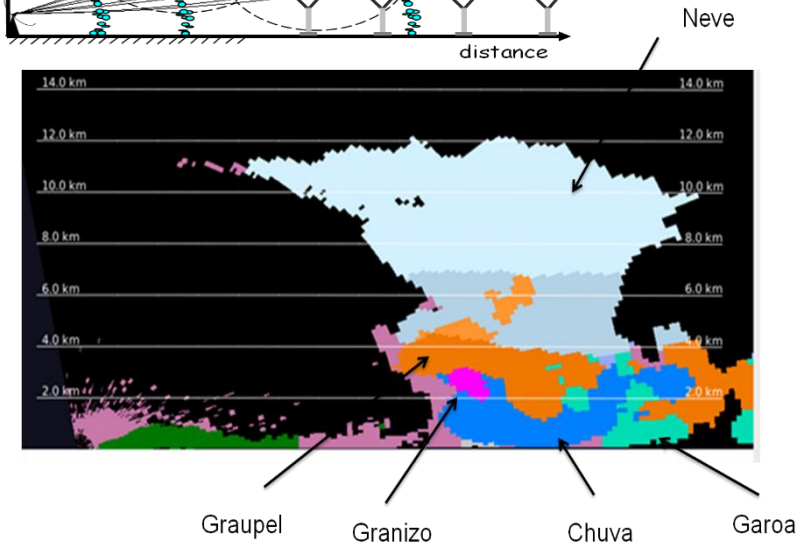

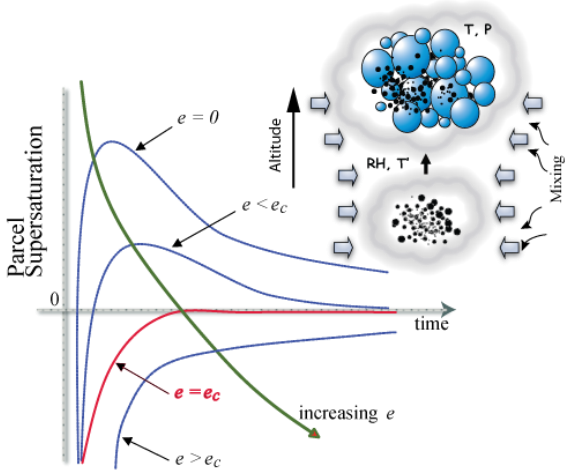

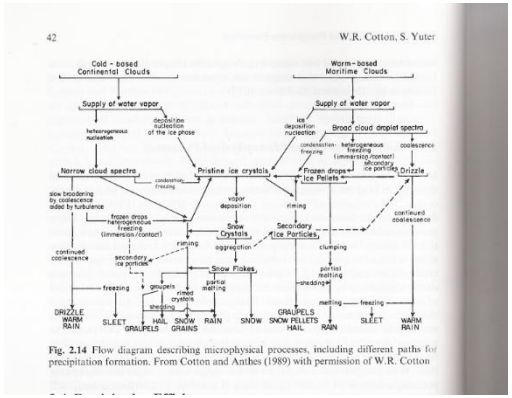

Fig. 2.14 Flow diagram describing microphysical processes, including different paths for precipitation formation. From Cotton and Anthes (1989) with permission of W.R. Cotton

:

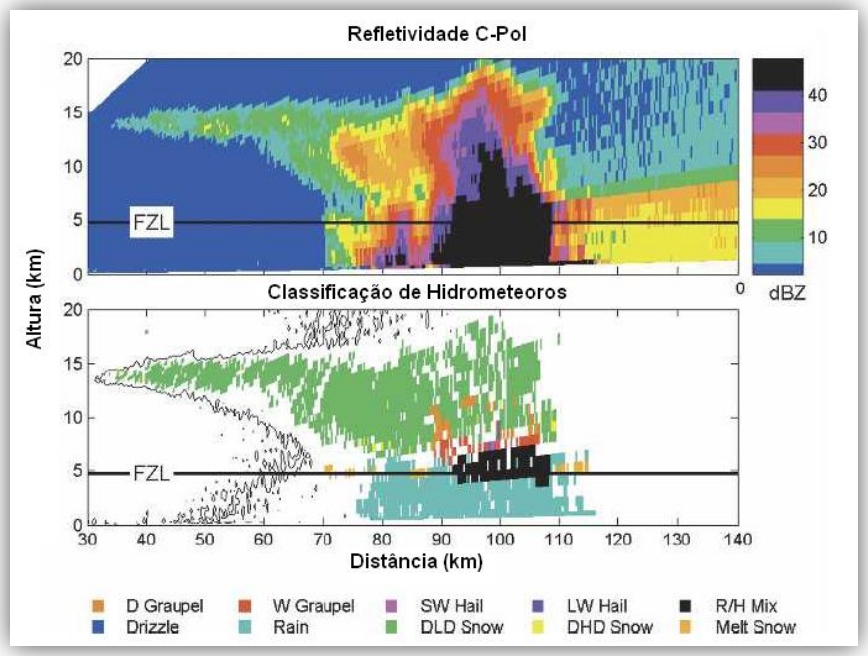

Coeficiente de correlação transversal mudança de fase diferencial

	Z_{HH} (dBZ)	Z_{DR} (dB)	$\rho_{HV}(0)$	K_{DP} (deg km^{-1})	Temperature (°C)
Drizzle	10-25	0.2 to 0.7	>0.97	0 to 0.06	>-10
Rain	25 to 60	0.5 to 4	>0.95	0 to 20	>-10
Snow (dry, low density)	-10 to 35	-0.5 to 0.5	>0.95	-1 to 1	< 0
Snow* (dry, high density)	-10 to 35	0.0 to 1	>0.95	0 to 0.4	<0
Snow (wet, melting)	20 to 45	0.5 to 3	0.5 to 0.9	0 to 1	0 to 5
Graupel, dry	20 to 35	-0.5 to 1	>0.95	0 to 1	<0
Graupel, wet	30 to 50	-0.5 to 2	>0.95	0 to 3	-15 to 5
Hail, small < 2 cm wet	50 to 60	-0.5 to 0.5	0.92 to 0.95	-1 to 1	-15 to 20
Hail, large > 2 cm wet	55 to 65	-1 to 0.5	0.90 to 0.92	-1 to 2	-25 to 20
Rain and hail	45 to 80	-1 to 6	>0.9	0 to 20	-10 to 25

Hydrometeor Classification – Amazon Stratiform Cloud

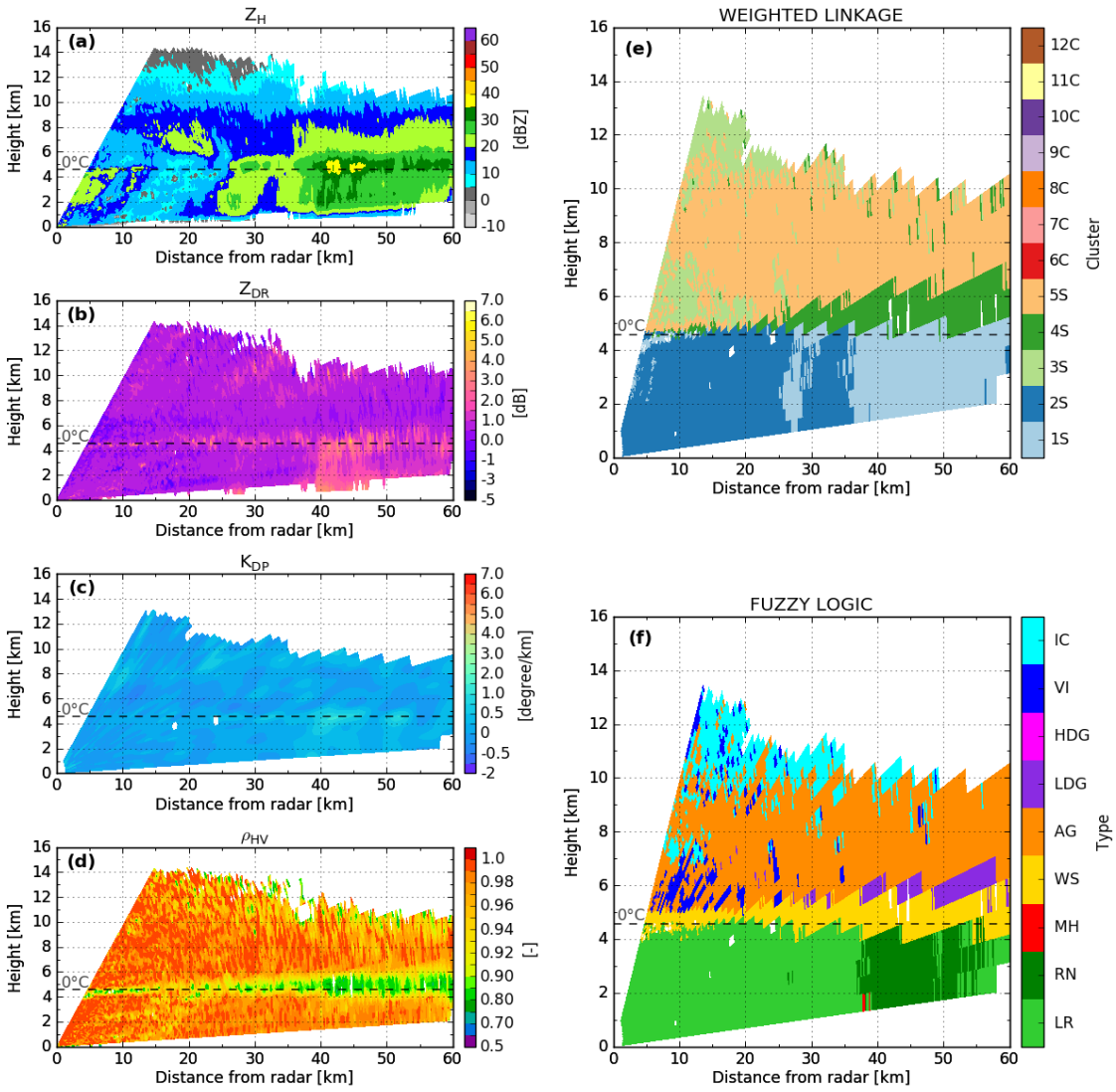

Ribaud, J.-F., Machado, L. A. T., and Biscaro, T.: X-band dual-polarization radar-based hydrometeor classification for Brazilian tropical precipitation systems, Atmos. Meas. Tech., 12, 811-837, https://doi.org/10.5194/amt-12-811-2019, 2019.

Hydrometeor Classification – Amazon Convective Cloud

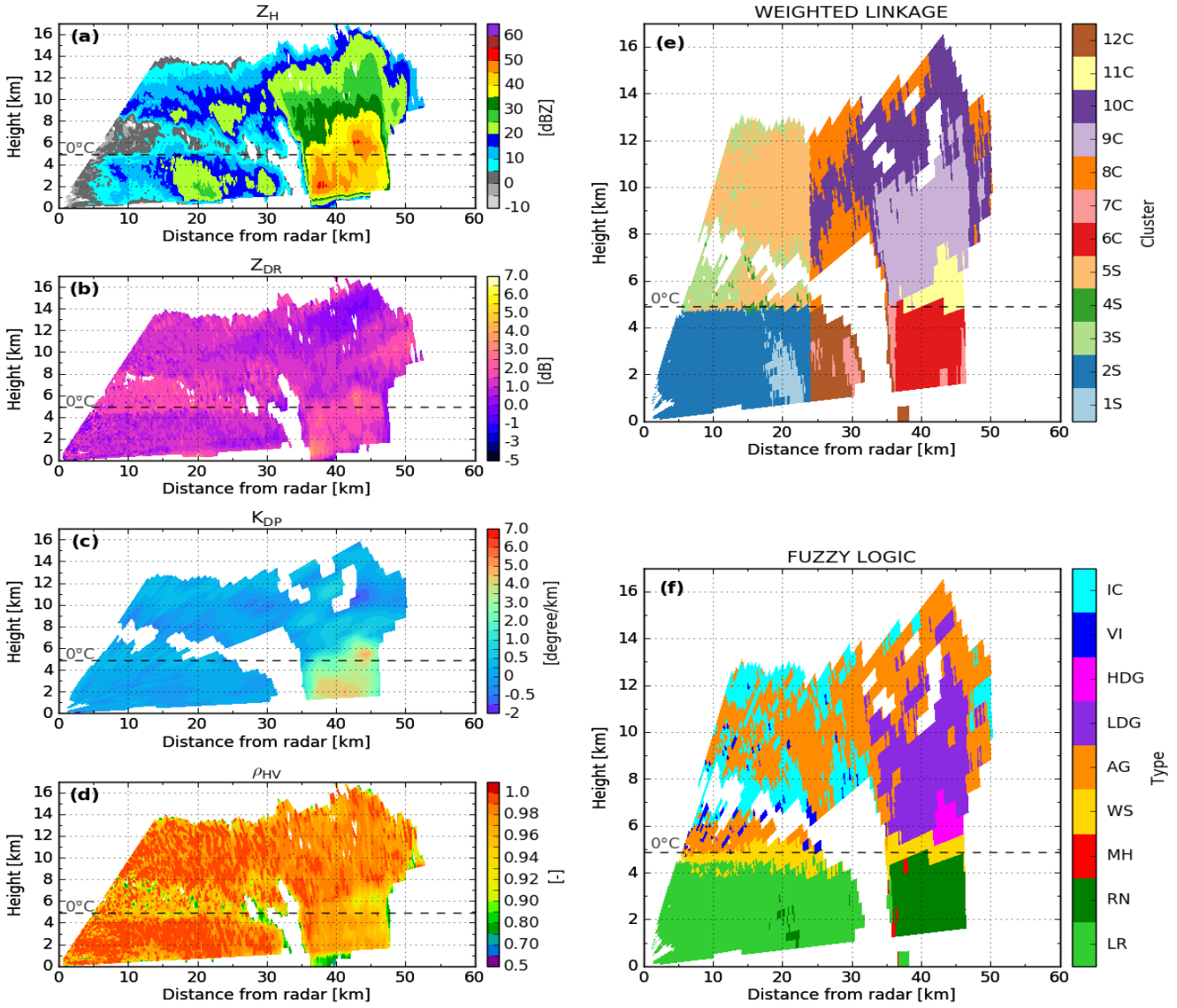

*Violin plot of cluster outputs retrieved for the **stratiform regime of the wet season** (DZ: drizzle, RN: rain, WS: wet snow, AG: aggregates, IC: ice crystals).*

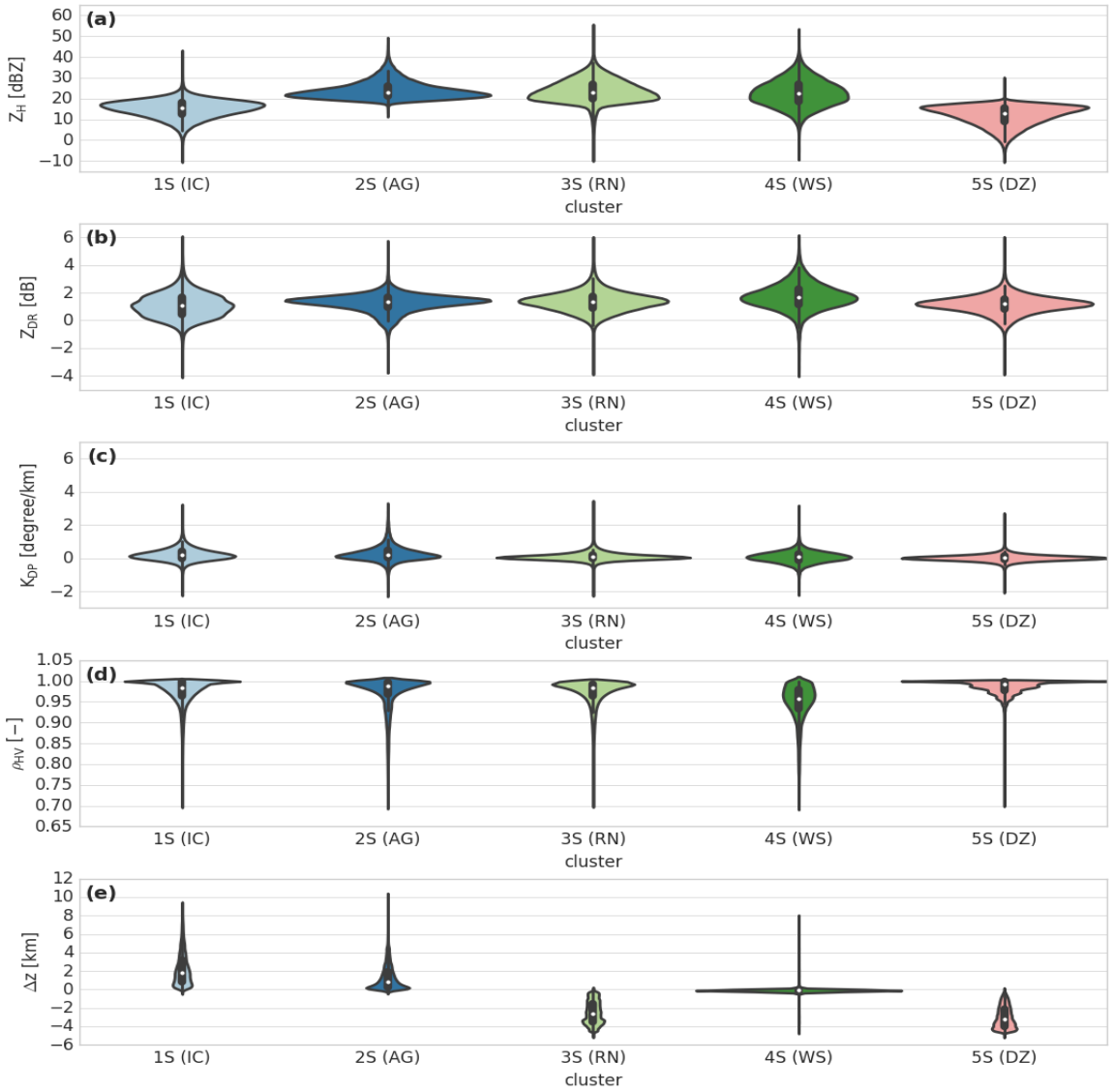

Violin plot of cluster outputs retrieved for the ***convective regime of the wet season***

LR: light rain, MR: moderate rain, HR: heavy rain, GR: graupel, AG: aggregates, IC: ice crystals

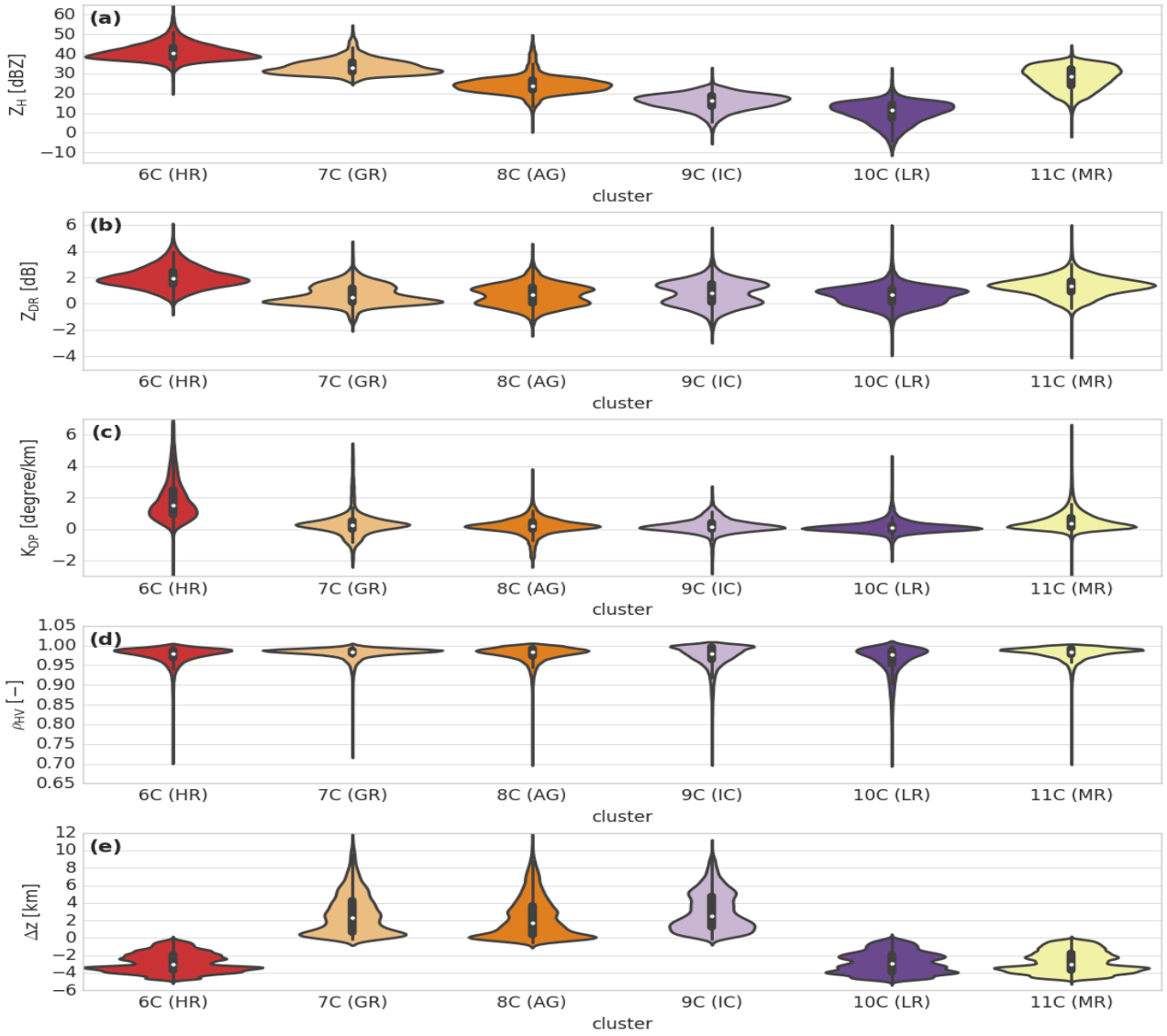

Amazon Wet and Dry Season Hydrometeor Differences – Stratiform and Convective Clouds

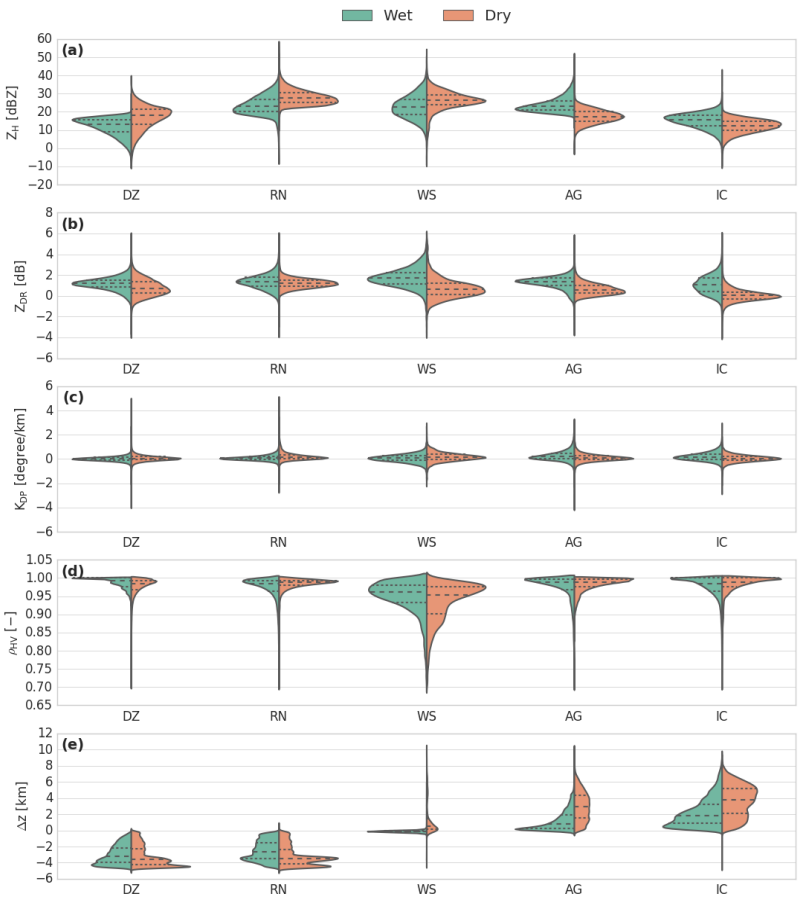

Violin plot comparison of pairs of stratiform hydrometeor types between the wet and dry seasons (DZ: drizzle, RN: rain, WS: wet snow, AG: aggregates, and IC: ice crystals).

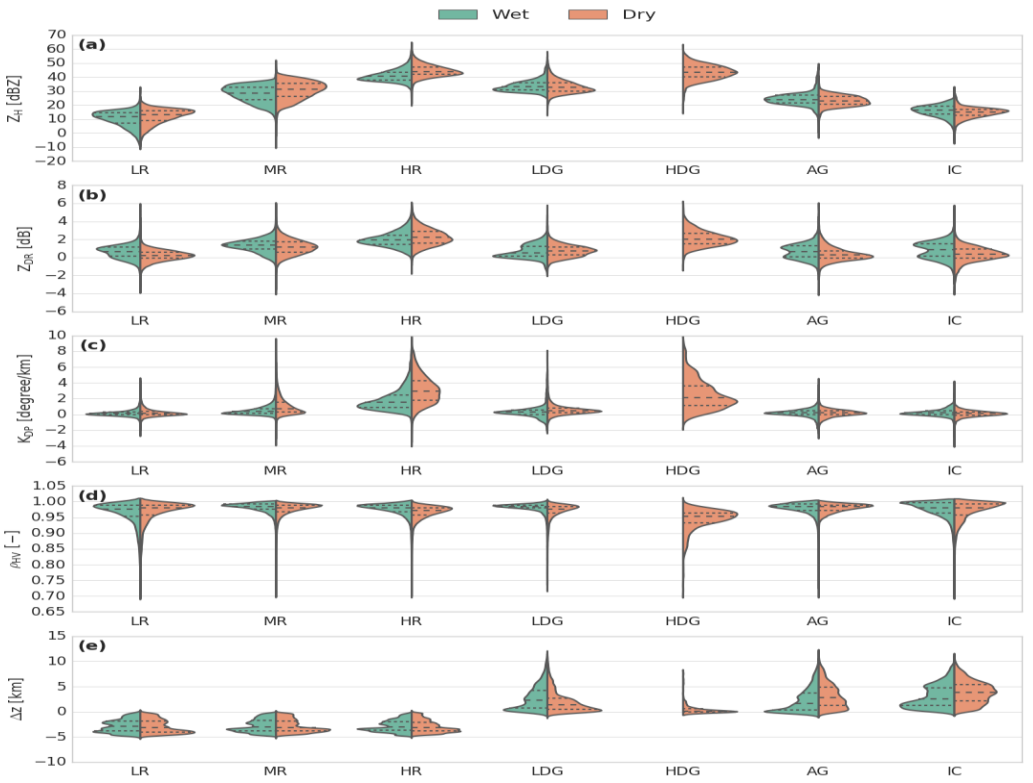

Violin plot comparison of pairs for the convective precipitation regime (LR: light rain, MR: moderate rain, HR: heavy rain, LDG: low-density graupel, HDG: high-density graupel, AG: aggregates, and IC: ice crystals).

São Borja Downburst – Severe Hail and Winds – November 2019 – RELAMPAGO Field Campaign

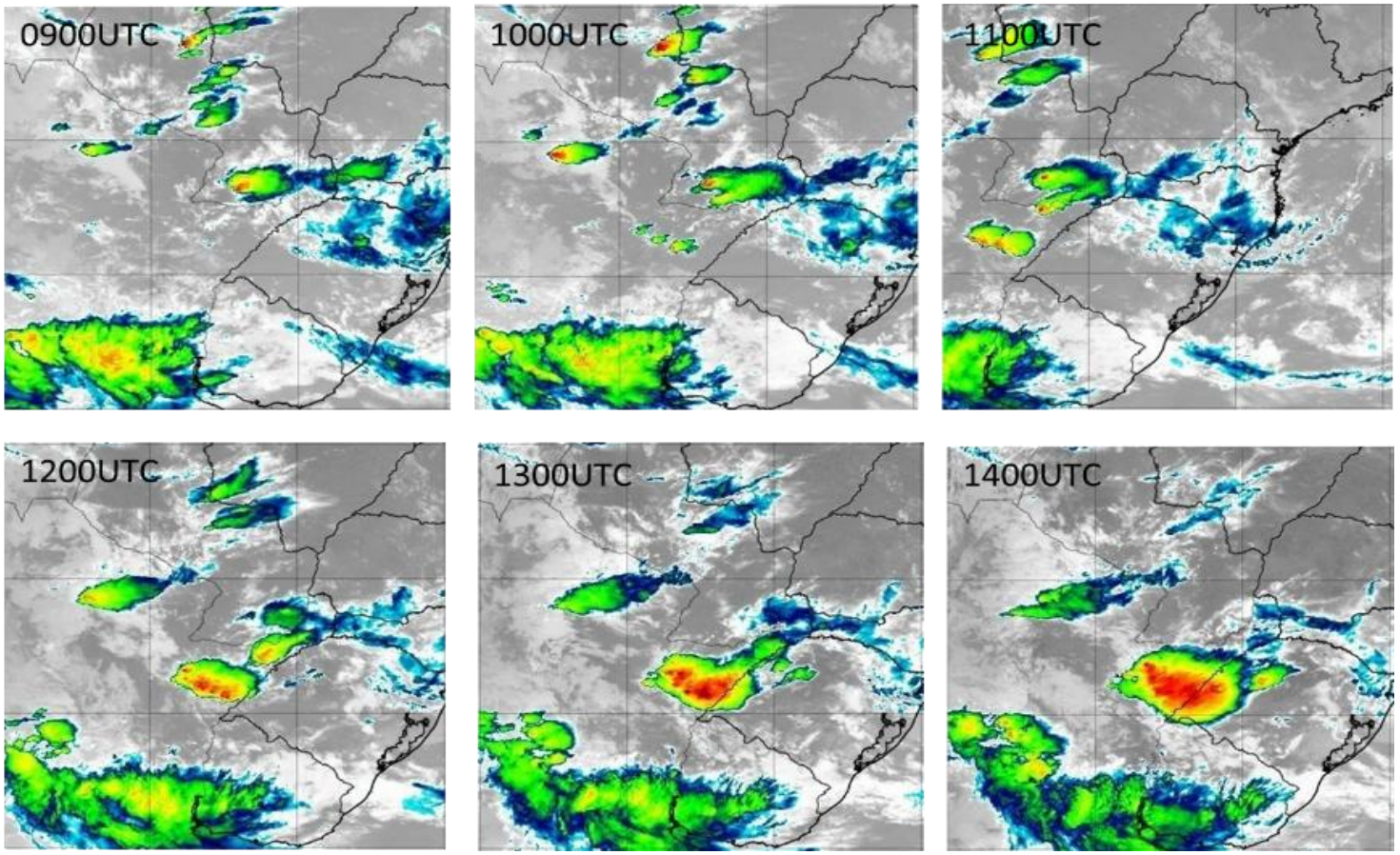

São Borja Downburst – Severe Hail and Winds – November 2019 – RELAMPAGO Field Campaign

The downburst occurred during RELAMPAGO in São Borja (SOS-CHUVA measurements) showed a change in VIL (Vertical Integrated Liquid water) from 235 kg/m^2 to 105 kg/m^2 in 10 minutes. Is hail evaporation the main feature of this physical process? This 130 kg/m2 of water drop in 10 minutes is too high to be explained by small hail evaporation. The only reasonable explanation for this 1.5 million tons of water fall in 10 minutes over 2000 km radius area is the cloud collapse.

São Borja Downburst – Severe Hail and Winds – November 2019 – RELAMPAGO Field Campaign

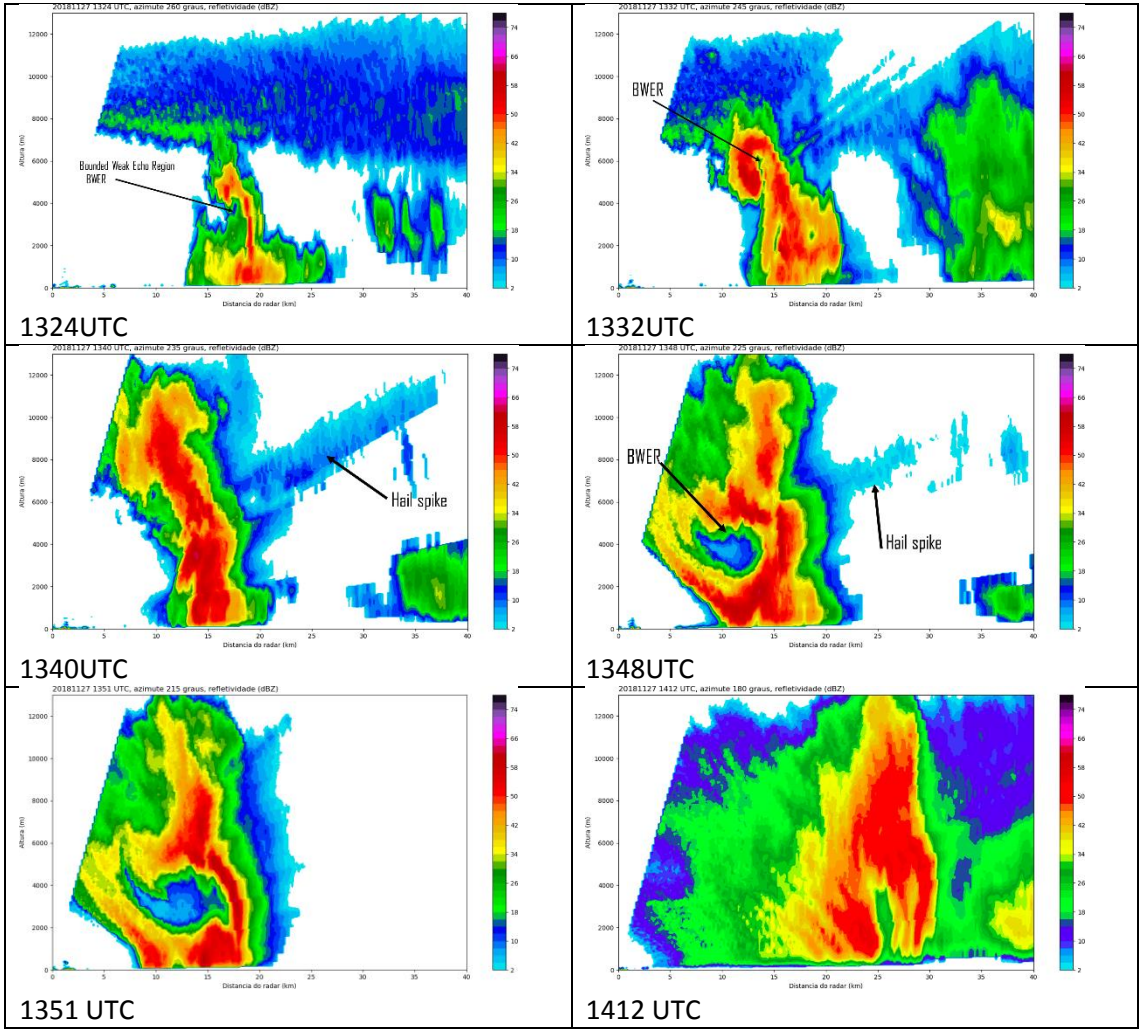

Bounded Weak Echo Region (BWER),

São Borja Downburst – Severe Hail and Winds – November 2019 – RELAMPAGO Field Campaign

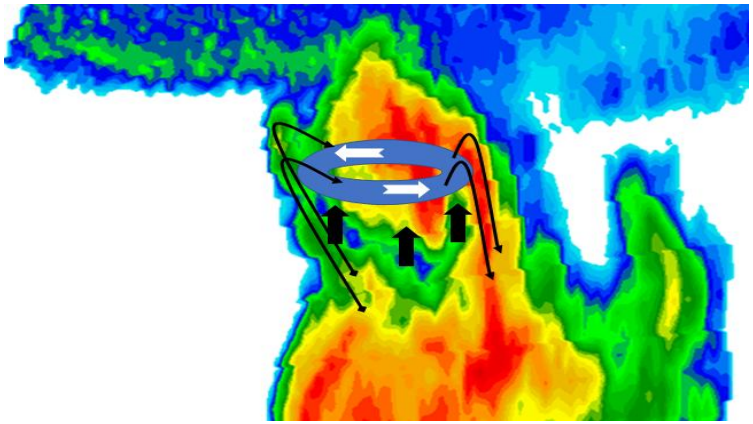

Figure V.1: Conceptual model of the mesocyclone above the layer of strong vertical motion.

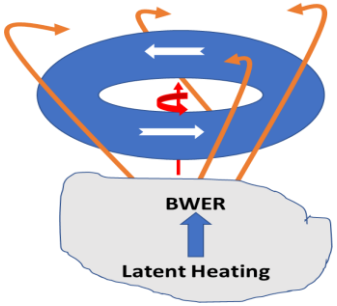

Figure V.2: Schematic view of the mesocyclone circulation supported by the BWER.

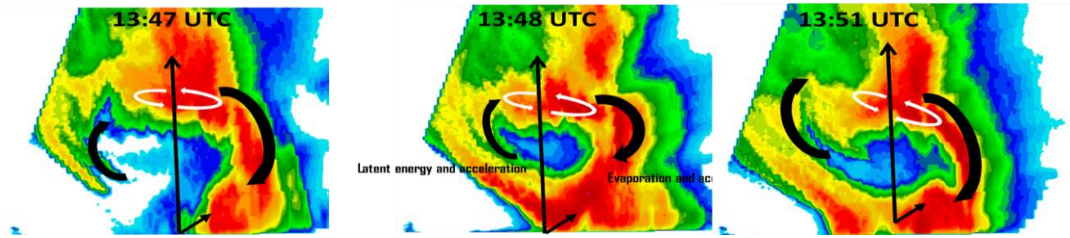

Figure V.3: Sequence of RHI just before the downburst.

A Modelagem - convecção seca

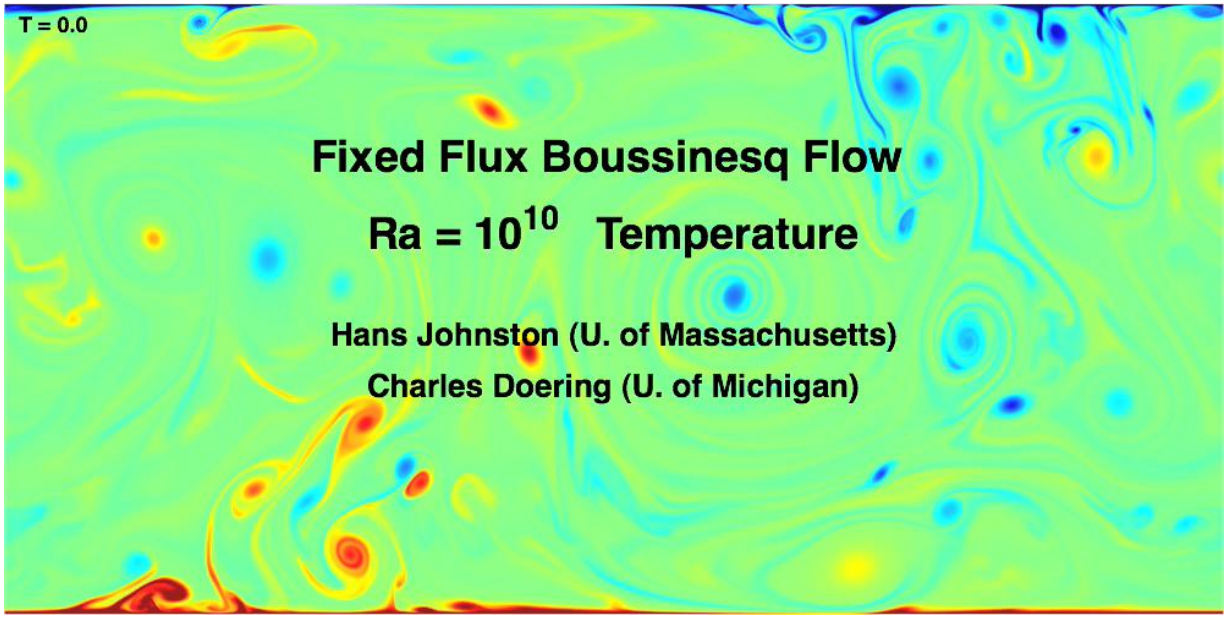

A convecção seca

Rayleigh Bernard Convection and the Lorenz System

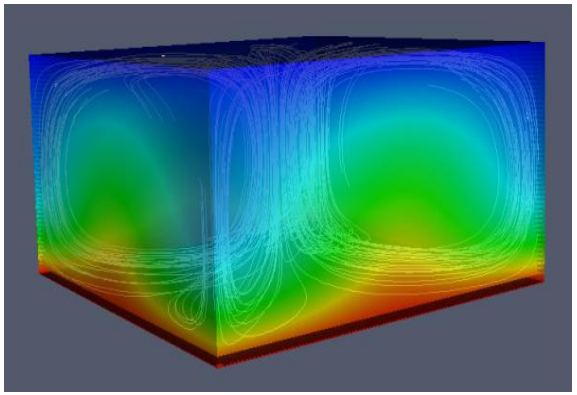

Bénard Cells as seen by Meteosat-7

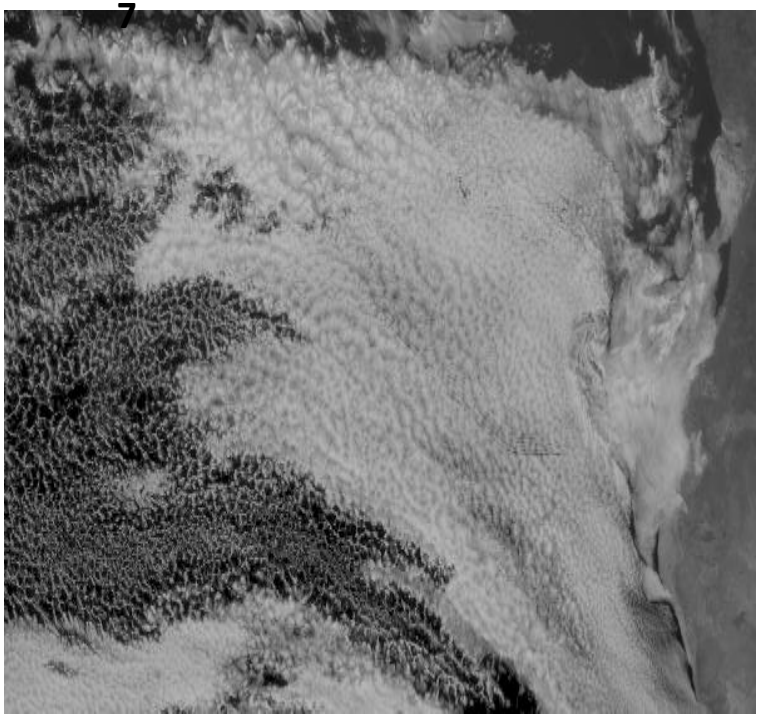

Convecção úmida

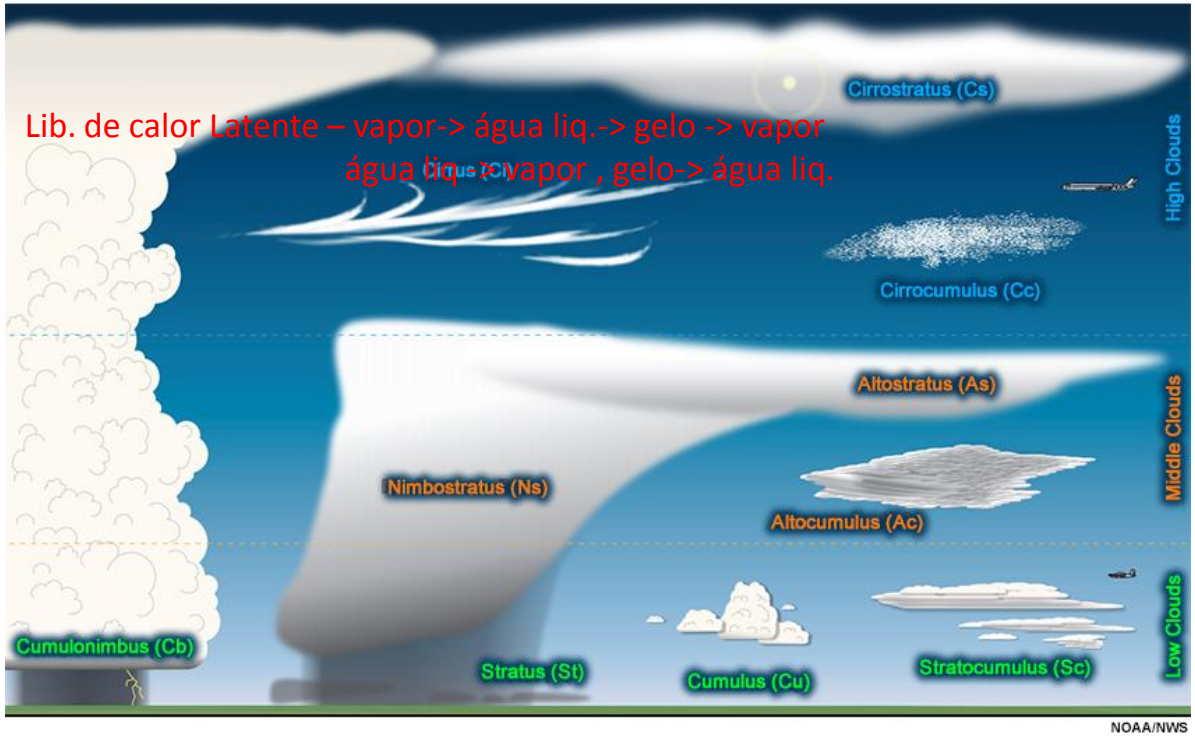

Water cycle in warm clouds

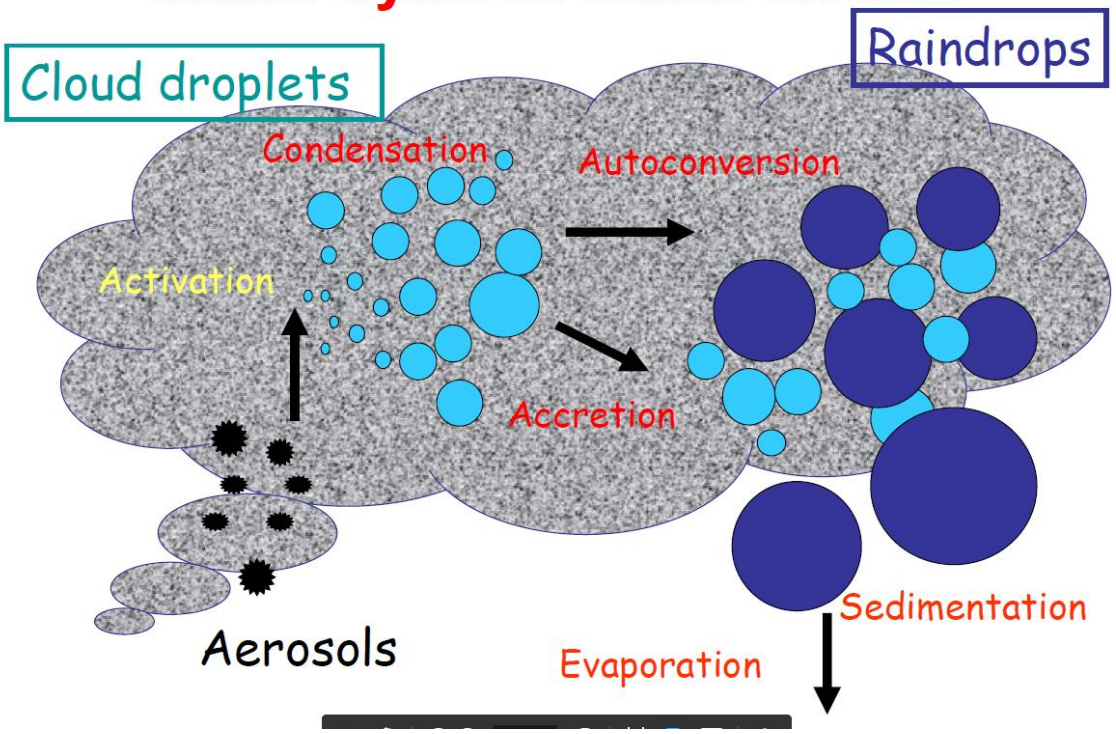

Mixed-phase clouds

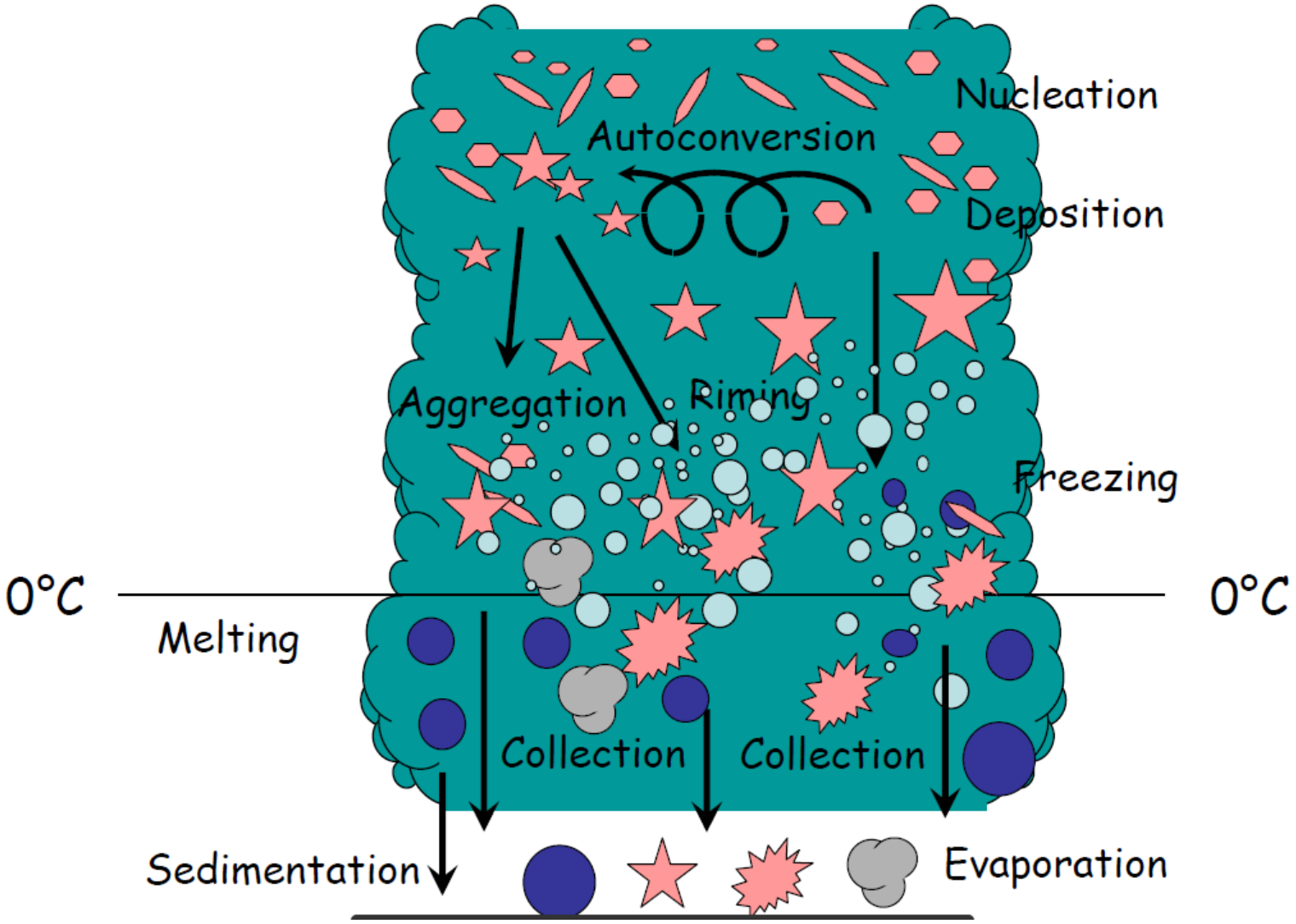

Chuva – contribuição a Modelagem

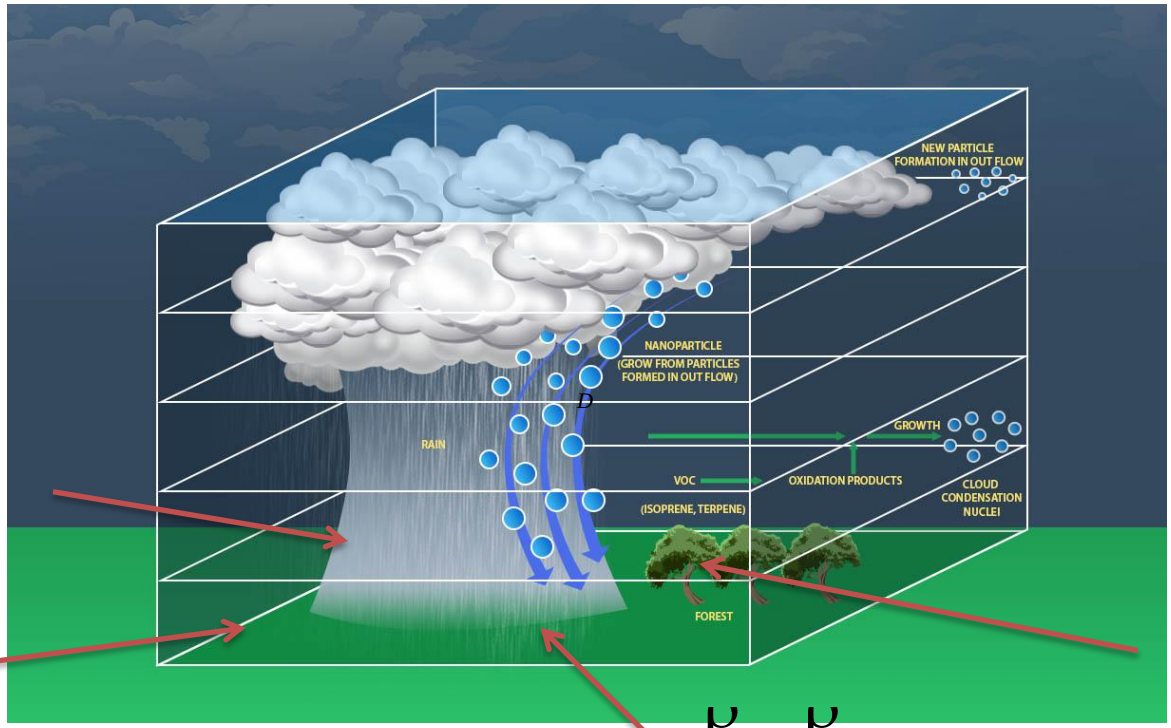

$$\text{Precipitação} = F(\lambda,\phi).\vec{\nabla}.q\vec{V}$$

Chuva – contribuição a Modelagem

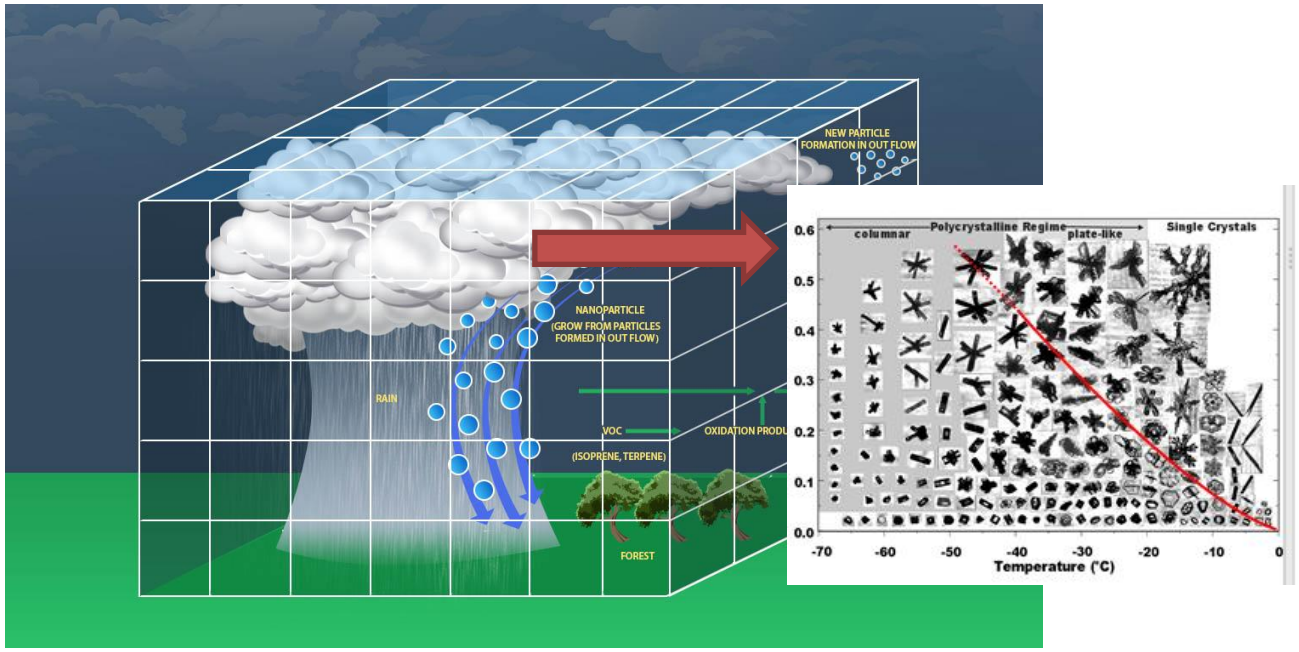

Cloud resolving models (CRM)
Large Eddy Simulation (LES)


a)

b)


c)


d)

Cloud Electrification

Conceptual View of Cloud-to-Ground Lightning Discharge Process

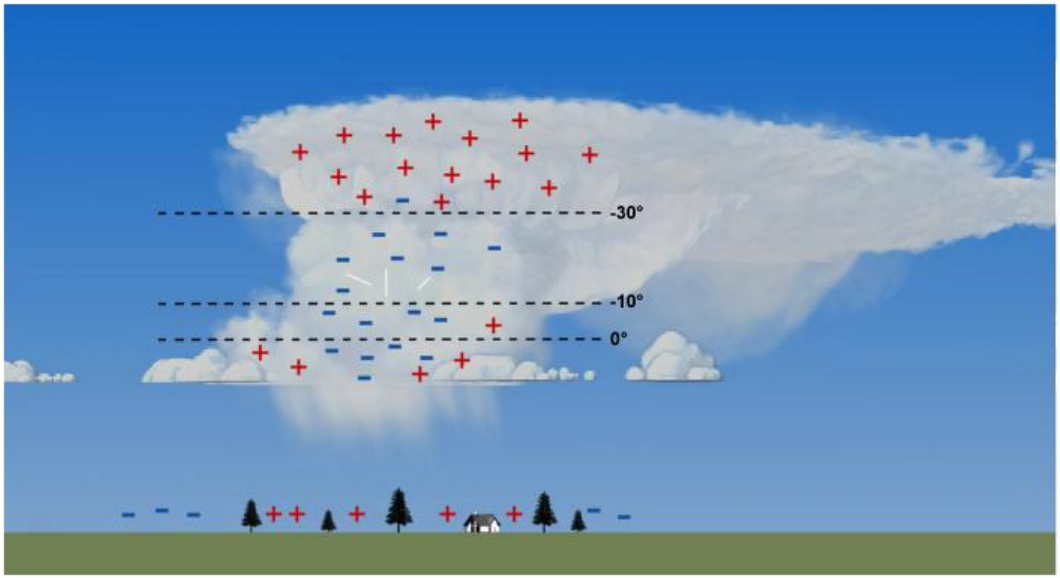

The Cloud Cluster and the Electrification Process

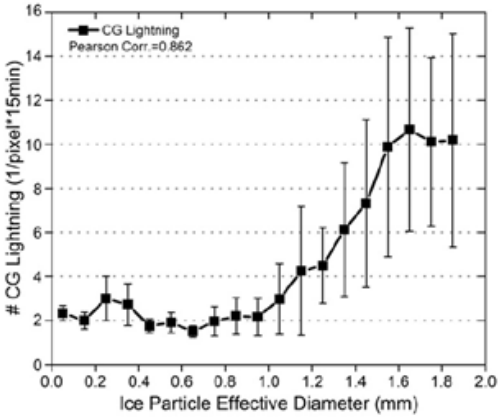

Fig. 8. Average and standard deviation of CG lightning occurrence in 15 min intervals by pixel (# CG lightning/pixel * 15 min) as a function of ice particle effective diameter (mm).

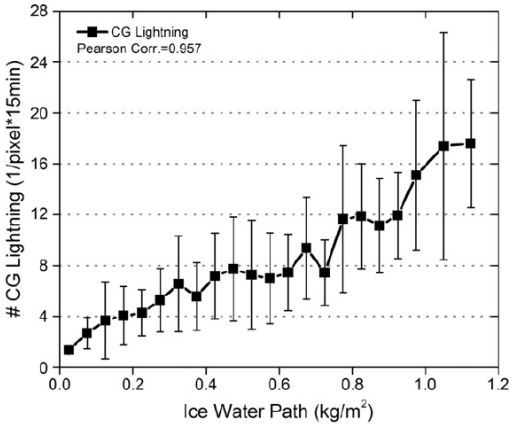

Fig. 9. Average and standard deviation of CG lightning occurrence in 15 min intervals by pixel (# CG lightning/pixel * 15 min) as a function of Ice Water Path (kg/m^2).

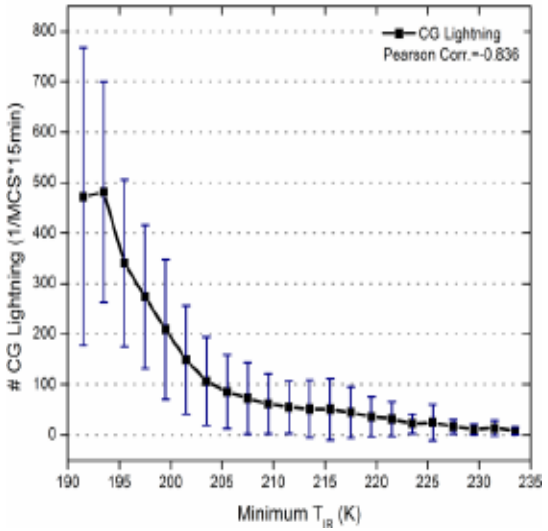

The Cloud cluster electrification processes depends from the ice water path, cloud top (Minimum Brightness Temperature and ice particles. Is interesting to see that for effective ice diameter smaller than 1 mm very few cloud to ground lighting is observed (CG). CG increases nearly linearly with the ice water path and exponentially with the minimum brightness temperature.

Mattos, E. V. and L.A.T. Machado. Cloud-to-ground lightning and mesoscale convective systems. Atmos. Res., 99 (2011), pp. 377-390

The Cloud Cluster and the Electrification Process

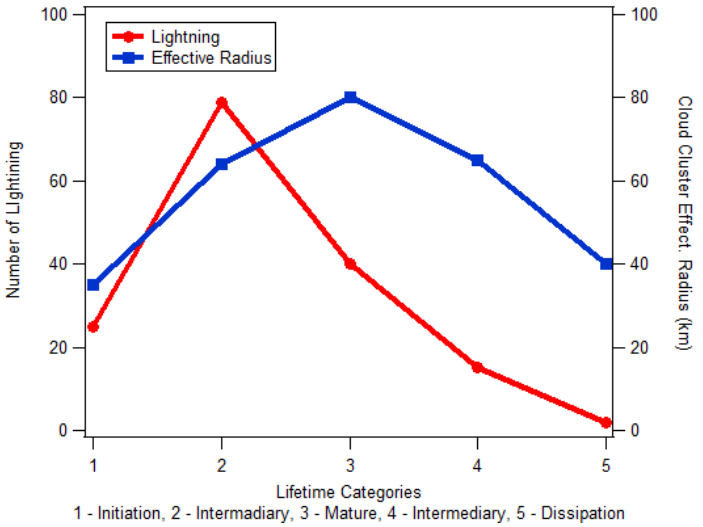

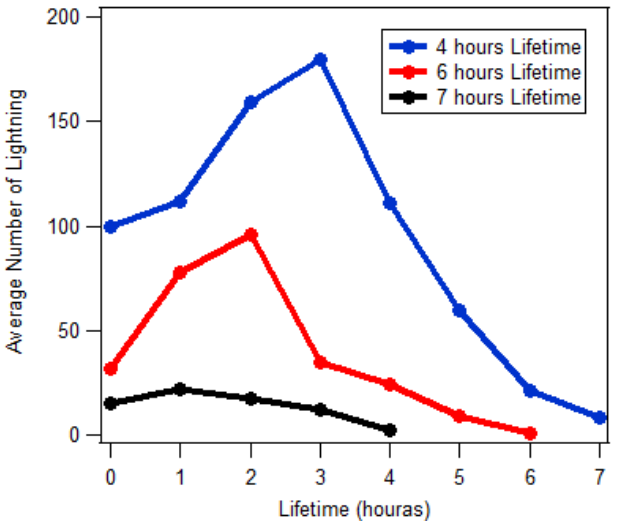

The maximum lightning activity occurs between the initiation and mature stage, this is the time of maximum convective activity. Larger the system more lightning is expect, but all system whatever the size the maximum occurs in the lifetime between initiation and mature stage.

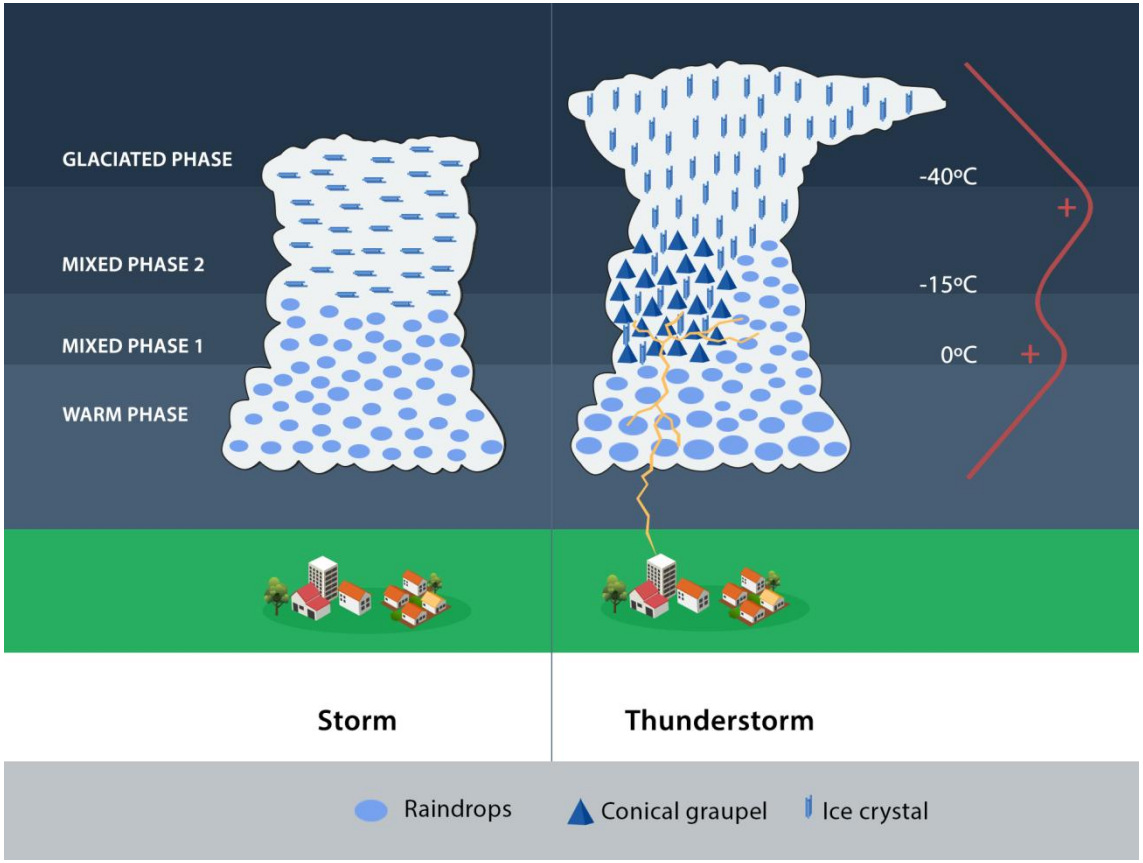
GLACIATED PHASE
MIXED PHASE 2
MIXED PHASE 1
WARM PHASE
-40ºC
-15ºC
0ºC
+
+
Storm
Thunderstorm
Raindrops
Conical graupel
Ice crystal

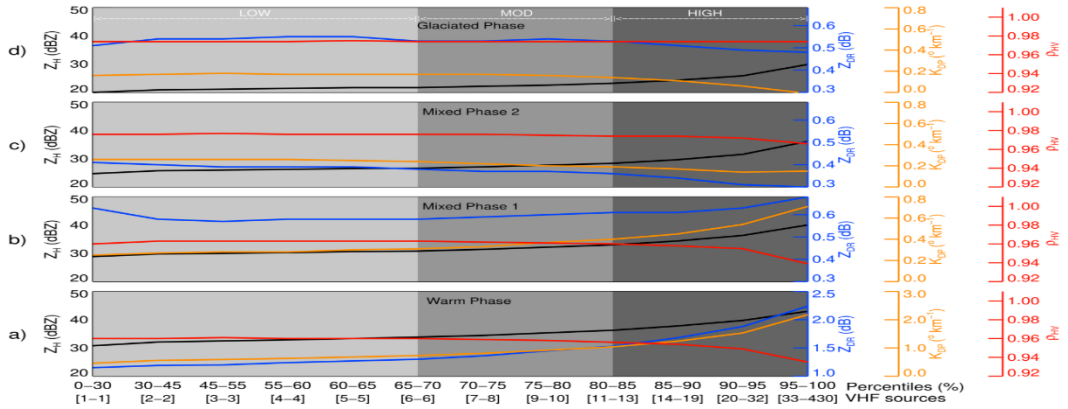
LOW
MOD
HIGH
Glaciated Phase
Mixed Phase 2
Mixed Phase 1
Warm Phase
d)
c)
b)
a)
Z_H (dBZ)
Z_{DR} (dB)
K_{DP} (° km⁻¹)
ρ_{HV}
0–30 [1–1]
30–45 [2–2]
45–55 [3–3]
55–60 [4–4]
60–65 [5–5]
65–70 [6–6]
70–75 [7–8]
75–80 [9–10]
80–85 [11–13]
85–90 [14–19]
90–95 [20–32]
95–100 [33–430]
Percentiles (%) VHF sources

The Cloud Cluster and the Electrification Process

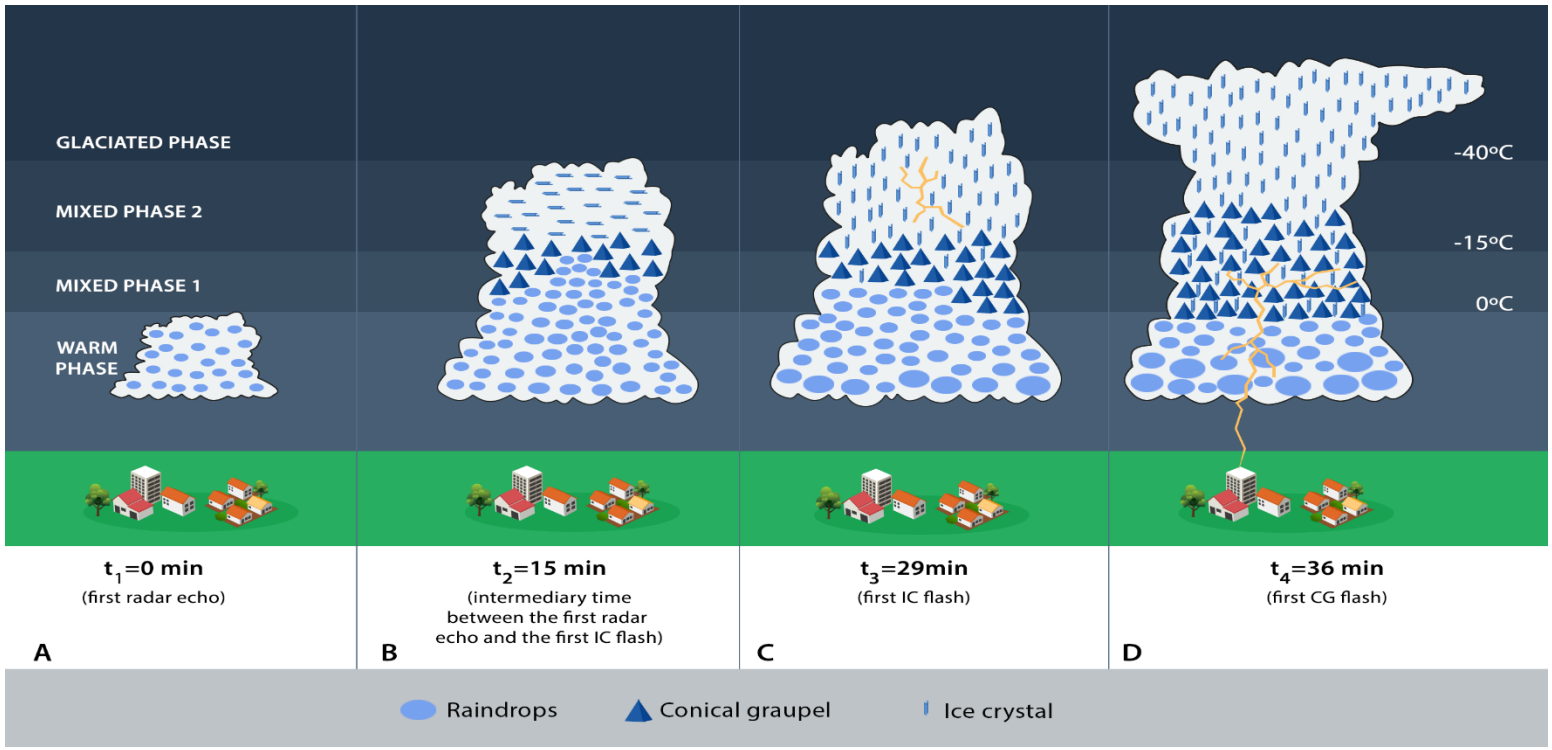

Conceptual model of the thunderstorm electrification life cycle. It is showed the evolution from the first radar echo up to the time of the first cloud-to-ground flash: (a) the time of the first radar echo (#1Echo, t_1=0 min), (b) the intermediate time between the first echo radar and the first intracloud lightning flash (Int., t_2=15 min), (c) the time of the first intracloud lightning flash (#1IC, t_3=29 min) and the (d) time of the first cloud-to-ground lightning flash (#1CG, t_4=36 min).

Mattos, E. V., L. A. T. Machado, E. R. Williams, S. J. Goodman, R. J. Blakeslee, and J. C. Bailey, 2017: Electrification life cycle of incipient thunderstorms. J. Geophys. Res. Atmos., ***122****, 4670–4697*

Evolution of Ice crystals in the eletrification processes

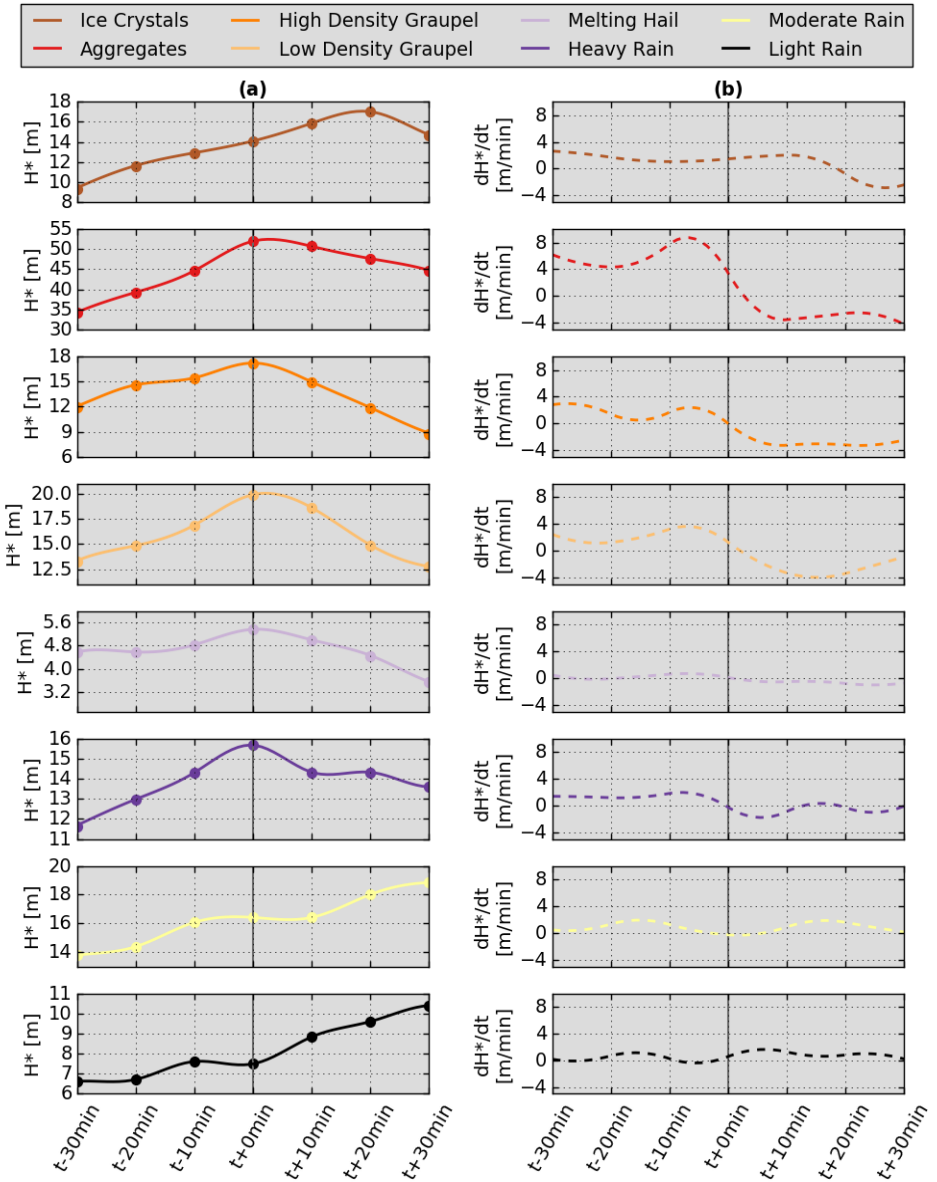

Time evolution of the mean altitude associated to solid hydrometeor types

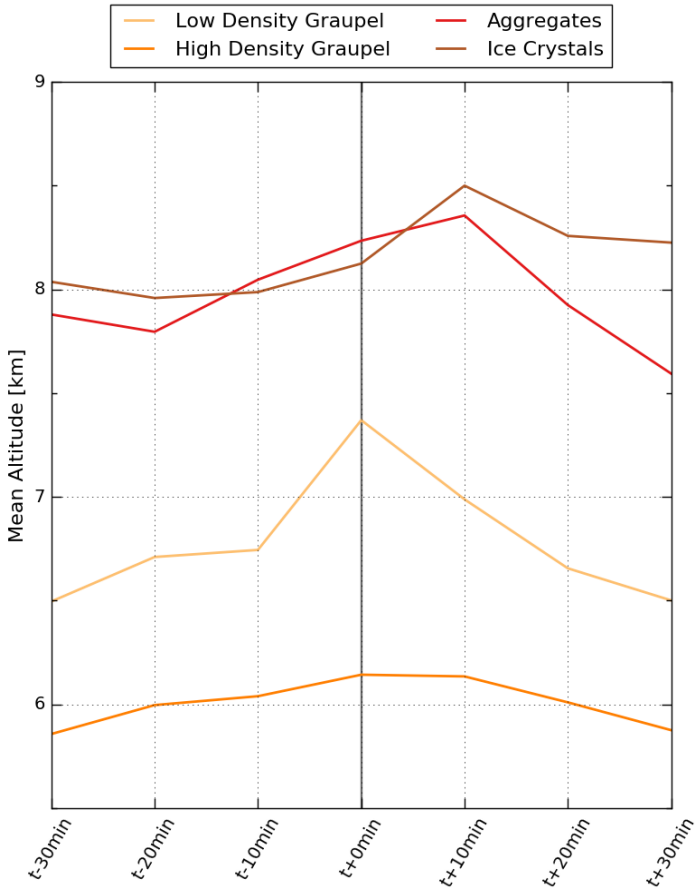

Jean-François Ribaud[1] and Luiz A. T. Machado. Hydrometeor Life Cycle Evolution of Tropical Thunderstorms Inferred from X-band dual-polarimetric Radar Observations. In submission processes - 2019

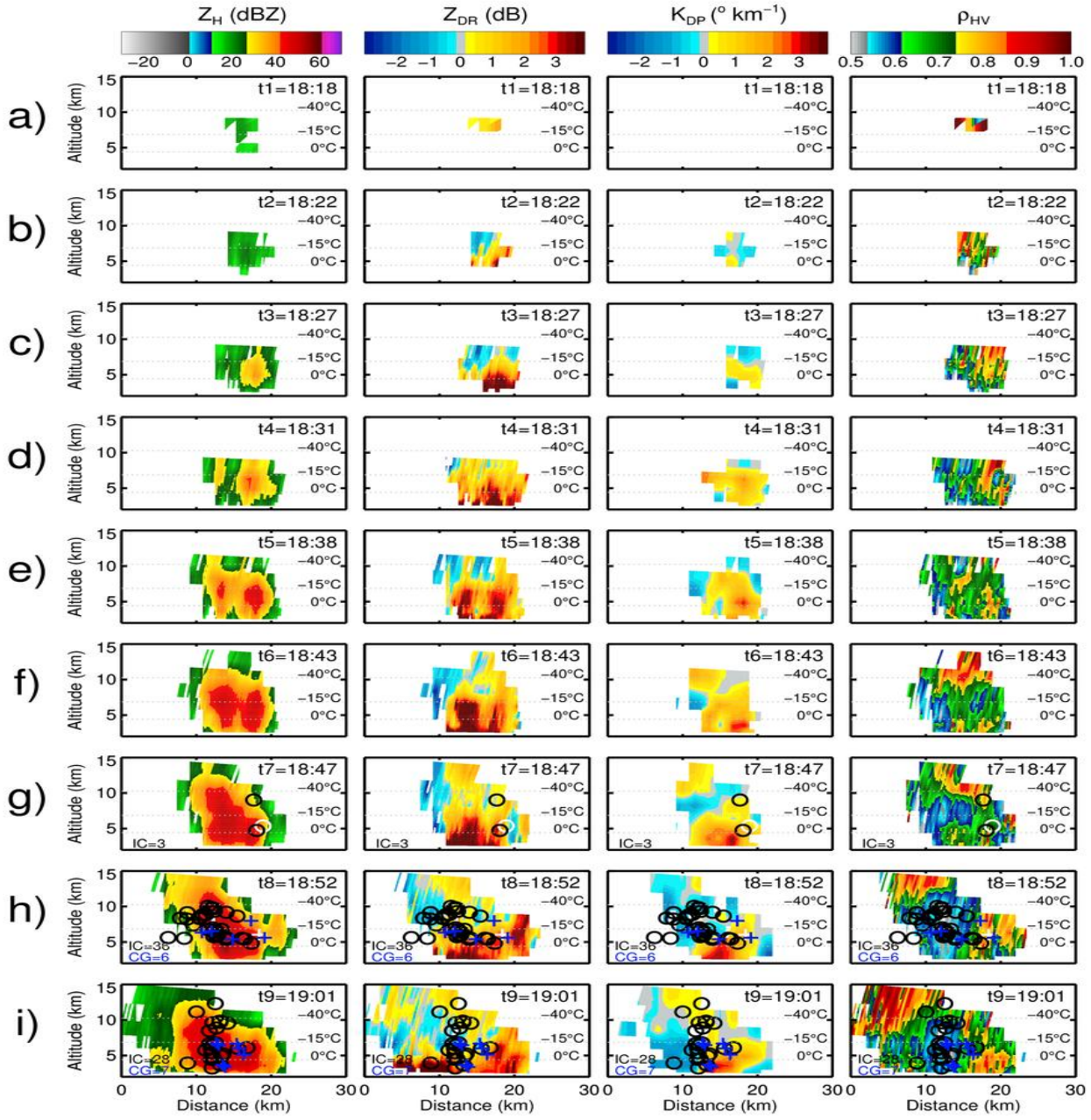
Z_H (dBZ)
−20 0 20 40 60
Z_{DR} (dB)
−2 −1 0 1 2 3
K_{DP} (° km^{-1})
−2 −1 0 1 2 3
ρ_{HV}
0.5 0.6 0.7 0.8 0.9 1.0
a)
b)
c)
d)
e)
f)
g)
h)
i)
Altitude (km)
15
10
5
t1=18:18
t2=18:22
t3=18:27
t4=18:31
t5=18:38
t6=18:43
t7=18:47
t8=18:52
t9=19:01
−40°C
−15°C
0°C
IC=3
IC=36
CG=6
IC=28
CG=7
0 10 20 30
Distance (km)

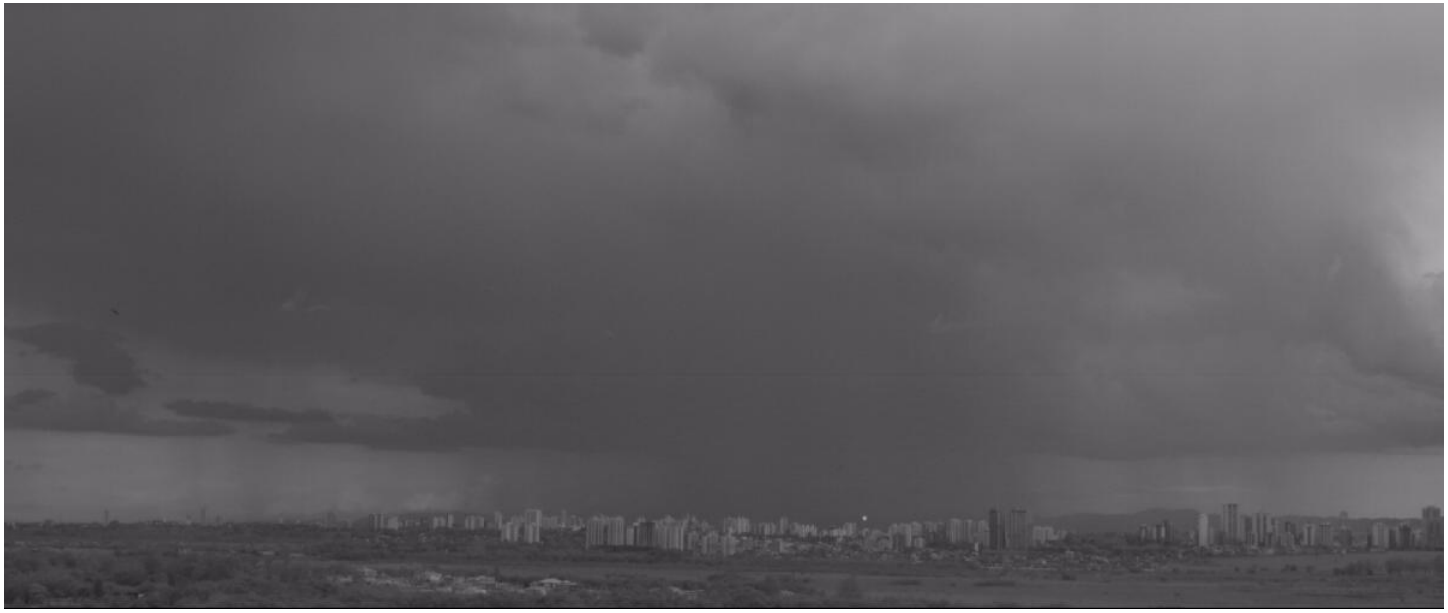

Contribuição do ELAT (Antônio Saraiva)

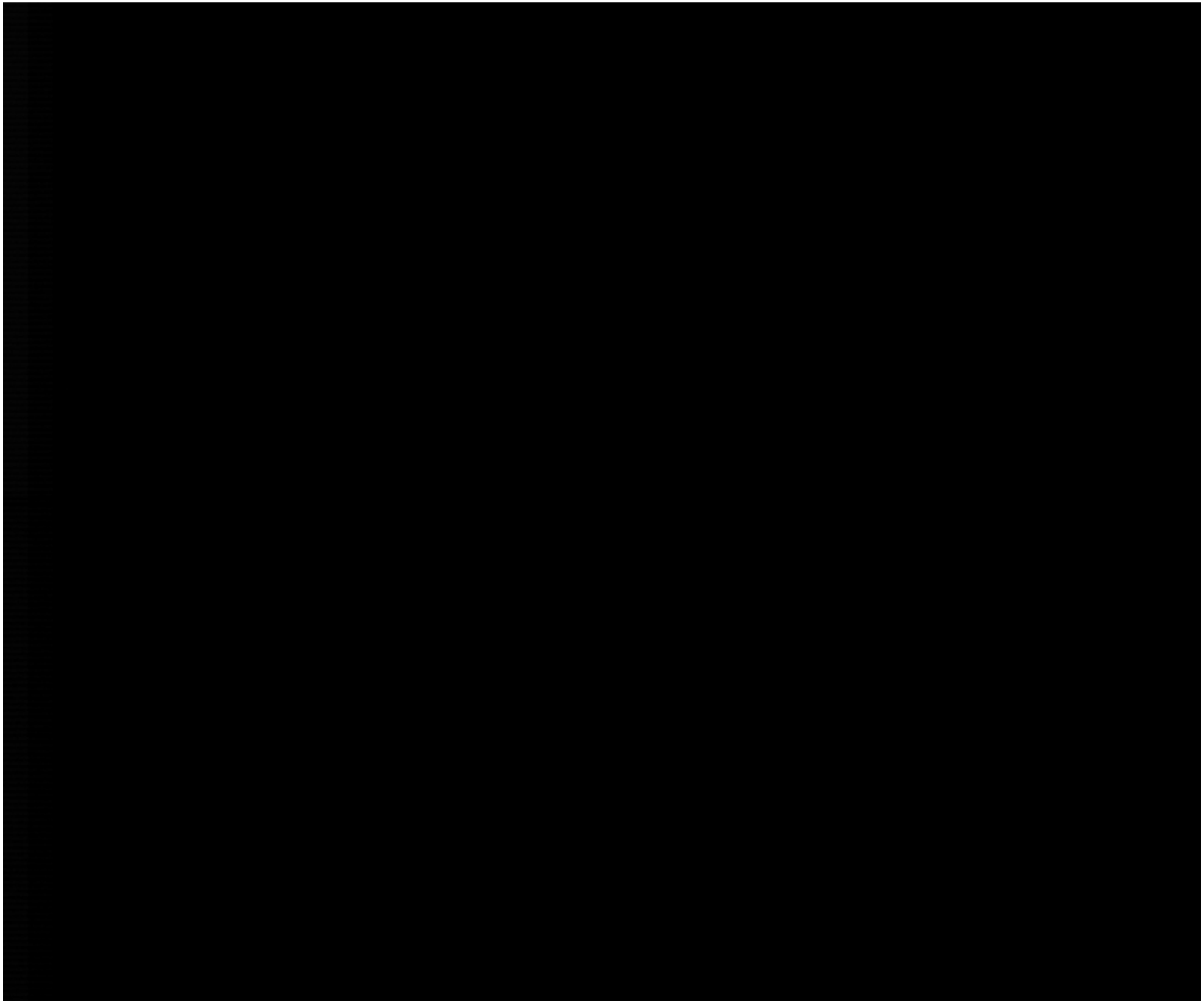

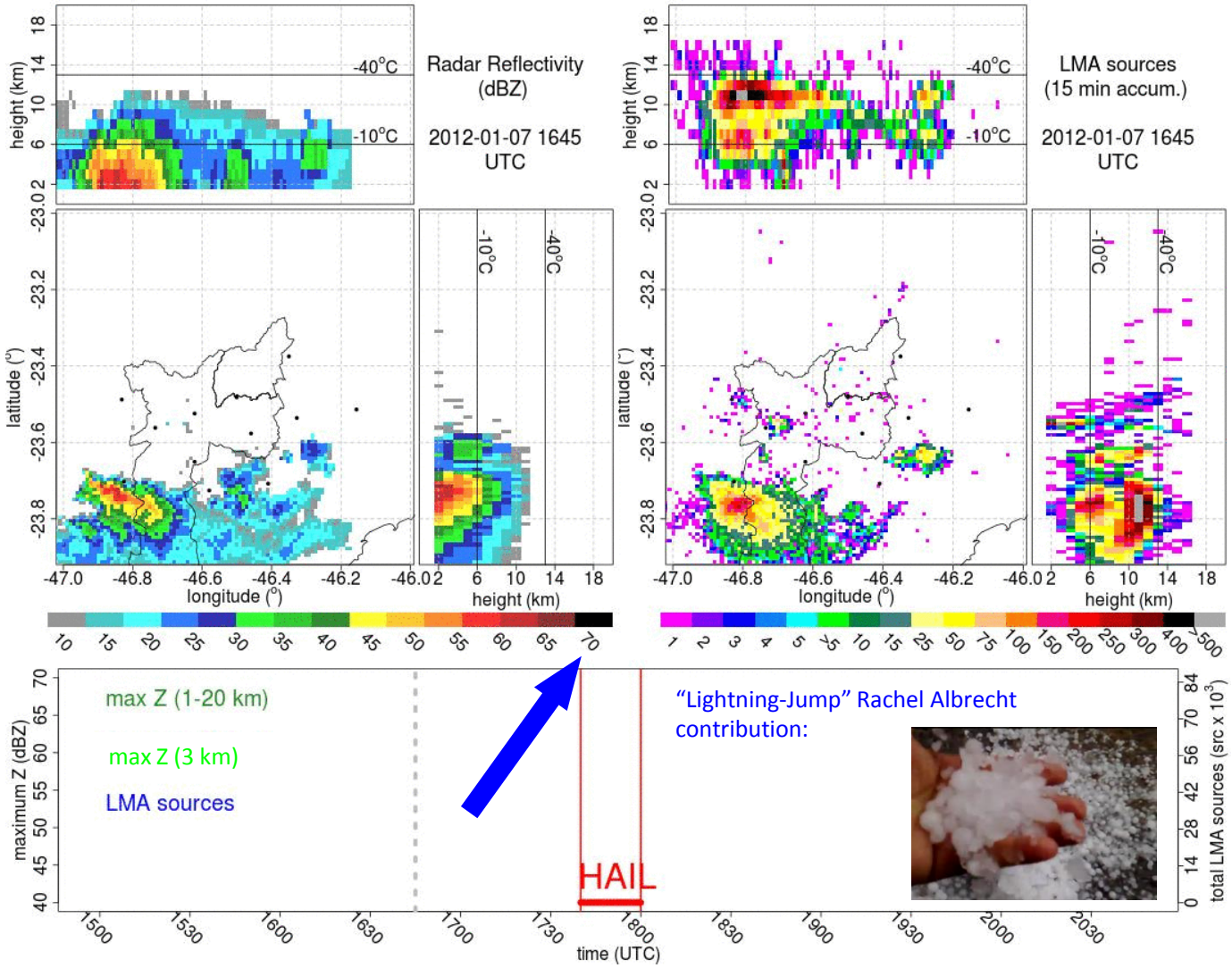
Radar Reflectivity (dBZ)
2012-01-07 1645 UTC
LMA sources (15 min accum.)
2012-01-07 1645 UTC
-40°C
-10°C
height (km)
latitude (°)
longitude (°)
max Z (1-20 km)
max Z (3 km)
LMA sources
maximum Z (dBZ)
total LMA sources (src x 10^3)
time (UTC)
HAIL
"Lightning-Jump" Rachel Albrecht contribution:

Raios durante a tempestade que gerou evento severo em Campinas
Dados STARNET 2016-06-06 0200 a 0400 UTC

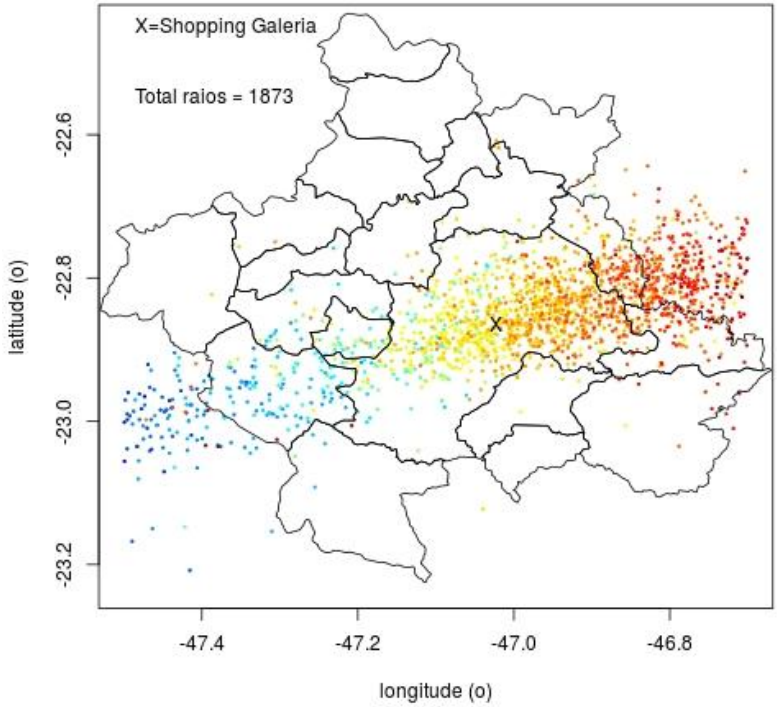

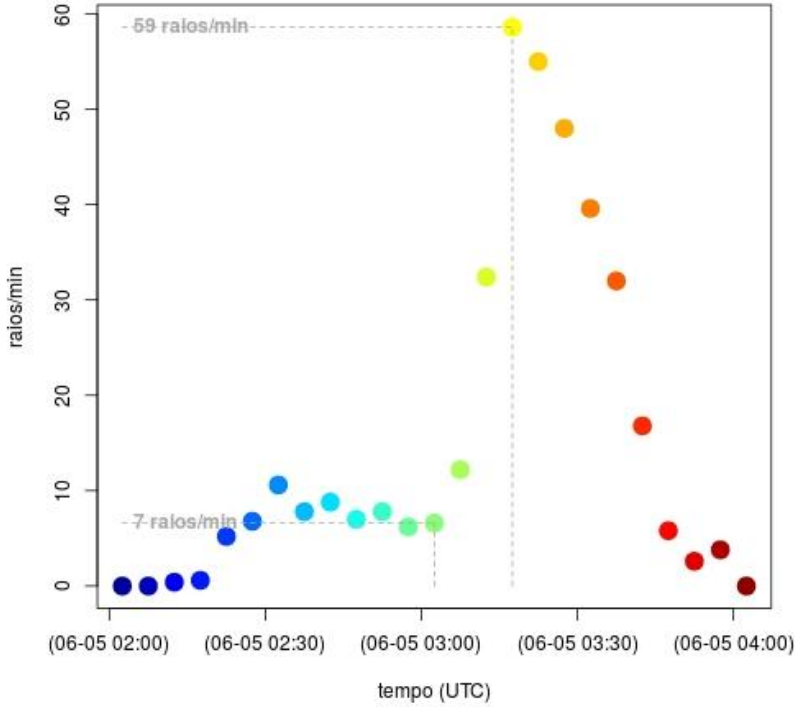

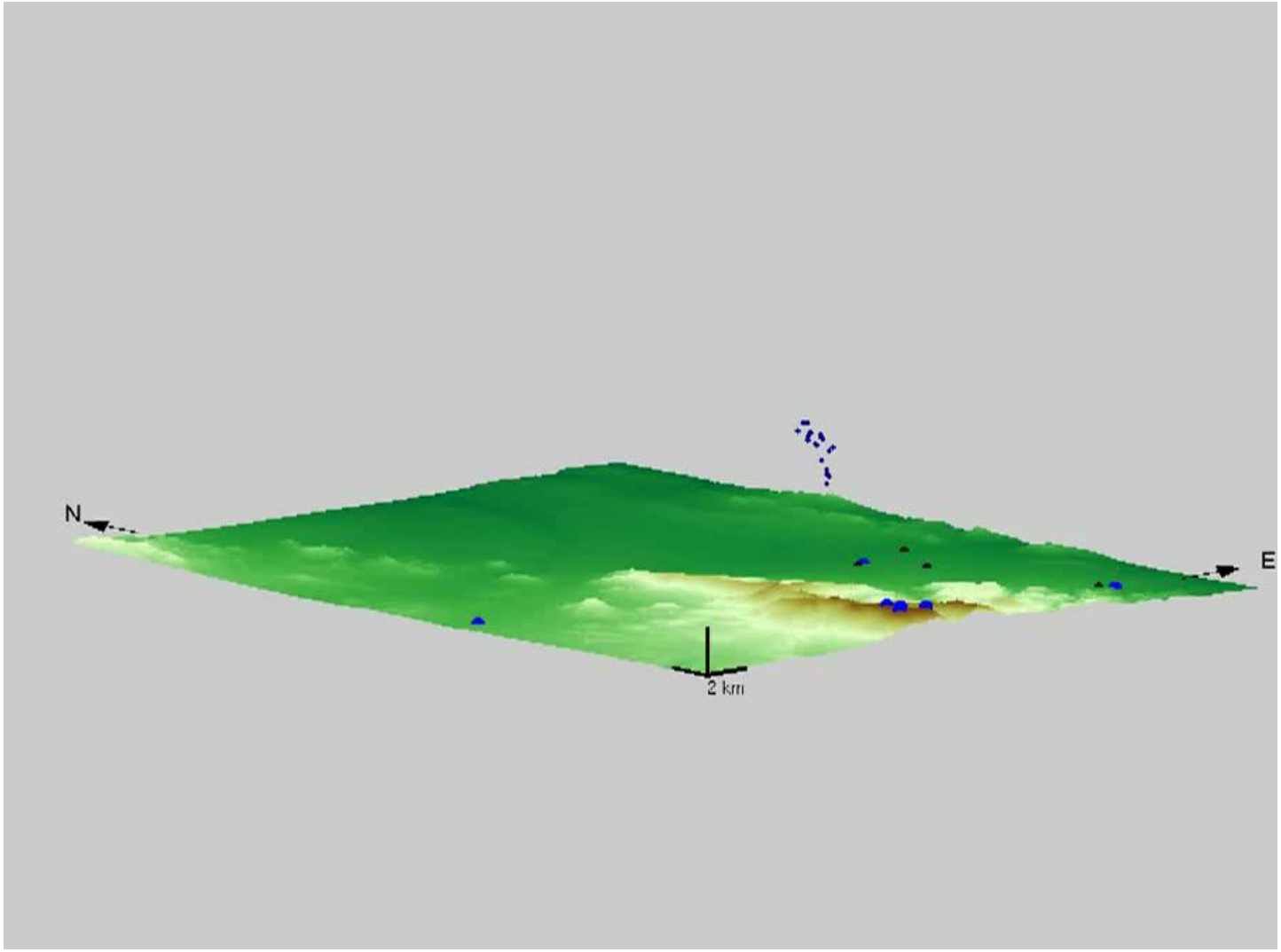
N
E
2 km

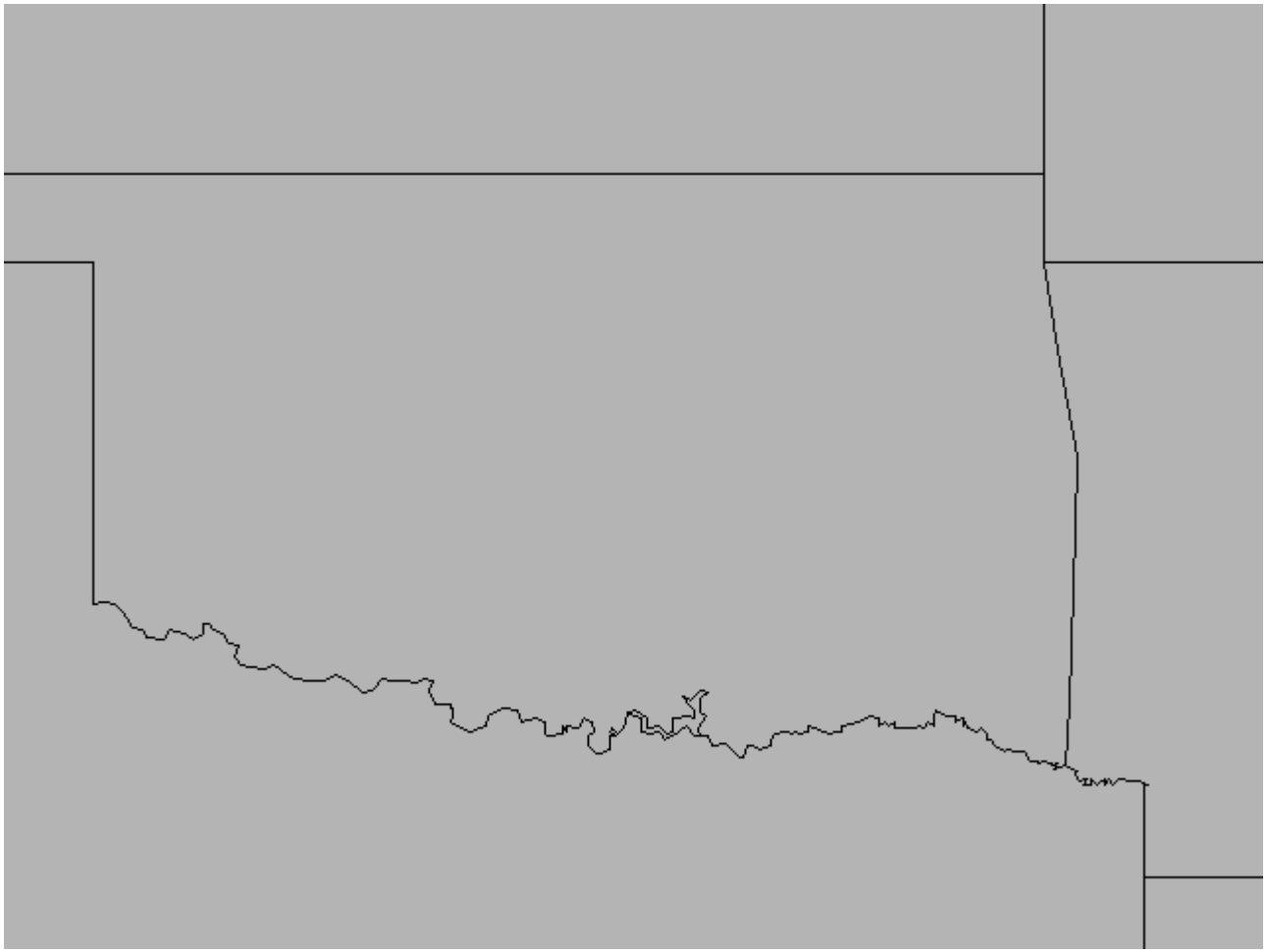

GOES-R Super Rapid Scan
Moving towards data fusion

Steven J. Goodman